AN ABSTRACT OF THE THESIS OF

Mohammad F. Azizian for the degree of Doctor of Philosophy in Civil Engineering

Presented on January 20, 1993

Title: Experimental Evaluation and Chemical Modeling of Hexavalent Chromium Adsorption, Desorption, and Reduction in a Natural Soil

Abstract approved: Peter O. Nelson
Peter O. Nelson

Chromium and its compounds are widely used by modern industries, resulting in large quantities of this element being discharged into the environment. To remove chromium from contaminated soils and ground water, it is necessary to predict chemical and physical processes that control the rate of reactions and transport of chromium in soils and aquifers. The goals of this experimental study were to determine (i) kinetics and equilibrium adsorption of chromium(VI) in a natural soil, (ii) reduction of Cr(VI) to Cr(III) in the soil, and (iii) the effect of competing oxyanions on Cr(VI) adsorption in the soil. The TLM was used to interpret surface complexation reactions of the chromate ions in the soil.

A laboratory investigation of reactions between hexavalent chromium, Cr(VI), and a natural soil was conducted to evaluate factors that influence

sorption and reduction of Cr(VI) in natural soils. Both batch and soil column experiments were conducted to study the chemical behavior and transport of Cr(VI) in the soil. Results indicated that adsorption and reduction of Cr(VI) are the major processes that control the rate of transport and mobility of chromium in natural soils. Cr(VI) removal from solution increased with increasing solute concentration and with decreasing solution pH. This experimental study provides insight on how the residual amount of ferrous ions in minerals such as magnetite can effect the redox speciation of chromium in natural soils. Experimental results indicated that the small amounts of magnetite Fe_3O_4 contained in the soil caused reduction of Cr(VI) to Cr(III) even at pH above 8. The ferrous iron contained in magnetite provides a source of electrons for the reduction of Cr(VI) to Cr(III). Competing oxyanions, phosphate ($H_2PO_4^-/HPO_4^{2-}$) and sulfate (SO_4^{2-}), increased Cr(VI) desorption by direct competition for adsorption sites. The equilibrium adsorption capacity of the soil was described with the Langmuir model, while a triple layer model (TLM) was employed to describe the surface complexation reactions. Outer–sphere surface complexation reactions and two–site (FeOH and AlOH) modeling were used to simulate adsorption of the chromate (CrO_4^{2-}) and bichromate ($HCrO_4^-$) ions.

Experimental Evaluation and Chemical Modeling of Hexavalent Chromium Adsorption, Desorption, and Reduction in a Natural Soil

by

Mohammad F. Azizian

A THESIS

submitted to

Oregon State University

in partial fulfillment of
the requirements for the
degree of

Doctor of Philosophy

Completed January 20, 1993

Commencement June 1994

APPROVED:

Peter O. Nelson

Professor of Civil Engineering in charge of major

Wayne C. Huber

Head of Department of Civil Engineering

John C. Ringle

Dean of Graduate School

Date thesis is presented January 20, 1993

Typed by Mohammad F. Azizian

ACKNOWLEDGEMENTS

I would like to thank Professor Peter O. Nelson for serving as my major advisor for his time, guidance, and support he provided throughout this study. I want to thank the members of my doctoral committee, Professor Kenneth J. Williamson, Professor Paul D. Komar, and Professor Sandra L. Woods. Each one provided assistance where and when it was needed. Special thanks to Professor John E. Baham for his time, suggestions, and permission to use lab space and equipment I needed to complete my research. I would also like to thank Mrs. Ann R. Kimerling for her help and valuable comments for my laboratory work.

Most of all, I thank my parents, Moluk Mahmudie, my mother, and Mirzababa Azizian, my father, for their encouragement, understanding and support throughout the years.

I would also like to thank Shahrnaz Badiee, my wife, Kasra, my son, and Kiana, my daughter, for their patience, continued love, and support.

I am especially grateful to my fellow graduate students, Heike K. Muller, Gregory R. Bean, Martin H. Schroth, Bruce L. Ball, Mark H. Smith, Gongming Wang, and Maoyu Yang, who have created an environment where ideas and experiences are freely shared.

Funding for this study was provided by the Office of Research and Development, U.S. Environmental Protection Agency, under agreement R–815738–01 through the Western Region Hazardous Substance Research Center.

TABLE OF CONTENTS

1. INTRODUCTION 1

2. LITERATURE REVIEW 3

2.1 Chromium chemistry in aquatic environment 3

2.2 Chromium chemistry in soils 7

2.3 Chromium(VI) adsorption and desorption in soils 8

2.4 Chromium(VI) precipitation/dissolution in soils 9

2.5 Chromium oxidation and reduction in soils 10

2.6 Chromium(VI) surface complexation 13

2.7 Triple layer model (TLM) 14

3. MATERIALS AND METHODS 18

3.1 Materials 18

3.1.1 Soil 18

3.1.2 Chemicals 18

3.2 Experimental procedures 20

3.2.1 Soil titration 20

3.2.2 Determination of soil specific surface area 20

3.2.3 Determination of inorganic carbon content (carbonates) 21

3.2.4 Determination of organic carbon content 22

3.2.5 Determination of soil reduction capacity 22

3.2.6 Determination of Fe(III) and Fe(II) in the soil 23

3.2.7 Batch experiments 23

3.2.7.1 Adsorption kinetics 23

3.2.7.2 Adsorption isotherms 24

3.2.8 Extraction of total chromium(VI) from the soil 25

3.2.9 Effects of the competing oxyanions on Cr(VI) adsorption 25

3.2.10 Soil column experiments 26

3.2.11 Determination of reduced Cr(VI) in the soil 27

3.3 Analytical Methods 29

3.3.1 Chromium(VI) analysis 29

3.3.2 Phosphate and sulfate determinations 30

3.3.3 Total Fe determination 30

3.3.4 pH determination 30

3.3.5 Conductivity determination 30

4. MODELING OF ADSORPTION DATA 31

4.1 Langmuir model 31

4.2 Triple layer model 36

4.2.1 Modeling approach 36

4.2.2 Triple layer model reactions 36

4.2.3 Triple layer model equilibrium constants 42

4.2.4 Triple layer model surface charge 43

4.2.5 Triple layer model surface potential 44

4.2.6 Application of triple layer model 44

4.2.7 Triple layer model parameters and values 45

4.3 HYDRAQL program 48

5. RESULTS 49

5.1 Soil analyses 49

5.1.1 pH of the piont–of–zero–charge 49

5.1.2 CHromium(VI) reduction capacity of the soil 51

5.2 Chromium(VI) batch reactor experiments 53

5.2.1 Adsorption kinetics 53

5.2.2 Adsorption isotherms 58

5.2.3 Effect of background electrolyte on Cr(VI) adsorption 61

5.2.4 Effects of competing oxyanions on Cr(VI) adsorption 62

5.3 Chromium(VI) soil column experiments 63

5.4 Chromium(VI) precipitation and Dissolution 79

5.5 Modeling Cr(VI) adsorption in batch experiments 81

5.5.1 Langmuir Model 81

5.5.2 Triple Layer Model 81

5.5.3 Effect of background electrolyte on Cr(VI) adsortpion 82

5.5.4 Effects of competing oxyanions on Cr(VI) adsorption 82

6. DISCUSSION OF THE RESULTS 86

6.1 Chromium(VI) reduction 86

6.2 Chromium(VI) adsorption kinetics 87

6.2.1 Effect of pH on chromium(VI) adsorption kinetics 88

6.2.2 Effect of chromium(VI) concentration on adsorption kinetics 89

6.3 Adsorption and desorption kinetics in soil columns 89

6.4 Chromium(VI) Adsorption isotherms 89

6.4.1 Effect of ionic strength on chromium(VI) adsorption isotherms 90

6.4.2 Effects of competing oxyanions on chromium(VI) adsorption isotherms 91

6.5 Chromium(VI) desorption in soil columns 91

6.6 Chromium(VI) reduction in soil columns 92

6.7 Adsorption modeling 93

6.7.1 Triple layer model 93

6.7.2 Langmuir adsorption model 95

7. SUMMARY AND CONCLUSIONS 97

8. ENGINEERING SIGNIFICANCE 100

9. REFERENCES 104

10. APPENDICES

APPENDIX 1: X–ray diffraction (XRD) curves of the soil and pH and flow rate curves of soil column experiments 112

APPENDIX 2: Batch and soil column experiment tables 125

APPENDIX 3: FITEQL and HYDRAQL input and output tables 151

LIST OF FIGURES

Figure		Page
1.	Areas of dominance of dissolved chromium species at equilibrium in the system Cr + H_2 + O_2 at 25 °C and 1 atm	4
2.	Predominance diagram showing the relative distribution of different Cr(VI) species in water as a function of pH and total Cr(VI) concentration	6
3.	Solubility diagram of $Cr(OH)_3$ and the solid phase solution $Fe_{.75}Cr_{.25}(OH)_3$(am) as a function of pH	11
4.	Schematic representation of TLM analogs of coordination (inner–sphere) and ion–pair (outer–sphere) surface complexes	15
5.	Soil pH of the point–of–zero–charge (pH_{pzc}) determination using acid and base titrations at various ionic strengths	50
6.	Chromium(VI) removal kinetics for 120 hour reaction time, 0.1 mM Cr(VI) in 0.01 M NaCl electrolyte solution, pH = 5.02–5.26, 40 g/L soil	54
7.	The effect of Cr(VI) reduction on Cr(VI) adsorption, 0.1 mM Cr(VI) in 0.01 M NaCl electrolyte solution, pH = 5.02–5.26, 40 g/L soil	55
8.	The effect of pH on Cr(VI) adsorption kinetics, 0.1 mM Cr(VI) in 0.01 M NaCl electrolyte solution, 40 g/L soil	56

9. The effect of Cr(VI) concentration on Cr(VI) adsorption kinetics, 0.01 M NaCl electrolyte solution, pH = 6.3–6.5, 40 g/L soil 57

10. The effect of Cr(VI) reduction on Cr(VI) adsorption isotherm, pH = 5.60–5.69 59

11. The effect of pH on Cr(VI) adsorption isotherm, 0.01 M NaCl electrolyte solution, 40 g/L soil. Solid lines represent fitted Langmuir equation 60

12. The effect of background electrolyte (NaCl) concentration on Cr(VI) adsorption as a function of pH, 0.1 mM Cr(VI), 40 g/L soil 61

13. The effects of competing oxyanions on Cr(VI) adsorption as a function of pH, 0.1 mM Cr(VI), 40 g/L soil 62

14. Chromium(VI) breakthrough curve for an initial concentration of 0.2 mM Cr(VI) in 0.01 M NaCl electrolyte solution. Desorption conducted using 0.01 M NaCl solution (column #1) 69

15. Chromium(VI) breakthrough curve for an initial concentration of 0.2 mM Cr(VI) in 0.5 M NaCl electrolyte solution. Desorption conducted using 0.01 M NaCl solution. Spike in desorption limb due to column shutdown (column # 2) 70

16. Chromium(VI) breakthrough curve for an initial concentration of 0.2 mM Cr(VI) in 0.01 M NaCl. Desorption conducted using 0.01 M phosphate solution at pH 7.21 (column # 3) 71

17. Chromium(VI) breakthrough curve for an initial concentration of 0.1 mM Cr(VI) in 0.01 M NaCl electrolyte solution. Desorption conducted using 0.01 M sulfate solution (column # 4) 72

18. Chromium(VI) breakthrough curve for an initial concentration of 0.1 mM Cr(VI) in 0.1 M NaCl electrolyte solution. Desorption conducted using 0.01 M sulfate solution (column # 5) 73

19. Cr(VI) breakthrough curve for an initial concentration of 0.1 mM Cr(VI) in 0.01 M NaCl solution at pH about 2. Desorption conducted using 0.5 M phosphate solution at pH = 8 (column # 6) 74

20. Cr(VI) breakthrough curve for an initial concentration of 0.1, 0.4, 1.0, and 10.0 mM, Cr(VI) in 0.01 M NaCl at pH = 2. Desorption with 0.5 M phosphate solution at pH = 8 (column # 7) 75

21. Cr(VI) breakthrough curve for an initial concentration of 10.0 mM Cr(VI) in 0.01 M NaCl solution. HCl added to the influent solution after 50 pore volumes at pH about 2. Desorption conducted using 0.5 phosphate solution at pH about 8 (column # 8)76

22. Solubility diagram of $BaCrO_4$(s) and $BaSO_4$(s) in 0.01 M NaCl solution versus pH at 25 °C for the shallow wells at the United Chrome Superfund site. Data points falling above the solubility lines indicate possible precipitation of solid phases 80

23. Comparison of Cr(VI) adsorption data, and triple–layer model (TLM) fit, as a function of pH, 0.1 mM Cr(VI) in 0.01 M NaCl electrolyte solution, 40 g/L soil 83

24. Effect of electrolyte concentration on Cr(VI) adsorption as a function of pH, and TLM fit, 0.1 mM Cr(VI), 40 g/L soil 84

25. The effect of 0.01 M sulfate on Cr(VI) adsorption, and triple–layer model fit, as a function of pH, 0.1 mM Cr(VI), 40 g/l soil 85

LIST OF TABLES

Table		Page
1.	Soil physical characterization experiments	19
2.	Soil chemical characterization experiments	19
3.	Description of the soil column #3 experiment	27
4.	Triple layer model complexation reactions and equilibrium constants for chromate and sulfate	46
5.	Surface area and the inner–layer and outer–layer capacitance	47
6.	Total reduction capacities of the soil	51
7.	Total magnetite separated from the soil	52
8.	Total Fe and Fe(II) determined by wet chemical analyses	52
9.	Organic and inorganic carbon content of the soil	53
10.	Langmiur adsorption constant and maxima calculated from equilibrium isotherms	58
11.	Chromium(VI) soil column experiments	68
12.	Sequential extraction data for residual chromium from soil column experiments	77
13.	Mass balance on Cr(VI) extraction from soil column experiments 1–8	78
14.	Intrinsic surface complexation constants for Cr(VI) adsorption on amorphous oxyhydroxide and on natural soils	93

LIST OF APPENDICES FIGURES

Figure		Page
26.	X–ray diffraction pattern of magnetically separated sample from a natural soil (#1)	113
27.	X–ray diffraction pattern of magnetically separated sample from from a natural soil (#2)	114
28.	X–ray diffraction pattern of the pure magnetite (#1)	115
29.	X–ray diffraction pattern of the pure magnetite (#2)	116
30.	Effluent pH of soil column #1 during adsorption and desorption	117
31.	Effluent flow rate of soil column #1 during adsorption and desorption	117
32.	Effluent pH of soil column #2 during adsorption and desorption	118
33.	Effluent flow rate of soil column #2 during adsorption and desorption	118
34.	Effluent pH of soil column #3 during adsorption and desorption	119
35.	Effluent flow rate of soil column #3 during adsorption and desorption	119
36.	Effluent pH of soil column #4 during adsorption and desorption	120
37.	Effluent flow rate of soil column #4 during adsorption and desorption	120
38.	Effluent pH of soil column #5 during adsorption and desorption	121

39. Effluent flow rate of soil column #5 during adsorption and desorption 121

40. Effluent pH of soil column #6 during adsorption and desorption 122

41. Effluent flow rate of soil column #6 during adsorption and desorption 122

42. Effluent pH of soil column #7 during adsorption and desorption 123

43. Effluent flow rate of soil column #7 during adsorption and desorption 123

44. Effluent pH of soil column #8 during adsorption and desorption 124

45. Effluent flow rate of soil column #8 during adsorption and desorption 124

LIST OF APPENDICES TABLES

Table		Page
15.	Description of the soil column experiment # 1	126
16.	Description of the soil column experiment # 2	126
17.	Description of the soil column experiment # 4	126
18.	Description of the soil column experiment # 5	127
19.	Description of the soil column experiment # 6	127
20.	Description of the soil column experiment # 7	127
21.	Description of the soil column experiment # 8	128
22.	Soil titration with 1.0 M HCl in H_2O	128
23.	Soil titration with 1.0 M HCl in 0.01 M NaCl	129
24.	Soil titration with 1.0 M HCl in 0.10 M NaCl	129
25.	Soil titration with 1.0 M HCl in 1.0 M NaCl	130
26.	0.1 mM Cr(VI) adsorption kinetic in 0.01 M NaCl, pH = 6.5	130
27.	0.1 mM Cr(VI) adsorption kinetic in 0.01 M NaCl, pH=5.25	131
28.	0.2 mM Cr(VI) adsorption kinetic in 0.01 M NaCl, pH=6.5	131
29.	Chromium(VI) adsorption isotherm in 0.01 M NaCl, pH=5.65	132
30.	Chromium(VI) adsorption isotherm in 0.01 M NaCl, pH=7.0	132
31.	0.1 mM Cr(VI) adsorption in 0.01 M NaCl for varying pH	133
32.	0.1 mM Cr(VI) adsorption in 0.1 M NaCl for varying pH	133
33.	0.1 mM Cr(VI) adsorption in 0.5 M NaCl for varying pH	134
34.	0.1 mM Cr(VI) adsorption in 0.01 M $NaNO_3$ for varying pH	134

35. 0.1 mM Cr(VI) adsorption in 0.01 M $NaHCO_3$ for varying pH 135
36. 0.1 mM Cr(VI) adsorption in 0.01 M Na_2SO_3 for varying pH 135
37. 0.1 mm Cr(VI) adsorption in 0.01 M KH_2PO_4 for varying pH 136
38. Soil column experiment # 1 137
39. Soil column experiment # 2 139
40. Soil column experiment # 3 141
41. Soil column experiment # 4 142
42. Soil column experiment # 5 143
43. Soil column experiment # 6 144
44. Soil column experiment # 7 146
45. Soil column experiment # 8 148
46. Thermodynamic calculations of $BaCrO_4$ 150
47. Thermodynamic calculations of $BaSO_4$ 150
48. Reaction stoichiometries considered for TLM calculations 152
49. TLM input data, 0.1 mM Cr(VI) adsorption for varying pH 153
50. TLM output data, 0.1 mM Cr(VI) adsorption for varying pH 155
51. HYDRAQL input, 0.1 mM chromate adsorption in 0.01 M NaCl 161
52. HYDRAQL output, 0.1 mM chromate adsorption in 0.01 M NaCl 162
53. HYDRAQL input, 0.1 mM chromate adsorption in 0.1 M NaCl 164
54. HYDRAQL output, 0.1 mM chromate adsorption in 0.1 M NaCl 165
55. HYDRAQL input , 0.1 mM chromate adsorption in 0.5 M NaCl 167
56. HYDRAQL output, 0.1 mM chromate adsorption in 0.5 M NaCl 168
57. HYDRAQL input, 0.1 mM chromate adsorption in 0.01 M sulfate 170
58. HYDRAQL output, 0.1 mM chromate adsorption in 0.01 M sulfate 171

EXPERIMENTAL EVALUATION AND CHEMICAL MODELING OF HEXAVALENT CHROMIUM ADSORPTION, DESORPTION, AND REDUCTION IN A NATURAL SOIL

1. INTRODUCTION

Groundwater contamination by chromium is a major problem in industrialized areas, particularly those have metal–plating industries. Chromium oxidation states range from –2 to +6, but only the +3 and +6 states are stable under most environmental conditions. The toxicity of chromium is confined to Cr(VI) compounds (Zachara et al., 1987). The harmful effects may be due to the oxidizing ability or the properties associated with heavy metals. Cr(VI) is a carcinogen, an irritant, and a corrosive, which can be absorbed by ingestion and through the skin (Nriagu and Nieboer 1988). The specific objectives of this study were to: 1. Determine the kinetics and equilibrium of Cr(VI) sorption in a natural soil as a function of pH, 2. Determine the effects of oxidation–reduction on Cr(VI) removal from the soil solution, 3. Determine the effects of competing oxyanions on Cr(VI) sorption in the soil, 4. Determine the surface complexation reactions of Cr(VI) in the soil.

Cr(VI) is mobile in most soils and water systems. The mobility of chromium in groundwater depends on its solubility and its tendency to be adsorbed by soil minerals. The amount of adsorption increases with decreasing

pH. Fortunately, environmental samples are typically alkaline and Cr(VI) is less reactive at these higher pHs. Cr(III) is rather immobile due to its limited solubility, sorption by negatively charged surfaces in soils, and complexation by organic material.

Oxidation–reduction processes play a major role in the mobility, transport, and fate of chromium in natural soils and waters. Cr(VI) can be reduced in many soil systems by reaction with organic matter, Fe(II), and sulfide compounds. The reduction potential of Cr(VI) decreases as the pH increases. Oxidation of Cr(III) to Cr(VI) in soil occurs readily in the presence of molecular oxygen and manganese oxides (Eary and Rai, 1987).

2. LITERATURE REVIEW

2.1 *Chromium chemistry in aquatic environment:* Of the possible oxidation states of chromium, only hexavalent and trivalent chromium (Cr(VI) and Cr(III)) are of interest in environmental systems. Chromium speciation in groundwater is affected by pE and pH conditions (Figure 1)(Calder, L. M. 1988). Chromium in natural waters exists in two oxidation states: +3, Cr(III) or trivalent form; and +6, Cr(VI) or hexavalent form. Chromium(VI) species are anionic (i.e., $HCrO_4^-$ and CrO_4^{2-}) and are generally mobile in most neutral to alkaline systems. The proportion of each ion in solution depends on pH and total chromium concentration. The following are the important equilibrium reactions for different Cr(VI) species (Sengupta and Clifford, 1986):

$H_2CrO_4 = H^+ + HCrO4^-$	log K_a (25 °C)	–0.8	(1)
$HCrO_4^- = H^+ + CrO_4^{2-}$	log K_a (25 °C)	–6.5	(2)
$2HCrO_4^- = Cr_2O_7^{2-} + H_2O$	log K_a (25 °C)	1.52	(3)
$HCr_2O_7^- = H^+ + Cr_2O_7^{2-}$	log K_a (25 °C)	0.07	(4)

Reactions 1, 2, and 4 show that the predominant species present, as a function of the pH, are H_2CrO_4 at pHs less than 0.8, $HCrO_4^-$ at pHs between 0.8 to 6.5, and CrO_4^{2-} at pHs above 6.5. Reaction 3 does not contain any H^+ terms, and

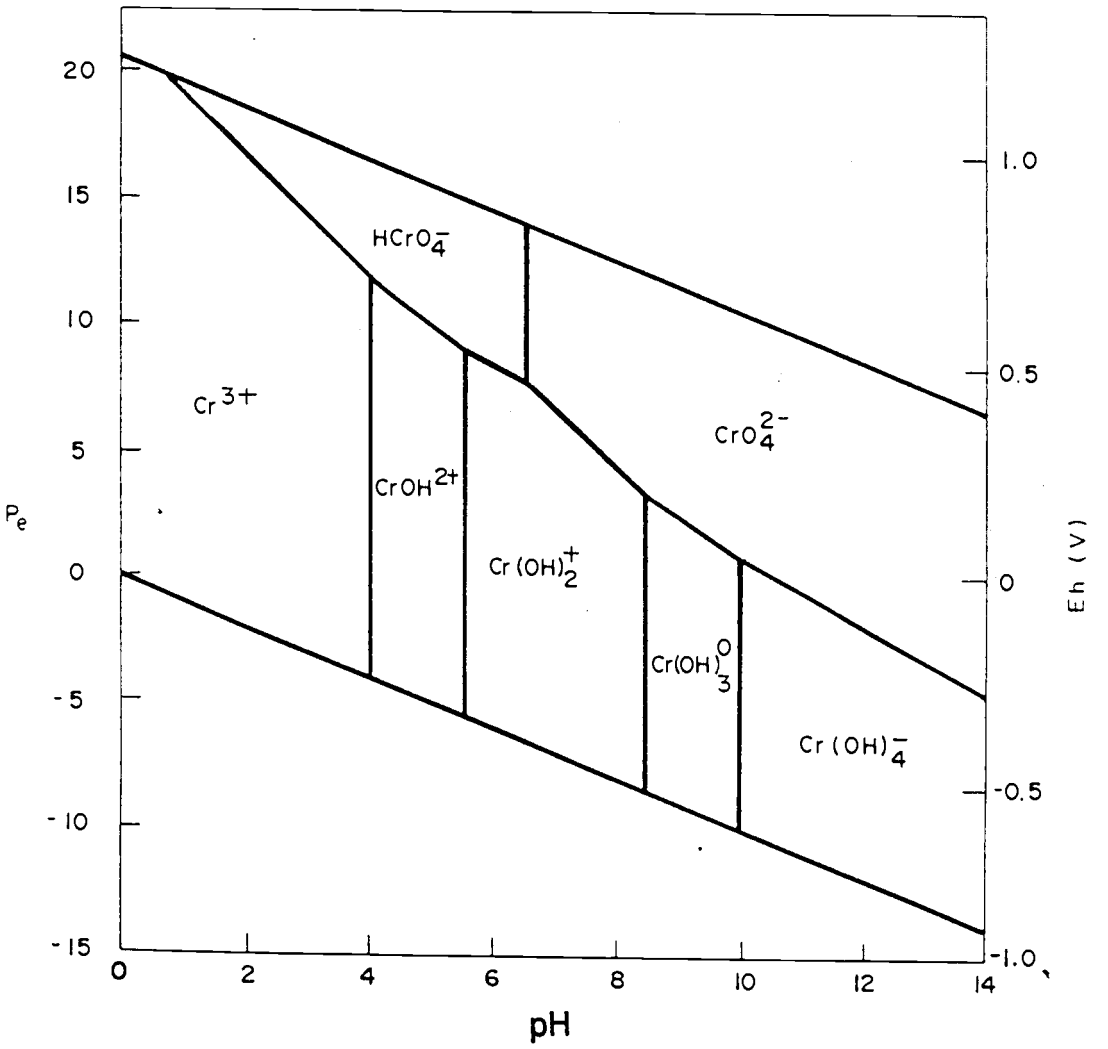

Figure 1: Areas of dominance of dissolved chromium species at equilibrium in the system Cr + H_2 + O_2 at 25°C and 1 atm. (Calder, 1988).

therefore, in a certain pH range (2–5) this reaction is nearly independent of pH and depends only on total Cr(VI) concentration. When the concentration of chromium exceed 10 mM and under acidic conditions bichromate ($HCrO_4^-$) polymerizes to form dichromate ($Cr_2O_7^{2-}$). A predominance diagram (Figure 2) shows relative distribution of chromate species as a function of pH and total Cr(VI) concentration (Sengupta and Clifford, 1986). Chromium (VI) species are strong oxidants that are reduced to the trivalent state by aqueous Fe(II) and organic compounds (Eary and Rai, 1988; Stollenwerk Grove, 1985). As the pH becomes lower, Cr(VI) species are removed from solution by adsorption onto positively charged sorption sites (Zachara et al., 1989). Chromium (VI) does not commonly form complexes with inorganic or organic ligands.

Chromium(III) predominates under more reducing conditions. The dominant Cr(III) species occurring in groundwater also depend on pH. Apparent stability constants (298 K, I=0.75) calculated for pertinent reactions revalent for chromium(III) speciations in seawater (Van and Reith, 1982) and the governing reactions are:

$Cr^{3+} + H_2O = CrOH^{2+} + H^+$	log K (25 °C)	–4.4	(5)
$Cr^{3+} + 2\ H_2O = Cr(OH)_2^+ + 2\ H^+$	log K (25 °C)	–10.6	(6)
$Cr^{3+} + 3\ H_2O = Cr(OH)_3^\circ + 3\ H^+$	log K (25 °C)	–19.2	(7)
$Cr^{3+} + 4\ H_2O = Cr(OH)_4^- + 4\ H^+$	log K (25 °C)	–28.2	(8)

$Cr(OH)_2^+$ is the dominant species in natural ground waters with a pH between 6–8. $CrOH^{2+}$ and Cr^{3+} predominate in more acidic environment. $Cr(OH)_3^\circ$ and

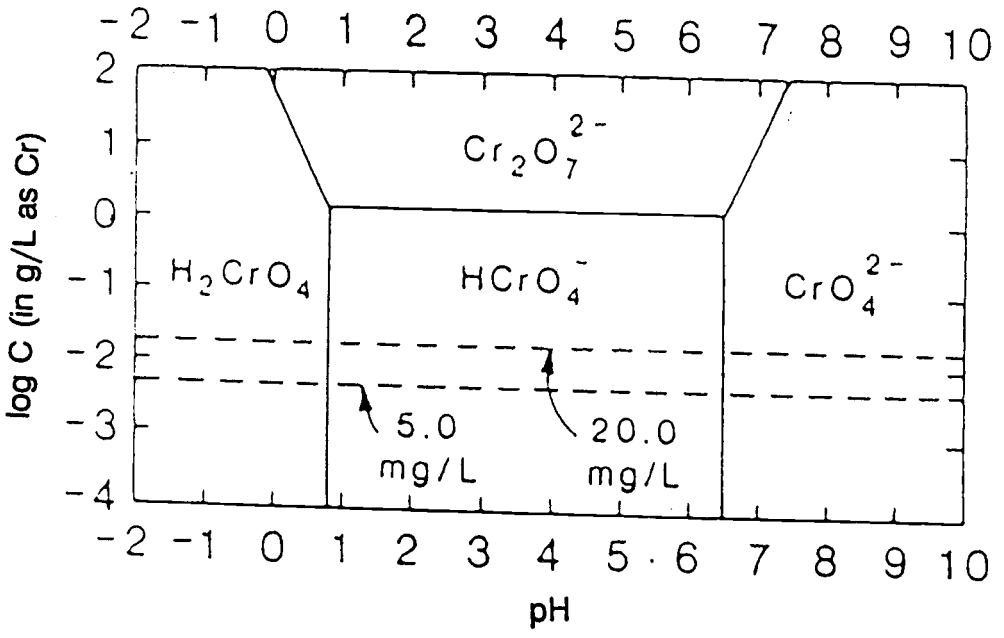

Figure 2: Predominance diagram showing the relative distribution of different Cr(VI) species in water as a function of pH and total Cr(VI) concentration (Sengupta and Clifford, 1986).

$Cr(OH)_4^-$ predominate in more alkaline environment (Figure 1). Cr(III) solubility is limited due to the formation of hydrous oxides, $Cr(OH)_3(s)$ and chromite $(Fe,Cr)(OH)_3(s)$, and the strong tendency to adsorb onto clays and other solid phases. Cr(III) can also form soluble organic complexes, particularly under acid conditions (Bartlett and Kimble, 1976a). However, Cr(III) could be converted to the more soluble Cr(VI) if the redox state changes from reducing to highly oxidizing. Cr(III) has been oxidized by manganese dioxide under natural conditions (Bartlett and James, 1979).

2.2 *Chromium chemistry in soils:* The literature indicates that chromium behavior in soil is complex, and depends on environment conditions such as pH, oxidation–reduction potential, and ionic composition of the groundwater. Chromite ($FeCr_2O_4$) is the major mineral form of chromium. Very little information is available concerning the chemical form of the element in the soils, but it is generally assumed to occur as the trivalent chromium oxide. Natural α–Al_2O_3 contains occasional Cr(III) ions in place of Al(III) ions. During weathering, chromium oxide in rocks tends to oxidize to soluble Cr(VI) anions. Cr(VI) is relatively stable and mobile in soils that are sandy or contain low organic matter concentration. In soils with high pH and lower organic matter content, Cr(VI) is readily mobilized by groundwater, but at lower pH and higher organic matter content Cr(VI) may adsorb or be reduced to Cr(III) and then adsorbed onto the soil.

Cr(VI) in soil is divided into two categories; *exchangeable*, which is the fraction of chromium easily removed from the soil, and *nonexchangeable*, which includes the fraction either very tightly adsorbed by the soil or precipitated on the soil (Hingston et al., 1967). Chemical and physical processes that control the rate of transport and mobility of chromium in soils include diffusion, adsorption–desorption, precipitation–dissolution, oxidation–reduction, and complexation.

2.3 *Chromium Adsorption and Desorption in Soils.* The adsorptive behavior of Cr(VI) by soils and subsurface minerals is not well understood. Most information on Cr(VI) adsorption comes from studies with pure mineral phase. Mineral phases with proton specific surface sites, particularly those with high pH of the point–of–zero–charge (pH_{pzc}), for example, iron and aluminum oxides [Fe_2O_3 (am), α–Al_2O_3], and clay minerals may adsorb Cr(VI) from pH 2 to 7 (Rai et al., 1984). As expected, the amount of adsorption generally increases with decreasing pH due to increasing positive surface charges on hydrous oxides and clays. Amorphous iron, with a pH_{pzc} = 8.5, is the adsorbate found at the highest concentrations in most aquifer materials. Cr(III) is adsorbed by clay minerals, which have low pH_{pzc} in the order of 2–2.5 (Stumm and Morgan, 1981). Cr(III) adsorption by soils and clays is high, with adsorption increasing with pH as the clay surface becomes negatively charged. Chromate adsorption on amorphous Fe oxide was reversible when the equilibrium pH was adjusted to higher values (Leckie et al., 1980). Reversible chromate adsorption was also observed in oxidic/kaolinitic soils (Zachara et al., 1989).

Competing oxyanions such as sulfate and phosphate decrease Cr(VI) adsorption in the soils by direct competition for Fe and Al hydrous oxides surface sites. Both sulfate (SO_4^{2-}) and phosphate ($H_2PO_4^-$) ions decrease Cr(VI) adsorption in the soils, with phosphate having a greater effect than sulfate. The effect of sulfate and phosphate was discussed by Stollenwerk and Grove, (1985). They found that SO_4^{2-}, $H_2PO_4^-$, and HPO_4^{2-} ions prevent adsorption of Cr(VI) by direct competition for hydroxy oxides surface sites. Anions such as sulfate and phosphate can also decrease adsorption of Cr(VI) by decreasing the electrostatic potential near the surface sites. One may consider the following specific and nonspecific surface competition reactions:

$$H_2PO_4^- + SHCrO_4 = SH_2PO_4 + HCrO_4^- \qquad (9)$$

$$H_2PO_4^- + SOH_2^+\text{–}CrO_4H^- = SOH_2^+\text{–}H_2PO_4^- + HCrO_4^- \qquad (10)$$

2.4 *Chromium(VI) Precipitation/Dissolution in Soils.* Both Cr(VI) and Cr(III) solid phases can play an important role in movement of chromium through soils. Existence of mineral phases can extend the time required to remove chromium from contaminated soils. The sodium, potassium, and magnesium salts of chromate are highly soluble. The calcium salt of chromate is moderately soluble. The solubility product (at 25 °C) of calcium chromate is 2.3×10^{-2}. Among the slightly soluble chromates are those of lead, silver, barium, mercury, and copper

(Cotton and Wilkinson, 1972). The solubility product (at 25°C) of slightly soluble chromates are: $PbCrO_4$, 1.8×10^{-14}; Ag_2CrO_4, 9.0×10^{-12}; $BaCrO_4$, 3.0×10^{-10} (Trotman–Dickenson, 1973). The solubility product of $BaCrO_4$ ($K_{sp} = \{Ba^{2+}\}\{CrO_4^{2-}\} = 3 \times 10^{-10}$) is low enough that Ba^{2+} might control the solubility of Cr(VI) in certain soils.

Cr(III) concentrations are limited by the formation of $Cr(OH)_3(s)$ at pH between 6 and 12 (Bartlett and Kimble 1976a). In some cases, chromium hydroxide solid solutions ($Cr(OH)_3^{\circ}$) may precipitate rather than pure $Cr(OH)_3$. If Fe(III) is present within the aquifer then an amorphous $Cr_{0.25}Fe_{0.75}(OH)_3$ solid solution will form (Eary and Rai, 1988). The solubility of the $Cr_{0.25}Fe_{0.75}(OH)_3$ decreases with decreasing fraction of Cr(III) (Figure 3).

2.5 *Chromium Oxidation and Reduction in Soils.* Oxidation–reduction processes play a major role in the mobility, transport, and fate of inorganic and organic chemical constituents in natural waters. Reduction of Cr(VI) to Cr(III) with subsequent adsorption or precipitation can be an important process for removing chromium from groundwater. Both oxidation of Cr(III) and reduction of Cr(VI) can be thermodynamically favorable in soils. The transformation of Cr(VI) to Cr(III) within soils is likely to occur in the presence of electron donors such as Fe(II) (James et al., 1983). The rate and amount of reduction of Cr(VI) in soils is difficult to predict. Reduction of Cr(VI) with organic compounds to insoluble Cr(III) forms has been studied by several workers. They found that at lower pH and higher organic matter conditions Cr(VI) was converted to Cr(III), which is insoluble

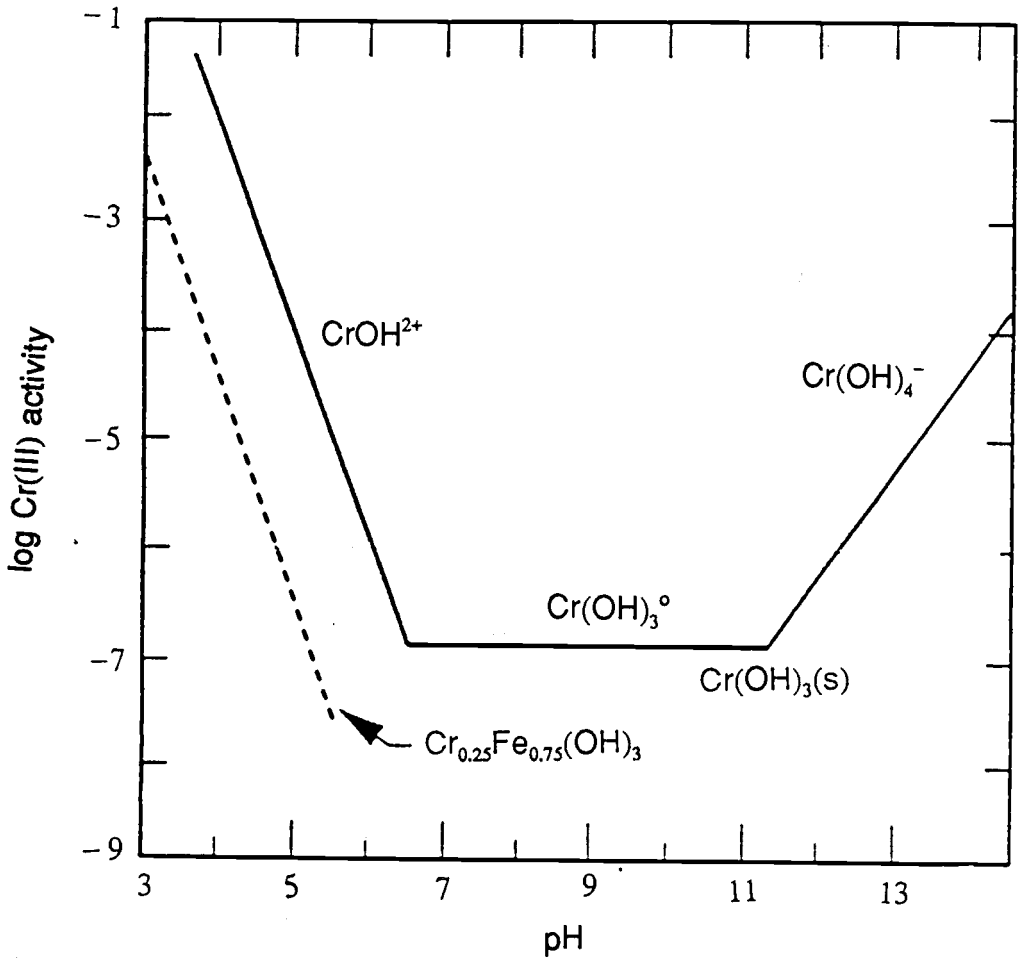

Figure 3: Solubility of $Cr(OH)_3$ and the solid solution $Fe_{.75}Cr_{.25}(OH)_3$ (am) as a function of pH (Eary and Rai, 1988).

and adsorbed to iron and aluminum oxide surfaces. Organic matter present in clays provides a sufficient source of electrons for reduction of Cr(VI) to Cr(III). Bartlett and Kimble (1976b), found no reduction of Cr(VI) in acidified organic–free samples. Only 2% of the Cr(VI) was lost in 48 hours by reduction in samples of the soil containing added cow manure when the pH was above 6, but when pH was lowered to 3, rapid reduction of all of the Cr(VI) resulted within 24 hours. The following equation was developed by Bartlett and Kimble (1976b) to explain the pH changes measured during reduction of Cr(VI):

$$\begin{aligned} &HOHC = R = CHOH + K_2Cr_2O_7 + 6\ HCl\ = \\ &KOOC - R - COOK + 2\ CrCl_3\ + 5H_2O \end{aligned} \qquad (11)$$

Another source of Cr(VI) reduction to Cr(III) is from Fe(II) in hematite and biotite. Past studies with pure mineral phases have shown that even the small amounts of Fe(II) contained in hematite and biotite can reduce aqueous Cr(VI) species to Cr(III), resulting in the precipitation of $(Fe,Cr)(OH)_3(am)$ (Eary and Rai, 1989). Reduction of chromate by the ferrous ions produced by dissolution of the ferrous iron components of hematite and biotite in acidic media is described by the reaction

$$3[FeO]_{biotite} + 9H^+ + HCrO_4^- = CrOH^{2+} + 3FeOH^{2+} + 3H_2O \qquad (12)$$

Bartlett and James (1979) and Eary and Rai (1987) found that the stable Cr(III) form in soil is oxidized to Cr(VI) by manganese dioxide, which serves as the electron acceptor in this reaction. The rate of Cr(III) oxidation by β–MnO_2 was found to increase with decreasing pH (Eary and Rai, 1987). Cr(III) concentration, pH, and the amount of initial available β–MnO_2 surface are the parameters controlling the degree of oxidation (Fendorf and Zasoki, 1992). The amount of Cr(III) oxidized to Cr(VI) was proportional to the manganese reduced. The following oxidation equation was proposed:

$$CrOH^{2+} + 1.5\ MnO_2(s) = HCrO_4^- + 1.5\ Mn^{2+} \qquad (13)$$

2.6 *Chromium(VI) Surface Complexation.* Surface complexation theory, which describes adsorption in terms of chemical reactions between surface functional groups and dissolved chemical species (Sposito, 1984), can be used to describe the adsorption phenomena of Cr(VI). Two types of surface complexes have been hypothesized: inner–sphere surface complexes and outer–sphere surface complexes. One may consider the following inner–sphere and outer–sphere surface complexation reactions of Cr(VI) with soil minerals:

Inner–sphere surface complexes or chemical binding mechanism,

$$SOH + H_s^+ + HCrO_4^- = SHCrO_4 + H_2O \qquad (14)$$

$$SOH + H_s^+ + CrO_4^{2-} = SCrO_4^- + H_2O \qquad (15)$$

Outer–sphere surface complexes or electrostatic binding mechanism,

$$SOH + H_s^+ + HCrO_4^- = SOH_2^+ - CrO_4H^- \quad (16)$$

$$SOH + H_s^+ + CrO_4^{2-} = SOH_2^+ - CrO_4^{2-} \quad (17)$$

where S is a metal cation associated with a solid surface, SOH is a surface hydroxyl group, and H_s^+ represents protons in the electrical double layer (EDL) and related to the bulk solution concentration by the Boltzmann distribution equation, e.g.,

$$[H^+_s] = [H^+_{aq}]\exp(-zF\psi/RT) \quad (18)$$

where the exponential term represents a coulombic activity correction due to difference in potential of the solution and surface, z is the charge of surface species, F is the Faraday constant, ψ is the surface potential (the difference in potential between the surface and the solution), R is the universal gas constant, and T is the absolute temperature.

2.7 *Triple Layer Model (TLM).* Because of the importance of ion adsorption on oxide surfaces, many adsorption models have been developed. The main difference between the various models lies in the assumed structure of surface complexes to be formed. The triple layer model (TLM) is shown schematically in Figure 4. In this model, there is a surface plane (o–layer), for adsorption of strongly bonding surface complexes, and a second adsorption plane for weakly

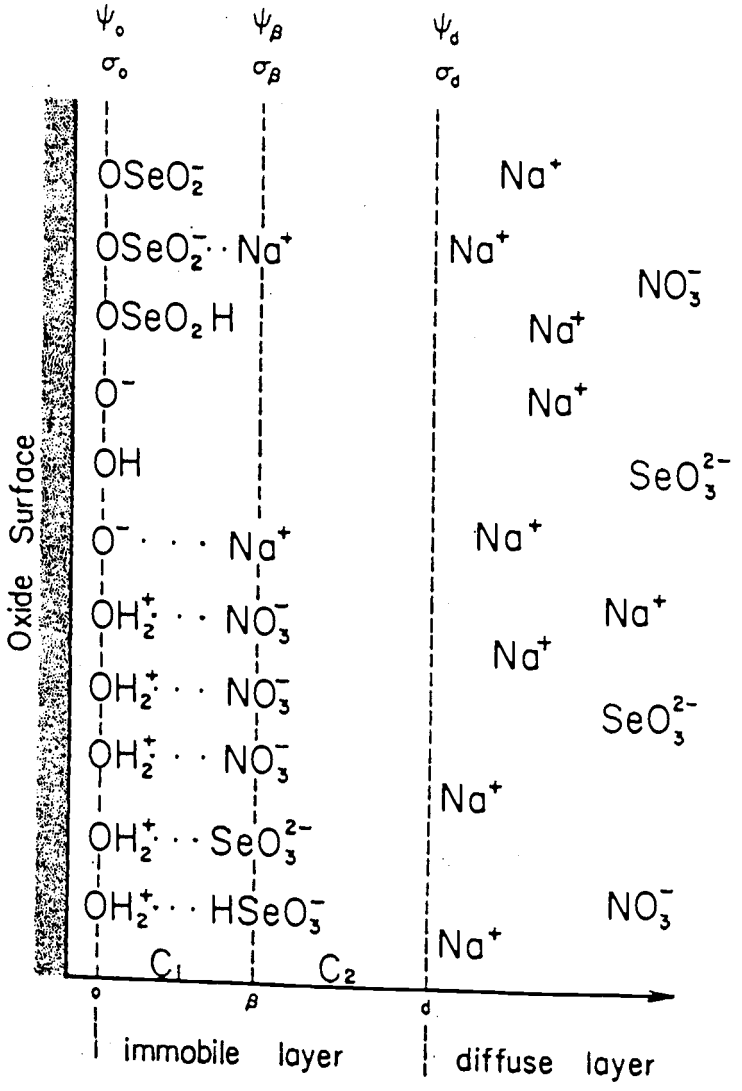

Figure 4: Schematic representation of TLM analogs of coordination (inner–sphere) and ion–pair (outre–sphere) surface complexes (Hayes, Papelis, and Leckie 1988).

bonded counterions (β–layer). The adsorbed ions can be located at both the o–layer or β–layer. Surface complexes formed at the o–layer are considered model analogs of inner–sphere complexes; those formed at the β–layer are considered outer–sphere analogs. It is possible to distinguish between inner–sphere and outer–sphere surface complexes (Hayes et al., 1988). The effect of ionic strength on the activity coefficient ratios is directly related to the o–plane potential or the β–plane potential or both and therefore depends on surface complexes. Since the outer–sphere surface reactions have a direct dependence on the β–plane potential, their activity coefficient ratios are more directly influenced by ionic–strength changes.

Chromate adsorption on hydrous oxides over ranges in pH, ionic strength, and competing ions has been well described using a Triple Layer Model (TLM) (Davis and Leckie, 1980; Zachara et al., 1987). The nature of the CrO_4^{2-} surface complexation reaction is not well known. The bichromate ion is calculated by the outer–sphere surface complexation model to be the preferred sorbate on pure oxide and kaolinite surfaces (Davis and Leckie, 1980). Two interesting applications of the TLM were recently made by Ainsworth et al. (1989) and Zachara et al. (1989) in studies of chromate adsorption by Al–substituted goethite and subsurface soil, where adsorption of chromate on mixed solid phases was modeled using outer–sphere surface species and two–site surface complexation reactions. However, application of the modeling approach to natural systems is considerably more difficult than when applied in simple mineral–water systems

(Zachara et al., 1989). In particular, there are severe difficulties associated with describing the reaction functional groups of soil and the electrical double layer properties of a mixture of mineral phases and their surface coatings.

3. MATERIALS AND METHODS

3.1 Materials

3.1.1 *Soil.* The soil used in the experiments was from the upper silts and aquitard layer and collected from an uncontaminated field at the United Chrome Products Superfund (UCPS) site, Corvallis, Oregon. The soil was taken from depths of 4.0–6.1, 8.0–10.3, 12.0–14.3, 16.0–18.3, and 18.6–20.9 ft in shelby tubes during drilling of a deep aquifer (DW–12) monitoring well. The soil was extruded from the shelby tubes and the outer portions were pared away with a stainless steel blade. Soil samples were air dried, ground and sieved to less than 200 mesh size, homogenized and placed in clean plastic bottles with tight lids. These samples were then stored at 4 °C until use. The mineral composition of these samples indicates that the major minerals present in the upper silts and aquitard layer are guartz, labradorite (an intermediate to calcic composition plagioclase) and clay minerals (CH2M–Hill, 1990). Physical and chemical soil characterization tests include: soil particle size analysis, surface area, pH of the point–of–zero–charge (pH_{pzc}), total organic carbon, and the concentration of anions and cations determinations are summarized in Table 1 and 2.

3.1.2 *Chemicals.* All reagents were of analytical–reagent grade and de–ionized water was used to prepare all solution. Fresh standards or reagent solutions were made up on each day analysis.

Table 1: Soil physical characterization experiments

Physical			Method
Clay	42	(%)	Hydrometer
Silt	52	(%)	Hydrometer
Sand	6	(%)	Hydrometer
Surface area	137	(m^2/g)	EGME*

EGME* = Ethylene Glycol Monoethyl Ether (Heilman et al., 1965)

Table 2: Soil chemical characterization experiments

Chemical			Method
pH	6.9		1:2, Soil:Water
pH_{pzc}	8.3		Soil Titration
Organic Content (TOC)	0.11	(%)	Carbon analyzer
Moisture Content	3.5	(%)	Oven at 105 °C
Soluble Manganese	10.7	(mg/L)	DTPA
Soluble Iron	454	(mg/L)	DTPA
Chromium (VI)	< 1	(mg/kg)	Phosphate Extraction
Total Chromium	31.3	(mg/kg)	Acid Digestion
Calcium	1603	(mg/kg)	Ammonium Acetate
Magnesium	145	(mg/kg)	Ammonium Acetate
Potassium	351	(mg/kg)	Ammonium Acetate
Phosphate	9.0	(mg/kg)	Ion Chromatography
Sulfate	14.2	(mg/kg)	Ion Chromatography
Nitrate	16.8	(mg/kg)	Ion Chromatography

All analyses and experiments were performed in duplicate or triplicate. Glass and plasticware were soaked in 10% nitric acid and rinsed well with glass distilled water prior to all uses.

3.2 Experimental Procedures

3.2.1 *Soil Titration.* A potentiometric titration of the soil suspensions in the presence of varying concentrations of background electrolyte solution was used to determine the pH of the point–of–zero–charge (pH_{pzc}). The soil suspensions were prepared in a jacketed 1000–ml reactor flask with 12.5 grams soil and 500 ml of 0.01, 0.1, and 1.0 M NaCl as background electrolyte solution. Suspensions were mixed to equilibrated under N_2 atmosphere. Mixing of the suspensions were provided by a Teflon–covered magnetic stirrer. The temperature was kept constant (at 25 °C) with a recirculating water bath. Various volumes of 1.0 or 0.1 M NaOH and HCl were added to adjust the pH. A Radiometer PHM 64 pH meter with Methrohm 665 Dosimat titrator, all interfaced to a personal computer (Beta PC–AT), were used for pH control.

3.2.2 *Determination of Soil Specific Surface Area.* Specific surface areas were determined by the ethylene glycol monoethly ether (EGME) technique of Heilman et al. (1965). Briefly, approximately 1 gram of the soil samples were dried to constant weight over P_2O_5 in an evacuated desiccator. Samples were treated with 3 milliliter EGME to form a soil–EGME slurry that was placed in a desiccator over $CaCl_2$ and allowed to equilibrate 30 minutes. The desiccator is then evacuated for 45 minutes. After about 24 hours, the samples were weighed. The following equation was used to calculate the specific surface area of the soil samples:

$$A = W_a/(W_s \times 0.000286) \qquad (19)$$

where A is the specific surface area in m^2/g, W_a is the weight of ethylene glycol monoethly ether (EGME) retained by the sample in grams, W_s is the weight of P_2O_5–dried sample in grams, and 0.000286 is the weight of EGME required to form a monomolecular layer on a square meter of surface.

3.2.3 *Determination of Inorganic Carbon (Carbonates).* Total inorganic carbon contents (TIC) of soil were determined by partial digestion of soil with concentrated hydrochloric acid as described by Bund and Bremner (1972). Briefly, the soil samples were treated with 2 M HCl at room temperature for 16–24 hours in a stoppered bottle containing 2 M KOH in a small beaker. The CO_2 released from decomposion of carbonates was adsorbed in 2 M KOH. Then KOH solution titrated with standard 0.1 M HCl from the phenolphthalein end–point (pH = 8.3) to the bromocresol green end–point (pH = 4.3). The following equation was used to calculate milligram of inorganic carbon in the soil samples:

$$N \times (S - C) \times 1.2 \qquad (20)$$

where N is the normality of standard HCl, S is the milliliter of standard 0.1 N HCl required to titrate from the phenolphthalein end–point to the bromocresol green end–point, and C is the milliliter of standard 0.1 M HCl required for this titration in a control analysis performed exactly as described for the sample analysis but with no soil sample added to the bottle.

3.2.4 *Determination of Organic Carbon Content.* Total organic carbon was measured by a DC–80 Dohrmann Carbon Analyzer. The analyzer was calibrated with 2000 mg/L standard carbon solution. The procedure used to analyze the soil samples was exactly as described in the Instruction Manual for the Dohrmann Carbon Analyzer. Briefly, about 50 mg soil was placed into a platinum boat and manually transferred into the furnace where all carbonaceous matter was oxidized to CO_2. The carbon dioxide was swept by the continuous oxygen flow to the infrared detector. The detector signal was integrated and displayed the analysis results in mg/L C concentration units.

3.2.5 *Determination of Soil Reduction Capacity.* The reduction capacities of the soil were measured by the acid dichromate reduction method (Barcelona and Holm, 1991). Approximately 0.5 gram dry soil was placed in each of the reaction tubes. Then 5 milliliters of cold concentrated sulfuric acid and dichromate reagent was added and allowed to react at room temperature for 15 minutes or until CO_2 evolution ceased. The tubes were then sealed and heated to 150 °C for 3 hours. After being cooled, the tubes were centrifuged and the unreacted Cr(VI) was determined colorimetrically (600 nm). Potassium hydrogen phthalate (KHP) standards of 100, 200, 300, 400, and 500 μg O_2 equivalent/ml were used to generate the standard curve. Concentrations of the soil samples were calculated from the standard curve by linear regression. The reduction capacity of soil was calculated according to

$$\text{reduction capacity} = \{Fe(II)\} + TOC/3 \qquad (21)$$

3.2.6 *Determination of Fe(III) and Fe(II) in the Soil.* The ferrous and total iron contents were determined according to the method of Begheijn (1979). Briefly, about 0.2 gram dry soil was placed into a platinum crucible (100 ml capacity). Added 2.0 ml sulfuric acid and homogenized. Then 6.0 ml of hydrofluoric acid was added and swirled gently for 10 seconds to allow temperature to rise to 60–67 °C. Transferred quickly into a silica beaker that contained 20 ml of boric acid solution and 2 ml of concentrated hydrochloric acid and boiled gently for 2 minute. Transferred into 200 ml polypropylene calibrated flask, which contained another 80 ml of boric acid solution. Fe(II) was determined by adding 2.0 ml of filtrate into 50–ml flask, 10 ml of potassium hydrogen phthalate buffer solution, and 4.0 ml of 1,10–phenanthroline solution and reading absorbance at 510 nm by spectrophotometer. Total iron was determined by adding 20 mg of hyroquinone to the remainder of the solution (about 40 ml) and reading absorbance at 510 nm after 10 to 30 minute.

3.2.7 *Batch Experiments.* Batch experiments were conducted in completely–mixed reactors in a temperature–controlled chamber. Adsorption and desorption experiments were run to determine kinetics and equilibrium sorption and desorption parameters of Cr(VI) on a natural soil. All batch experiments were conducted under oxic conditions.

3.2.7.1 *Adsorption Kinetics.* Short–term and long–term kinetics experiments were used to determine the time required for Cr(VI) to approach equilibrium during sorption and desorption. For short–term and long–term adsorption kinetics,

identical reactor tubes were left on the shaker bath at varying pH values and for various times, ranging from 1 to 24 hours and 1 to 120 hours, respectively. Adsorption experiments were conducted in 250 milliliter, screw–top plastic centrifuge tubes. The soil (4 grams) was reacted with 100 milliliter solution. Hexavalent chromium was added to yield concentrations ranging between 1×10^{-4} and 5×10^{-4} M. The pH was adjusted by adding various volumes of 1.0 M HCl or NaOH. The soil suspensions were mixed by continuous shaking in a 20 °C constant–temperature shaker bath. After mixing for the desired reaction time, the suspensions were centrifuged at 10,000 rpm for 10 minutes and the supernatant solutions were passed through 0.45 μm Millipore filters. Chromium concentration in the supernatant solutions was determined by ion chromatography (IC) and adsorbed chromium was determined by difference from initial and final solution concentrations. The pH of each sample was also determined.

3.2.7.2 *Adsorption Isotherms.* Adsorption isotherms were also determined in completely–mixed batch reactors in a temperature–controlled chamber. The soil suspensions were prepared with 4 grams soil and 100–ml of 0.01 M NaCl background electrolyte solution. Cr(VI) was added to yield ten concentrations ranging between 3×10^{-5} M and 5×10^{-4} M and equilibrated at 20°C constant–temperature. After 120 hours equilibration time, suspensions were centrifuged and dissolved chromium and pH were determined as described in the adsorption kinetic experiments. The effects of varying pH values and supporting electrolyte concentrations were also determined on Cr(VI) equilibrium isotherms.

3.2.8 *Extraction of Total Chromium(VI) from the Soil.* The soil suspensions were first equilibrated with Cr(VI), and the solution and soil were separated by centrifugation. Then varying quantities of NaOH (1.0 M) or phosphate (2.0 M NaOH and 0.5 M KH_2PO_4 at a 1:4 (V/V) ratio, pH = 8.0) were added to the soil, and after 24 hours reaction time, the solution and soil were separated by centrifugation. This method was based on laboratory studies reported in the literature on Cr(VI) adsorption (Stollenwerk and Grove, 1985; Zachara, et al., 1987). Extracted (desorbed) Cr(VI) was determined as described in the adsorption isotherm experiments. The Cr(VI) removed by this reversible reaction is defined as the adsorbed fraction. This method was found to be effective in desorbing Cr(VI) in experiments where reduction of Cr(VI) to Cr(III) occurred. This procedure was used in all adsorption kinetic and isotherm experiments to differentiate between adsorbed and reduced chromium.

3.2.9 *Effects of the Competing Oxyanions on Cr(VI) Adsorption.* Addition of oxyanions to the soil solution influenced Cr(VI) sorption on the soil by the competition of Cr(VI) and oxyanions for available surface sites. The effects of competing oxyanions such as phosphate (PO_4^{3-}), sulfate (SO_4^{2-}), bicarbonate (HCO_3^-), and nitrate (NO_3^-) on Cr(VI) sorption were examined in equilibrium isotherm experiments. The soil suspensions were prepared with the same method as described in adsorption isotherms, but instead of NaCl background electrolyte solution, 0.01 M sulfate, 0.01 M bicarbonate, or 0.01 M phosphate solutions were used. After 120 hours reaction time, suspensions were centrifuged and chromium concentration was determined by ion chromatography.

3.2.10 *Soil Column Experiments.* Soil column experiments were conducted to more closely simulate field conditions of continuous hydraulic flow through a stationary porous medium. The 25.5 cm long by 2.5 cm inside diameter columns were packed with about 165 grams soil to a porosity of 50% (approximate field porosity). The column was packed by adding about 2 cm layers of soil and gently tamping with a glass rod. The soil was saturated by capillary action from the bottom–up to ensure that no air pockets formed within the soil column. A four liter constant head (approximately 5 meters) reservoir and needle valves controlled hydraulic flow (5 ml/hr) through soil columns to approximate field conditions. The column influents were sparged with N_2 (gas) and a CO_2 trap containing 2 M KOH was used to remove background carbonate species. Column effluent samples were taken by a 250–ml plastic bottle at the outlet of the column and the exact volume was determined. Temperature, pH, flow rate, and conductivity were also measured at the time of sample collection. The following equations were used to calculate physical characteristics of soil columns:

$$\rho_b = M_s/V_t \tag{22}$$

where ρ_b = soil bulk density (g/cm^3)

M_s = soil mass (g)

V_t = column volume (cm^3)

$$\eta = 1 - \rho_b/\rho_s \tag{23}$$

where η = porosity

ρ_s = particle density

In addition:

$$V_p = \eta V_t \tag{24}$$

where V_p = pore volume (cm^3)

The experimental parameters for column experiment # 3 are summarized in Table 3.

Table 3: Description of soil column #3 experiment

Column Length, L		25.5	(cm)
Column Diameter, D		2.5	(cm)
Column Volume, V_t		125.1	(cm^3)
Pore Volume, V_p		63.6	(cm^3)
Mass of Soil, M_s		163.1	(g)
Porosity, η		51	(%)
Particle Density, ρ_s		2.65	(g/cm^3)
Influent Cr(VI) Conc., C_o		10.0	(mg/L)
Background Electrolyte,	NaCl	0.01	(M)
Desorption with H2PO4–		0.01	(M)

The experimental parameters for column experiments (#1, 2, 4, 5, 6, 7, 8) are also summarized in Tables 15–21 in Appendix 2.

3.2.11 *Determination of Reduced Cr(VI) in the Soil.* Sequential extractions were performed on subsamples from the soil columns after the desorption phase to determine Cr(III) solid phases. Distilled water was used to extract some readily desorbed chromate. Following the water extraction, a phosphate extraction was conducted to remove adsorbed chromate (Bartlett and James, 1988). Both amorphous and crystalline forms of Cr(III) and Fe(III) were extracted by ammonium oxalate and dithionite–citrate–bicarbonate (DCB), respectively. The

ammonium oxalate extraction method (McKeague and Day, 1966) was used to remove amorphous hydroxide of Cr and Fe. The general procedure used for the oxalate extraction was as follows:

1. Ten milliliters of 0.2 M acidified ammonium oxalate (pH = 3) were added to the sample (250 milligrams) in a 25 milliliters tube which was stoppered tightly.
2. The tubes were mixed by continuous shaking in a 20 °C constant–temperature shaker bath.
3. An aliquot of the extract (filtered) was digested with HNO_3 and H_2SO_4, and Cr and Fe were determined by atomic absorption spectrophotometry.

Crystalline and amorphous Fe–containing oxides were extracted with dithionite–citrate–bicarbonate (Mehra and Jackson, 1960). The test consists of adding 40 milliliters of 0.3 M Na–citrate solution and 5 milliliters of 1 M $NaHCO_3$ solution to 4 grams soil in a 250 milliliters Erlenmeyer flask. The temperature is brought to 80 °C in a water bath, then 1 gram of solid $Na_2S_2O_4$ is added and the mixture is stirred constantly for 1 minute and then occasionally for a total of 15 minutes. At the end of the 15 minutes digestion period, 10 milliliters of saturated NaCl solution is added to the tube to promote flocculation. The suspension is then mixed and centrifuged for 5 minutes. The supernatant is decanted into a 500 milliliters volumetric flask for Cr(III) and Fe(III) determinations. Finally 1 M HCl was used to extract residual chromium soil phases.

3.3 Analytical Methods

3.3.1 *Chromium(VI) Analysis.* Chromium(VI) concentrations in solution were determined by anion chromatography using a DIONEX Series 2000i ion chromatograph (IC) equipped with UV–VIS detector. The columns used in the IC are HPIC–CG5 cation guard column and HPIC–CS5 cation separator column. The eluent solution is a 2.0 mM pyridinediycarboxylic acid (PDCA), 2.0 mM disodium hydrogen phosphate, 10.0 mM sodium iodide, 50.0 mM ammonium acetate, and 2.8 mM lithium hydroxide at flow rate of 1.0 ml/min. Post column reagent is a 0.49 g/L 1,5–diphenyl carbazide and 25 milliliters sulfuric acid. Detection limit for Cr(VI) was determined to be 10 ppb. Total chromium in solution was determined by flame atomic absorption spectroscopy using Perkin Elmer Model 360 AAS. Detection limit was determined to be 0.05 mg/L. Chromium concentrations in samples analyzed by both methods were equal within analytical error, indicating that all of the dissolved chromium was present as Cr(VI). Trivalent chromium, Cr(III), concentrations were calculated by difference, subtracting the Cr(VI) from total chromium concentrations.

3.3.2 *Phosphate and Sulfate Determinations.* Phosphate and sulfate concentrations were determined by anion chromatography using a DIONEX series 4000i ion chromatography (IC) equipped with a conductivity detector. The column used in the IC were a HPIC–AG4A guard column and a HPIC–AS4A separator column. The eluent solution injected was a 1.8 mM Na_2CO_3 + 1.7 mM

$NaHCO_3$ at a flow rate of 2.0 ml/min. 25 mN H_2SO_4 solution were injected into the column as regenerant. Phosphate standards of 5, 8, 10, 15 mg/l (as HPO_4^-) and sulfate standards of 10, 20, 30, and 50 mg/l (as SO_4^{2-}) were used to generate standard curves. Detection limit for phosphate and sulfate was 50 and 10 ppb respectively.

3.3.3 *Total Fe Determination.* Iron concentration in solutions was determined by flame atomic absorption spectroscopy as described for total chromium. The detection limits was determined to be 0.01 mg/L.

3.3.4 *pH Determination.* The pH values were determined with an Orion research grade Ag/Ag/Cl glass combination electrode. Calibration were performed with appropriate pH buffer solutions.

3.3.5 *Conductivity Determination.* The conductivity of the samples were measured on the Lab–Line Lectro Mho–meter, model MC–1 Mark IV utilizing a cell constant = 0.1. Measurements were made at 25 °C. The ionic strengths were calculated by the following formula (Snoeyink and Jenkins, 1980).

$$\mu = C \times 1.6 \times 10^{-5} \qquad (25)$$

where C is specific conductance (μmho/cm) and μ is ionic strength (M).

4. MODELING OF ADSORPTION DATA

4.1 *Langmuir Model.* The equilibrium model was expressed as an adsorption isotherm and fitted to either the Langmiur or the Freunlich equations. Adsorption isotherms of Cr(VI) indicated that the Langmuir equation is the best fit to the experimental data. Two Cr(VI) sorption parameters, the maximum sorption capacity and the Langmuir adsorption constant, were determined in 120 hours batch isotherm experiments. The Langmuir equation was also used to determine the intrinsic equilibrium constants of adsorption reactions.

In this study, Langmuir adsorption isotherms at constant pH were represented by,

$$\Gamma = \Gamma_M[CrO_4^{2-}]/(K_L + [CrO_4^{2-}]) \qquad (26)$$

where Γ is the amount of the ion adsorbed per unit weight of adsorbent, Γ_M is the maximum adsorption at the particular pH, K_L is the Langmuir adsorption constant, and $[CrO_4^{2-}]$ is the equilibrium solution concentration of chromate. This model does not explicitly include the effect of the electrical potential (ψ) and electrolyte concentration on adsorption.

The Cr(VI) adsorption reaction, assuming formation of outer–sphere surface complexes and pH less than 6.5, can be written as:

$$SOH + 2H^+ + CrO_4^{2-} = SOH_2^+\text{–}CrO_4H^- \qquad (27)$$

where SOH represents the surface oxide functional group, SOH_2^+ is the protonated surface, and SOH_2^+–CrO_4H^- is the surface complex for bichromate. The corresponding equilibrium constant for surface complexation, called the "intrinsic" adsorption constant, is:

$$K^{int}_{SOH_2^+-CrO_4H^-} = [SOH_2^+-CrO_4H^-]\ \exp(2F(\psi_o-\psi_\beta)/RT)/[SOH][H^+]^2[CrO_4^{2-}] \qquad (28)$$

where terms in brackets are the concentrations of species at equilibrium, the exponential terms represent coulombic activity correction due to differences in potentials of the solutions and the double–layer planes, F is the Faraday constant, R is the universal gas constant, T is absolute temperature, ψ is the surface potential (the difference in potential between the surface and the solution), and the subscript o and β indicate the o and β counterion layers, respectively.

In the case of low adsorption density, using similar assumptions as those of Davies–Colley et al. (1982), we can write:

$$S_T = k\{S_T\} \simeq [SOH] \qquad (29)$$

where $S_T = [SOH] + [SOH_2^+-CrO_4H^-]$ and k is a constant (the moles of surface sites per unit mass (or unit area) of surface) and { } denotes mass (or areal) concentration of the adsorbent;

For the adsorption density:

$$\Gamma = [SOH_2^+-CrO_4H^-]/[SOH] \tag{30}$$

Substituting Eq. (30) into Eq. (28)

$$K^{int}_{SOH2^+-CrO4H^-} = (\Gamma)\exp(2F(\psi_o-\psi_\beta)/RT)/[H^+]^2[CrO_4^{2-}] \tag{31}$$

Substituting Γ from Langmuir equation (Eq. (26)) and rearranging:

$$K^{int}_{SOH2^+-CrO4H^-} = (\Gamma_M)\exp(2F(\psi_o-\psi_\beta)/RT)/[H^+]^2(K_L + [CrO_4^{2-}]) \tag{32}$$

ψ_o is related to pH by the Nernst equation (Stumm and Morgan, 1970):

$$\psi_o = 2.3\ RT(pH_{pzc} - pH)/F \tag{33}$$

where pH_{pzc} is the pH of the point–of–zero–charge and F is the Faraday constant.

Substituting ψ_o in Eq. (32) and rearranging:

$$K^{int}_{SOH2^+-CrO4H^-} = (\Gamma_M)\exp(2F(2.3RT(pH_{pzc}-pH)/F-\psi_\beta)/RT)/[H^+]^2(K_L + [CrO_4^{2-}]) \tag{34}$$

Under the condition of low adsorption density, e.g., dilute solutions, ψ_β=0, and Eq. (34) becames

$$K^{int}_{SOH2^+-CrO4H^-} = (\Gamma_M)\exp(2.3(2pH_{pzc}-2pH)/[H^+]^2(K_L + [CrO_4^{2-}]) \quad (35)$$

and in negative logarithmic form,

$$pK^{int}_{SOH2^+-CrO4H^-} = p\Gamma_M - 2pH_{pzc} + \log(K_L + [CrO_4^{2-}]) \quad (36)$$

In addition, $[CrO_4^{2-}]$ can be represented by:

$$[CrO_4^{2-}] = C_{TCr}/(1 + K_{a2}[H^+]) \quad (37)$$

Substituting $[CrO_4^{2-}]$ as a function of C_{Tcr} and pH from Eq. (37) and rearranging:

$$pK^{int}_{SOH2^+-CrO4H^-} = p\Gamma_M - 2pH_{pzc} + \log(K_L + C_{TCr}/(1 + K_{a2}[H^+]) \quad (38)$$

For Cr(VI) adsorption assuming formation of outer–sphere surface complexes, and assuming pH is above 6.5, then, the reaction can be written as

$$SOH + H^+ + CrO_4^{2-} = SOH_2^+-CrO_4^{2-} \quad (39)$$

$$K^{int}_{SOH_2^+-CrO_4^{2-}} = [SOH_2^+-CrO_4^{2-}]\exp(F(\psi_o-2\psi_\beta)/RT)/[SOH][H^+][CrO_4^{2-}] \quad (40)$$

Using similar assumptions as for pH < 6.5, we can write:

$$pK^{int}_{SOH_2^+-CrO_4^{2-}} = p\Gamma_M - pH_{pzc} + \log(K_L + [CrO_4^{2-}]) \quad (41)$$

Substituting $[CrO_4^{2-}]$ as a function of C_{Tcr} and pH from Eq. (37), we can write:

$$pK^{int}_{SOH_2^+-CrO_4^{2-}} = p\Gamma_M - pH_{pzc} + \log(K_L + C_{Tcr}/(1 + K_{a2}[H^+]) \quad (42)$$

Thus it is shown that the intrinsic equilibrium constant is related to the Langmuir adsorption constant (K_L) in dilute solutions by including terms for maximum site adsorption density (Γ_M), pH of the point–of–zero–charge, dissociation constant of $HCrO_4^-$ (K_{a2}), and total chromate concentration.

4.2 Triple Layer Model

4.2.1 *Modeling Approach.* An alternative to the empirical modeling approaches are the surface complexation models (SCM), which treat surface functional groups as analogs of complexing ligands in solution (Sposito, 1984). Use of the triple layer model (TLM) to represent the adsorption of dilute cations and anions by hydrous oxides was first reported by Davis and Leckie (1978a, 1980). The molecular hypotheses of the TLM model as implemented by Davis et al. (1978) are as follows:

There are three planes in the interfacial region:

1. A surface plane for adsorption of H^+, OH^-, and strongly adsorbed ions.
2. A near–surface plane (the β–plane) for weakly adsorbed ions.
3. A diffused layer plane, representing the closest distance of approach of dissociated charge.

4.2.2 *Triple Layer Model Reactions.* The TLM reactions for adsorption of chromate on Fe oxide including surface protonation and deprotonation, electrolyte reactions, and outer–sphere surface complexation reactions are written as:

Surface protonation and deprotonation

$$FeOH_2^+ = FeOH + H^+ \tag{43}$$

$$FeOH = FeO^- + H^+ \tag{44}$$

where FeOH represents the iron oxide surface functional group, $FeOH_2^+$ is the protonated iron oxide surface, and FeO^- is the deprotonated iron oxide surface, analogous to the nonspecific SOH oxide surface.

Electrolyte reactions

$$FeOH + Na^+ = (FeO^- - Na^+)^o + H^+ \tag{45}$$

$$FeOH + Cl^- + H^+ = (FeOH_2^+ - Cl^-)^o \tag{46}$$

Chromate outer–sphere adsorption

$$FeOH + CrO_4^{2-} + H^+ = FeOH_2^+ - CrO_4^{2-} \tag{47}$$

$$FeOH + CrO_4^{2-} + 2\ H^+ = FeOH_2^+ - HCrO_4^- \tag{48}$$

Surface complexation reactions for competing oxyanion, SO_4^{2-}

$$FeOH + SO_4^{2-} + H^+ = FeOH_2^+ - SO_4^{2-} \tag{49}$$

$$FeOH + SO_4^{2-} + 2\ H^+ = FeOH_2^+ - HSO_4^- \tag{50}$$

The mass law equation for reaction (43) is written as:

$$K_{a1}^{int} = \frac{[FeOH][H^+]}{[FeOH_2^+]} \quad \frac{\gamma^s_{FeOH}\ \gamma_{H^+}}{\gamma^s_{FeOH2^+}} \tag{51}$$

where γ_i^s and γ_i are the activity coefficients of surface and solution species, respectively. In the TLM as used by Davis et al. (1978), the following chemical potential is defined for both solution and surface species i:

$$\mu_i = \mu_i^o + RT \ln[i] + zF\psi \tag{52}$$

where μ_i and μ_i^o are the electrochemical and standard electrochemical potential, respectively; $zF\psi$ represents the free energy required to bring a species with charge z from the reference state potential to the given potential ψ.

Applying Eq. (52) to each species in Eq. (43), e.g.,

$$\mu_{FeOH_2^+} = \mu^o_{FeOH_2^+} + RT \ln[FeOH_2^+] + F\psi_{FeOH_2^+} \tag{53}$$

$$\mu_{FeOH} = \mu^o_{FeOH} + RT \ln[FeOH] + 0F\psi_{FeOH} \tag{54}$$

$$\mu_{H^+} = \mu^{o+}_H + RT \ln[H^+] + F\psi_{H^+} \tag{55}$$

gives

$$\Delta\mu = \Delta\mu^o + RT \ln \left[\frac{[FeOH][H^+]}{[FeOH_2^+]} \right] + F(\psi_{H^+} - \psi_{FeOH_2^+}) \tag{56}$$

where

$$\Delta\mu = \Delta\mu^{o} + \mu_{H^+} - \mu_{FeOH_2^+} \tag{57}$$

$$\Delta\mu^{o} = \mu^{o}_{FeOH} + \mu^{o+}_{H} - \mu^{o}_{FeOH_2^+} \tag{58}$$

at equilibrium ($\Delta\mu = 0$)

$$\exp\left(\frac{-\Delta\mu^{o}}{RT}\right) = \frac{[FeOH][H^+]}{[FeOH_2^+]} \exp((\psi_{H^+} - \psi_{FeOH_2^+})F/RT) \tag{59}$$

or

$$K^{int}_{a1} = \frac{[FeOH][H^+]}{[FeOH_2^+]} \exp((\psi_{H^+} - \psi_{FeOH_2^+})F/RT) \tag{60}$$

Equating the difference in the potential of the surface species $\psi_{FeOH_2^+}$ and bulk potential ψ_{H^+} with the TLM potential ψ_o (the difference in potential between the surface and the solution) gives the model reaction:

$$K^{int}_{a1} = \frac{[FeOH][H^+]}{[FeOH_2^+]} \exp(-F\psi_o/RT) \tag{61}$$

Comparison of Eq. (51) with (61) shows that:

$$\frac{\gamma^{s}_{FeOH}\,\gamma_{H^+}}{\gamma^{s}_{FeOH_2^+}} = \exp(-F\psi_o/RT) \tag{62}$$

Typically, the ratio of the surface activity coefficients (γ^s) is taken to be unity (Brownawell et al., 1990). Thus:

$$\gamma_H^+ = \exp(-F\psi_o/RT) \tag{63}$$

Thus, it is shown that the exponential term, the difference in the electrostatic potential of solution and the o–plane, is related to the activity coefficient. The TLM makes use of concepts of the electrical double layer to provide estimates of the activity coefficients. Although the mass action equations are written in terms of activities, the TLM uses concentrations and modifies the thermodynamic stability constants for nonideal solutions (Davis et al., 1978).

The mass action expressions can be written in terms of bulk concentrations and electrostatic potentials at the o– and β–planes by the Boltzmann distribution law, e.g.,

$$[H^+_s] = [H^+_{aq}] \exp(-F\psi_o/RT) \tag{64}$$

$$[CrO_4^{2-}{}_s] = [CrO_4^{2-}{}_{aq}] \exp(2F\psi_\beta/RT) \tag{65}$$

where $[CrO_4^{2-}{}_s]$ represents the surface species concentration in the electrical double layer (EDL), $[CrO_4^{2-}{}_{aq}]$ represents the bulk solution concentration, the exponential terms represent coulombic activity correction due to difference in

potential of the solution and TLM planes, z is the charge of surface species, ψ is the surface potential (the difference in potential between the surface and the solution), and F, R, and T have their usual meanings.

Using similar approach for the mass action equation for Eq. (47), we can write:

$$K^{int}_{FeOH2^+-CrO4^{2-}} = \frac{[FeOH_2^+ - CrO_4^{2-}]}{[FeOH][CrO_4^{2-}][H^+]} \frac{\gamma^s_{[FeOH2^+-CrO4^{2-}]}}{\gamma^s_{[FeOH]}\,\gamma_{[CrO4^{2-}]}\,\gamma_{[H^+]}} \qquad (66)$$

where γ_i and γ^s are the solution and surface activity coefficients, respectively.

Substituting for $[CrO_{4\,s}^{2-}]$ and $[H^+_s]$ from Eq. 64 and 65 into Eq. (66)

$$[FeOH][CrO_{4\,aq}^{2-}]\exp(2F\psi_\beta/RT)\,[H^+_{aq}]\exp(-F\psi_o/RT)\,K^{int}_{FeOH2^+-CrO4^{2-}} = [FeOH_2^+ - CrO_4^{2-}] \qquad (67)$$

or

$$[FeOH][CrO_4^{2-}][H^+]\,\exp(F(2\psi_\beta - \psi_o)/RT)\,K^{int}_{FeOH2^+-CrO4^{2-}} = [FeOH_2^+ - CrO_4^{2-}] \qquad (68)$$

and the intrinsic adsorption constant, can be calculated as follows:

$$K^{int}_{FeOH2^+-CrO4^{2-}} = \frac{[FeOH_2^+ - CrO_4^{2-}]}{[FeOH][CrO_4^{2-}][H^+]}\,\exp(F(\psi_o - 2\psi_\beta)/RT \qquad (69)$$

4.2.3 *Triple Laye Model Equilibrium Constants.* The intrinsic equilibrium constants for the TLM reactions including surface protolysis, electrolyte binding, and surface complexation reactions are represented in equations 70–77, which correspond to reactions 43–50, respectively:

$$K_{a1}^{int} = \frac{[FeOH]\,[H^+]}{[FeOH_2^+]} \exp(-F\psi_o/RT) \tag{70}$$

$$K_{a2}^{int} = \frac{[FeO^-]\,[H^+]}{[FeOH]} \exp(F\psi_o/RT) \tag{71}$$

$$K_{FeO^-\text{-}Na^+}^{int} = \frac{[FeO^-\text{–}Na^+]\,[H^+]}{[FeOH]\,[Na^+]} \exp(F(\psi_\beta - \psi_o)/RT) \tag{72}$$

$$K_{FeOH2^+\text{-}Cl^-}^{int} = \frac{[(FeOH_2^+ - Cl^-]}{[FeOH]\,[Cl^-]\,[H^+]} \exp(F(\psi_o - \psi_\beta)/RT) \tag{73}$$

$$K_{FeOH2^+\text{-}CrO4^{2-}}^{int} = \frac{[FeOH_2^+ - CrO_4^{2-}]}{[FeOH]\,[CrO_4^{2-}]\,[H^+]} \exp(F(\psi_o - 2\psi_\beta)/RT) \tag{74}$$

$$K_{FeOH2^+\text{-}HCrO4^-}^{int} = \frac{[FeOH_2^+ - HCrO_4^-]}{[FeOH]\,[CrO_4^{2-}]\,[H^+]^2} \exp(F(\psi_o - \psi_\beta)/RT) \tag{75}$$

$$K^{int}_{FeOH_2^+-SO_4^{2-}} = \frac{[FeOH_2^+ - SO_4^{2-}]}{[FeOH]\,[SO_4^{2-}]\,[H^+]} \exp(F(\psi_o - 2\psi_\beta)/RT) \qquad (76)$$

$$K^{int}_{FeOH_2^+-HSO_4^-} = \frac{[FeOH_2^+ - HSO_4^-]}{[FeOH]\,[SO_4^{2-}]\,[H^+]^2} \exp(F(\psi_o - \psi_\beta)/RT) \qquad (77)$$

A complete description of the relationships among the mass–action equations, charge, and potential has been given by Davis et al., 1987. Surface charge density (σ_o) on hydrous oxides is defined by the net uptake of protons by the surface and is determined by potentiometric titration, e.g.,

$$\sigma_o = F(\Gamma_H^+ - \Gamma_{OH}^-) \qquad (78)$$

$$\sigma_o = F(C_A - C_B + [OH^-] - [H^+])/A \qquad (79)$$

where A is the surface area of oxide available in solution in cm^2/liter, σ_o is the surface charge density and has the units of microcoulombs per square centimeter ($\mu C/cm^2$).

4.2.4 *Triple Layer Model Surface Charge.* The surface charges σ_o (o–layer) and σ_β (β–layer) include the surface reactions of all ions:

$$\sigma_o = 10^6 F([FeOH_2^+] + [FeOH_2^+ - Cl^-] + [FeOH_2^+ - CrO_4H^-] + [FeOH_2^+ - CrO_4^{2-}] - [FeO^-] - [FeO^- - Na^+])/A \qquad (80)$$

$$\sigma_\beta = 10^6\ F([FeO^- - Na^+] - [FeOH_2^+ - Cl^-] - [FeOH_2^+ - CrO_4H^-] - [FeOH_2^+ - CrO_4^{2-}])/A \quad (81)$$

Electroneutrality requires that:

$$\sigma_o + \sigma_\beta + \sigma_d = 0 \quad (82)$$

where σ_d is the diffuse layer surface charge.

4.2.5 *Triple Layer Model Surface Potential.* The o–plane potential ψ_o, β–layer potential ψ_β, and the diffuse layer surface potential ψ_d are related to o–plane charge σ_o, β–layer surface charge σ_β, and the diffuse layer surface charge σ_d as

$$\psi_o - \psi_\beta = \sigma_o/C_1 \quad (83)$$

$$\psi_\beta - \psi_d = \sigma_d/C_2 \quad (84)$$

where C_1 and C_2 are the inner–layer and outer–layer capacitances, respectively. C_1 and C_2 have units of F/m^2.

4.2.6 *Application of Triple Layer Model.* In this study, a triple layer model was employed using a similar approach to that of Zachara et al. (1989) to describe the adsorption phenomena of chromate on a natural soil. The TLM was used with three assumptions: 1. Fe oxide is the controlling sorbent and its surface area

could be approximated by the change in total surface area after DCB extraction, 2. Al in the DCB extract directly represents Al substitution in a mixed solid phase, and 3. Al–substituted Fe oxide in a mixed solid phase exhibits the same surface acidity and reactivity to CrO_4^{2-} as a pure–phase reference adsorbent.

The computer program FITEQL (Westall, 1982), including ionization, electrolyte complexation, chromate reactions, and competing oxyanion (SO_4^{2-}) complexation reactions, was used to simulate the chromate adsorption data. Modeling of experimental data requires a choice of the type of surface complexation and site binding reactions. Outer–sphere surface complexation reactions and two–site (FeOH and AlOH) modeling were used in this study. Table 4, lists surface complexation, aqueous speciation reactions and equilibrium constants for the two–site TLM. Reaction stoichiometries used in TLM calculations are summarized in Table 48 in Appendix 3.

4.2.7 *Triple Layer Model Parameters and Values.* In addition to the equilibrium constants listed in Table 4, modeling of experimental data requires surface area and the inner–layer and outer–layer capacitances, C_1 and C_2, respectively. Total surface area (A, m^2/kg) of the soil was determined as described by Mehra and Jackson, (1960). The surface area of the soil was measured before and after dithionite–citrate–bicarbonate (DCB) extraction and is presented in Table 5. The inner–layer and outer–layer capacitance were taken from data in Zachara et al., (1989).

Table 4: Triple Layer Model surface complexation reactions and equilibrium constants for chromate and sulfate

	Surface complexes	Constants (log K^{int})
1.	$FeOH_2^+ = FeOH + H^+$	–4.3
2.	$FeOH = FeO^- + H^+$	–9.8
3.	$AlOH_2^+ = AlOH + H^+$	–6.3
4.	$AlOH = AlO^- + H^+$	–12.0
5.	$FeOH + Na^+ = (FeO^- – Na^+)^\circ + H^+$	–9.3
6.	$FeOH + Cl^- + H^+ = (FeOH_2^+ – Cl^-)^\circ$	5.4
7.	$AlOH + Na^+ = (AlO^- – Na^+)^\circ + H^+$	–9.2
8.	$AlOH + Cl^- + H^+ = (AlOH_2^+ – Cl^-)^\circ$	7.9
9.	$FeOH + CrO_4^{2-} + H^+ = FeOH_2^+ – CrO_4^{2-}$	10.4
10.	$FeOH + CrO_4^{2-} + 2\ H^+ = FeOH_2^+ – HCrO_4^-$	18.9
11.	$AlOH + CrO_4^{2-} + H^+ = AlOH_2^+ – CrO_4^{2-}$	9.4
12.	$AlOH + CrO_4^{2-} + 2\ H^+ = AlOH_2^+ – HCrO_4^-$	15.9
13.	$FeOH + SO_4^{2-} + H^+ = FeOH_2^+ – SO_4^{2-}$	1.6
14.	$FeOH + SO_4^{2-} + 2\ H^+ = FeOH_2^+ – HSO_4^-$	17.3
	Aqueous speciation reactions	
15.	$H^+ + CrO_4^{2-} = HCrO_4^-$	6.51
16.	$2H^+ + CrO_4^{2-} = H_2CrO_4$	5.56
17.	$Na^+ + CrO_4^{2-} = NaCrO_4^-$	0.70
18.	$2H^+ + 2CrO_4^{2-} = Cr_2O_7^{2-}$	14.56

Table 5: Surface area and the inner–layer and outer–layer capacitance

Surface area (A), (m^2/kg):	
Untreated soil	1.37×10^5
DCB treated	1.19×10^5
Difference (Δ)	1.8×10^4
Outer–layer capacitance, F/m^2	1.25
Inner–layer capacitance, F/m^2	0.20

What remains to be determined are the surface complexation constants for CrO_4^{2-} adsorption on the Fe oxide surface ($K^{int}_{FeOH2^+-CrO4^{2-}}$ and $K^{int}_{FeOH2^+-HCrO4^-}$) for reactions 9 and 10 in Table 4 and surface site concentrations. The equilibrium constants and the surface site concentrations are the adjustable parameters in the TLM model. Equilibrium adsorption constants ($K^{int}_{FeOH2^+-CrO4^{2-}}$ and $K^{int}_{FeOH2^+-HCrO4^-}$) and the surface site concentrations are varied in FITEQL to yield an optimum fit to the experimental adsorption data while simultaneously satisfying the mass and charge constraints for all aqueous and surface equilibria considered. By use of the FITEQL program, the electrostatic parameters such as surface charge and surface potential at the o and β layers were calculated. In addition, the FITEQL program is able to compute the equilibrium concentration of each surface species ($[FeOH_2^+–CrO_4H^-]$ and $[FeOH_2^+–CrO_4^{2-}]$) and the equilibrium concentration of each solution species (e.g., $[H^+]$, $[CrO_4^{2-}]$, and $[CrO_4H^-]$) in the reaction system based on Cr(VI) experimental adsorption data. The main indicator of goodness of fit is the overall variance (V_y), which is the weighted sum of squares of residuals divided by the degree of freedom. Values of V_y between 0.1 and 20 are typical

for a good fit (Westall, 1982). The estimated concentration of surface sites along with the surface area estimated from DCB extraction data (Table 5) and the solid–to–solution ratio were used in the following equation (Zachara et al., 1989), to calculate the site density (N_s) of extractable Fe:

$$N_s = (FeOH \times a)/(ss \times S) \tag{85}$$

where FeOH is the surface sites (mol/L), a is Avogadro's number, ss is the solid–to–solution ratio (kg/L), and S is the surface area (nm^2/kg).

4.3 *HYDRAQL Model.* HYDRAQL is a computer program for the computation of chemical equilibria in aqueous and solid systems. This program can solve problems involving adsorption of ions on oxides using five different surface complexation models (SCMs), namely the constant capacitance, diffuse–layer, stern, triple–layer, and four–layer model. HYDRAQ was developed directly from MINEQL (Westall, 1986) by Papelis et al. (1988). In this study, the HYDRAQL program was used to simulate adsorption of the chromate and bichromate ions using the formation constants calculated from the FITEQL program.

5. RESULTS

5.1 Soil Analyses

5.1.1 *pH of the Point-of-Zero-Charge.* The pH of the point–of–zero–charge (pH_{pzc}) of soil is defined as the pH value at which the total net charge on the surface of a solid particle is zero (Sposito, 1984). This value is commonly determined by soil titration experiments performed in background electrolyte solutions at two or more ionic strengths (Sposito, 1984; Stumm and Morgan, 1981). When the net surface charge is zero, the activity of sorbed species is unaffected by ionic strength. Therefore, plots of proton or hydroxide surface densities versus pH intersect at the pH_{pzc}. The point–of–zero–charge on this soil was measured as a function of pH and ionic strength by the potentiometric titration method as described by Parks and De Bruyn (1962) except that NaCl was used as the supporting electrolyte in place of KNO_3. The variation in moles of acid added (H^+) with pH and supporting electrolyte concentration is shown in Figure 5. For each titration shown (Figure 5), some ions were dissolved from the soil into solution. However, no effort was made to quantify their contribution to the total ionic strength. Tables 22–25 in Appendix 2 list the data for soil titrations.

Two crossover points corresponding to zero points of charges were observed in the titration data for the soil. This phenomenon sometimes has been observed for the titration of soil materials, but is usually attributed to unknown artifacts (personal communication, Sabine Goldberg, Feb. 1993). At both pH

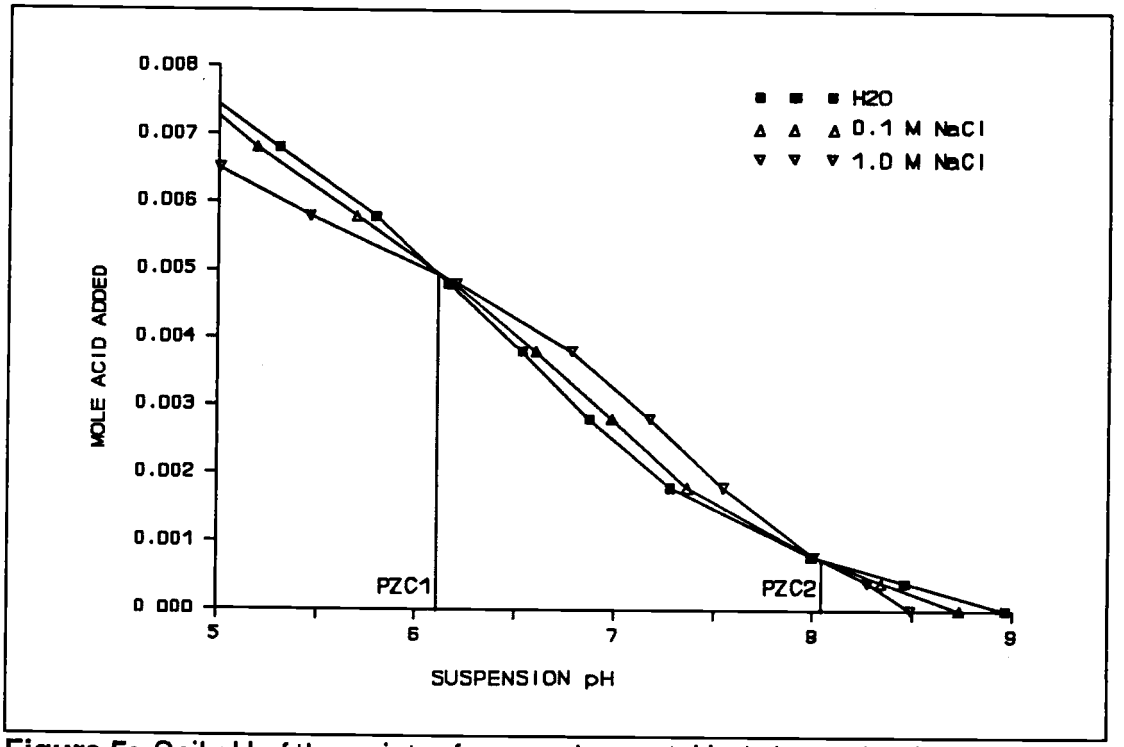

Figure 5: Soil pH of the point–of–zero–charge (pH_{pzc}) determination using acid and base titrations at various ionic strengths.

values 8.1 and 6.2 the observed point–of–zero–charges were determined which correspond approximately to the pH_{pzc} of the two pure solids, α–Fe_2O_3 (Goethite) and Fe_3O_4 (Magnetite) with pH_{pzc} 7.8 and 6.5, respectively. The slight deviation of the determined pH_{pzc} values from the literature values can be accounted for by complications such as those caused by structural or adsorbed impurities. Therefore, pH_{pzc} values of 8.1 and 6.2 are assumed to be the pH of point–of–zero–charges of the mixed solids, α–Fe_2O_3 and Fe_3O_4, in the soil. The determined point–of–zero–charge at pH 8.1 indicates that the soil has a positive net charge at the ground water pH of 6.9, and should electrostatically favor anion adsorption.

5.1.2 *Chromium(VI) Reduction Capacity of the Soil.* The reduction capacities of the soil at varying depths were measured by the acid dichromate reduction method as described by Barcelona and Holm (1991) (see section 3.2.5). The results are shown in Table 6.

Table 6: Total reduction capacities of the soil

Soil Depth (ft)	Geologic Unit	Reduction Capacity (mmol Cr(VI)/kg soil)
4.0–6.1	Upper Silts	218
8.3–10.3 & 12.0–14.3	Upper Silts	168
18.6–20.9	Aquitard	273

The greatest reduction capacity was in the aquitard, 18.3–20.9 ft depth, and 273 mmol of Cr(VI) was reduced to Cr(III) per kilogram soil. The reduction capacity in the upper silts, 4–6.1 ft depth, was 218 mmol Cr(VI) reduced to Cr(III) per kilogram soil. The lower reduction capacity was in the upper silts, a mixture of 8.3–10.3 ft and 12–14.3 ft depth, and 168 mmol Cr(VI) was reduced to Cr(III) per kilogram soil.

Magnetite was separated from the upper silts and aquitard samples magnetically and was determined by powder X–ray diffraction (XRD). Figures 26 and 27 in Appendix 1 show the X–ray diffraction pattern. Figures 28 and 29 also show the XRD of pure magnetite. Results of chemical analysis of magnetically separated samples from the soil are listed in Table 7.

Table 7: Total magnetite separated from the soil

Soil Depth (ft)	Geologic Unit	Fe_3O_4 (w/w)	Fe(II)[a] (mmol/kg)
4.0–6.1	Upper Silts	0.78 %	33.6
8.3–10.3 & 12.0–14.3	Upper Silts	0.75 %	32.3
18.6–20.9	Aquitard	0.89 %	38.4

[a]mmol Fe(II)/kg soil

The ferrous and total iron contents were determined according to the method of Begheijn (1979) (see section 3.2.6). Results for Fe(II) and total Fe (II plus III) are shown in Table 8. As Table 8 shows, ferrous iron also exists in the soil structure in other than magnetite and is probably in oxides such as hematite and biotite and in silicate minerals.

Table 8: Total Fe and Fe(II) determined by wet chemical analyses

Soil Depth (ft)	Geologic Unit	Fe_{total} (w/w)	Fe(II) (w/w)	Fe(II) (mmol/kg)
4.0–6.1	Upper Silts	4.99 %	0.85 %	151.8
8.3–10.3 & 12.0–14.3	Upper Silts	4.98 %	0.83 %	148.2
18.6–20.9	Aquitard	5.85 %	0.92 %	164.3

Organic matter content of the soil was considered an important factor for Cr(VI) reduction to Cr(III) (Bartlett and Kimbel 1976b). To estimate the organic reduction capacity of the soil, total organic carbon content of the soil was measured (see section 3.2.4). Table 9 shows total organic and inorganic carbon content of the soil in the upper silts and aquitard samples.

Table 9: Organic and inorganic carbon content of the soil

Soil Depth (ft)	Geologic Unit	TC[a] (w/w)	TIC[b] (w/w)	TOC[c] (w/w)
4.0–6.1	Upper Silts	0.32 %	0.17 %	0.14 %
8.3–10.3 & 12.0–14.3	Upper Silts	0.29 %	0.18 %	0.11 %
18.6–20.9	Aquitard	0.55 %	0.38 %	0.17 %

[a]Total carbon, [b]Total inorganic carbon, [c]Total organic carbon

5.2 Chromium(VI) Batch Reactor Experiments

5.2.1 *Adsorption Kinetics.* Chromium(VI) adsorption kinetics were determined in completely–mixed reactors in a temperature–controlled chamber. Kinetic experiments were conducted to investigate the time dependence of the adsorption process for different pH values. Kinetic experiments were also conducted to determine the effects of initial concentration and pH on Cr(VI) adsorption on a natural soil. The effects of supporting electrolyte concentration were also determined in kinetic batch experiments. Figure 6 shows Cr(VI) removal from solution as a function of time. Cr(VI) removal from solution showed a rapid initial uptake followed by very slow uptake kinetics. Figure 7 shows Cr(VI) removal kinetics in which the effects of adsorption and reduction are included. Similar results were found for all kinetics and pH values. Results of Cr(VI) adsorption kinetics show that equilibrium was approached within 58 hours reaction time. Adsorption kinetics of 0.1 mM Cr(VI) as a function of time and at

pH values of 5.25 and 6.50 are demonstrated by plots of solid phase concentration against time (Figure 8). As Figure 8 shows, adsorption increases with decreasing pH. Adsorption kinetics of 0.1 and 0.2 mM Cr(VI) as a function of time are shown in Figure 9 showing the effect of Cr(VI) concentration. The data used for constructing Figures 6–9 are summarized in Tables 26–28 in Appendix 2.

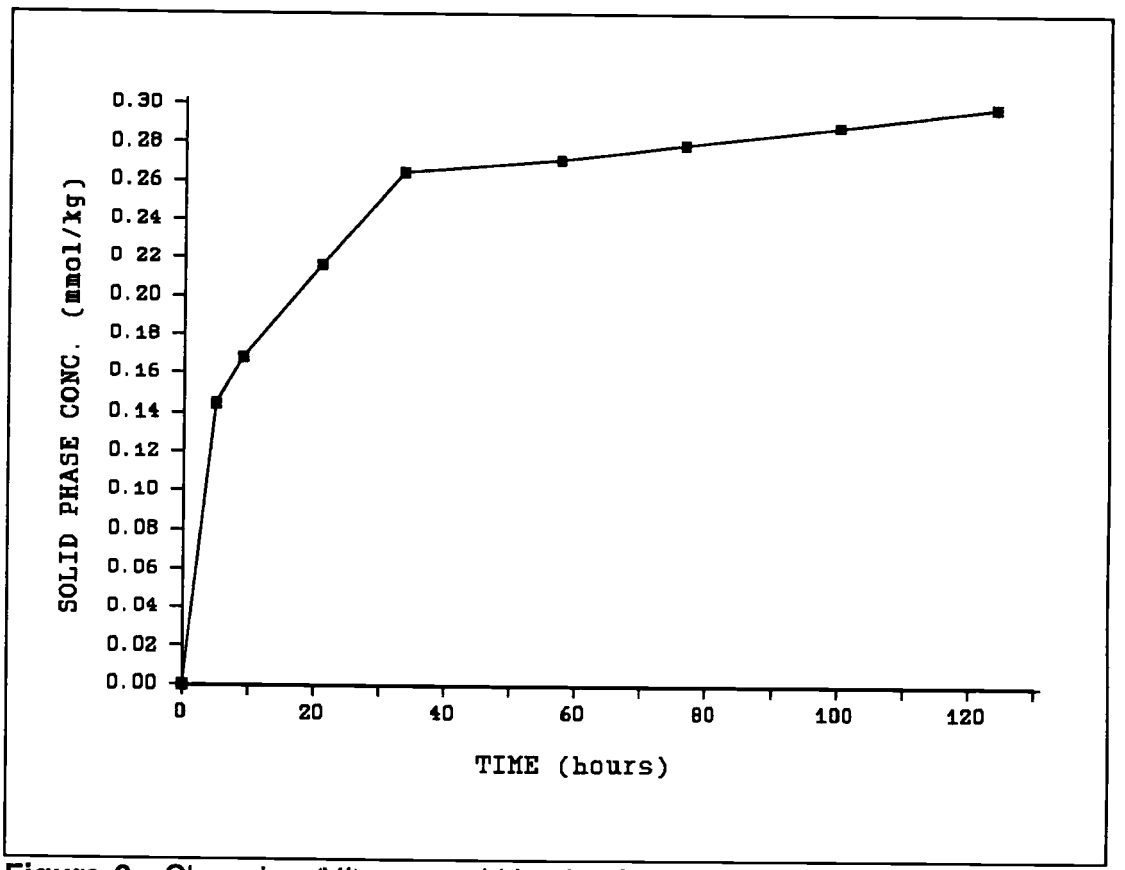

Figure 6: Chromium(VI) removal kinetics for 120 hour reaction time, 0.1 mM Cr(VI) in 0.01 M NaCl electrolyte solution, pH = 5.02–5.26, 40 g/L soil.

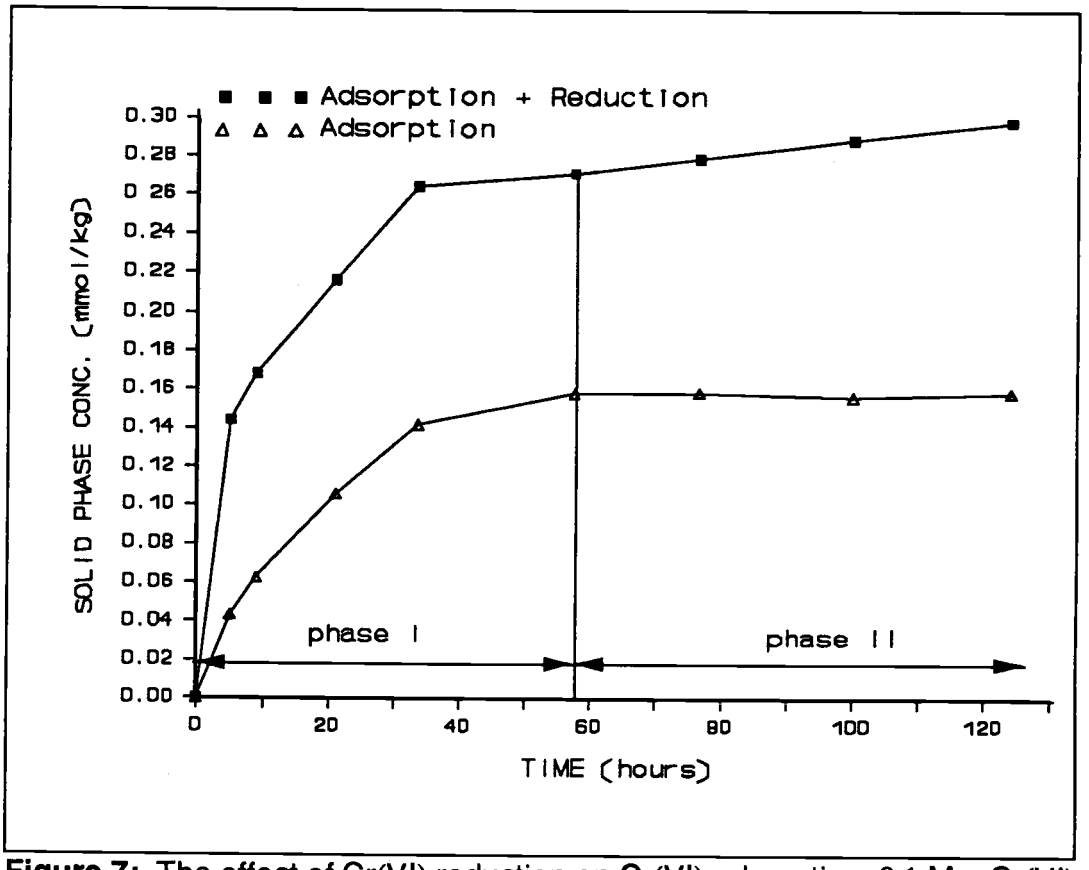

Figure 7: The effect of Cr(VI) reduction on Cr(VI) adsorption, 0.1 Mm Cr(VI) in 0.01 M NaCl electrolyte solution, pH = 5.02–5.26, 40 g/L soil.

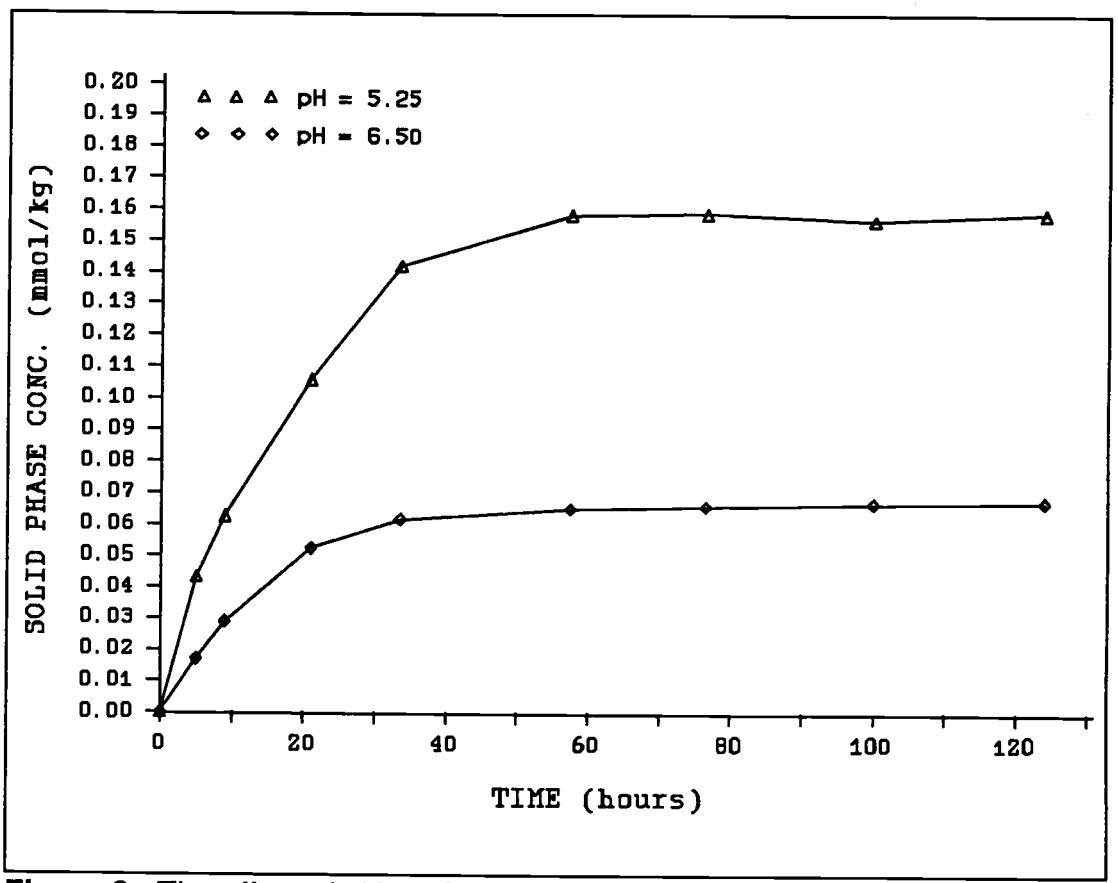

Figure 8: The effect of pH on Cr(VI) adsorption kinetics, 0.1 mM Cr(VI) in 0.01 M NaCl electrolyte solution, 40 g/L soil.

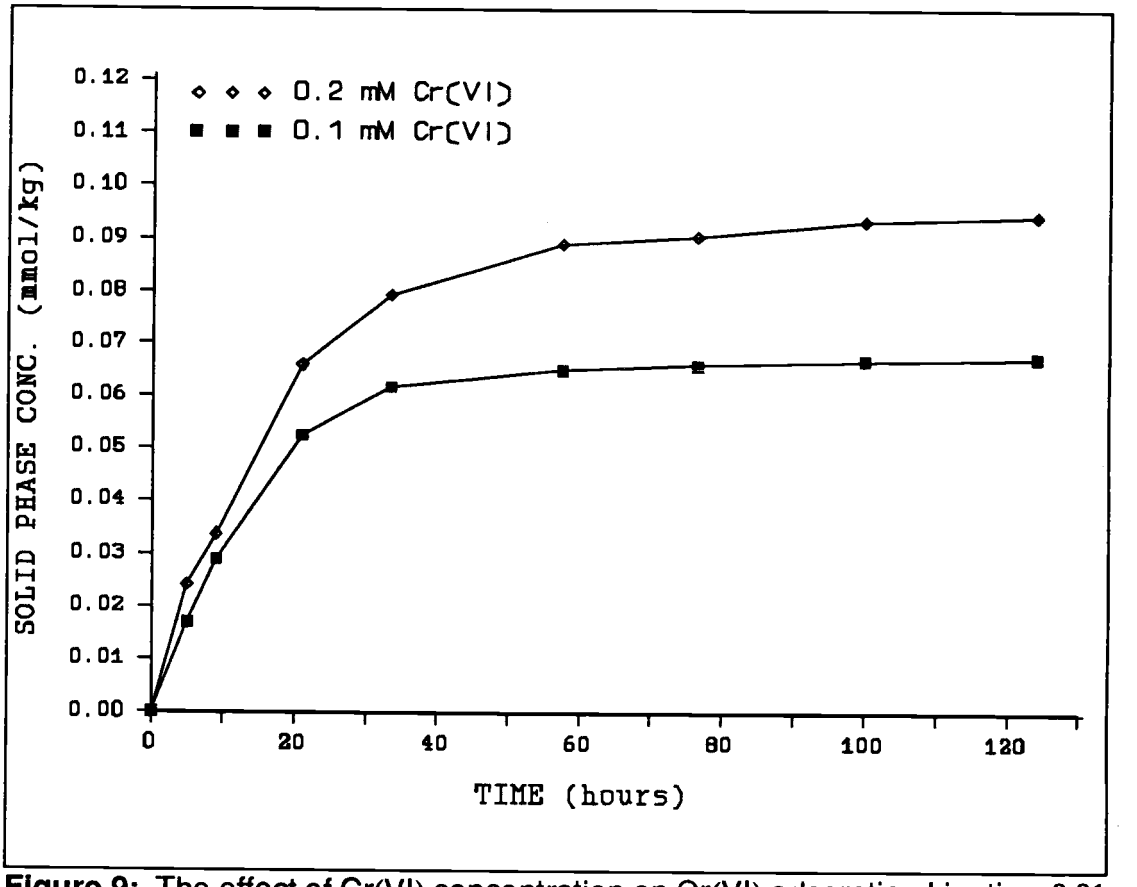

Figure 9: The effect of Cr(VI) concentration on Cr(VI) adsorption kinetics, 0.01 M NaCl electrolyte solution, pH = 6.3–6.5, 40 g/L soil.

5.2.2 *Adsorption Isotherms.* Adsorption isotherms were determined in batch reactors after 120 hours reaction time. Figure 10 shows an adsorption isotherm in which the effects of Cr(VI) reduction are included. The dependence of the amount of Cr(VI) adsorption on pH and solution concentration of Cr(VI) is illustrated by the curves in Figure 11. The adsorption isotherms for this soil conformed to the Langmuir equation (see section 4.1). Figure 11 shows that the amount of Cr(VI) uptake by soil approaches a maximum value (Γ_M) at constant pH which can not be exceeded by increasing the solution concentration and which varies only with pH. Two Cr(VI) sorption parameters, the maximum sorption capacity (Γ_M) and Langmuir adsorption constant (K_L), were determined in 120 hours isotherm experiments. Table 10 reports the maximum adsorption capacity and Langmuir constant of Cr(VI) equilibrium sorption at pH 5.65 and 7.00. The intrinsic equilibrium constants obtained from equations (38) and (42) at pH values 5.65 and 7.00, using K_L and Γ_M from Table 10 and $pH_{pzc} = 8.1$, were log $K^{int}_{SOH_2^+-CrO_4H^-} = 8.95$ and log $K^{int}_{SOH_2^+-CrO_4^{2-}} = 16.5$.

Table 10: Langmuir adsorption constant and maxima calculated from equilibrium isotherms.

pH	K_L(mol/L)	Γ_M(mol/kg)
5.65	5.9×10^{-5}	2.6×10^{-4}
7.00	1.1×10^{-4}	1.4×10^{-4}

Tables 29 and 30 in Appendix 2 report the data for adsorption isotherm experiments.

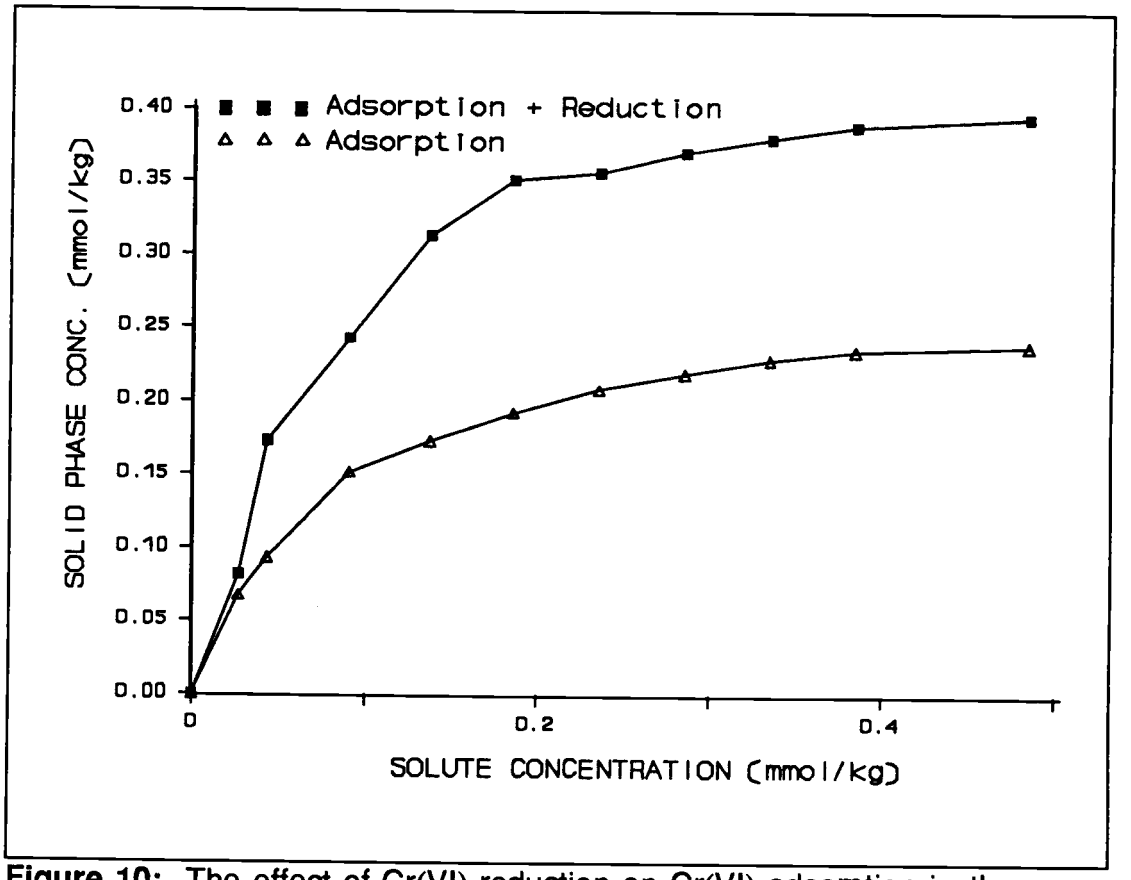

Figure 10: The effect of Cr(VI) reduction on Cr(VI) adsorption isotherm, pH = 5.60–5.69.

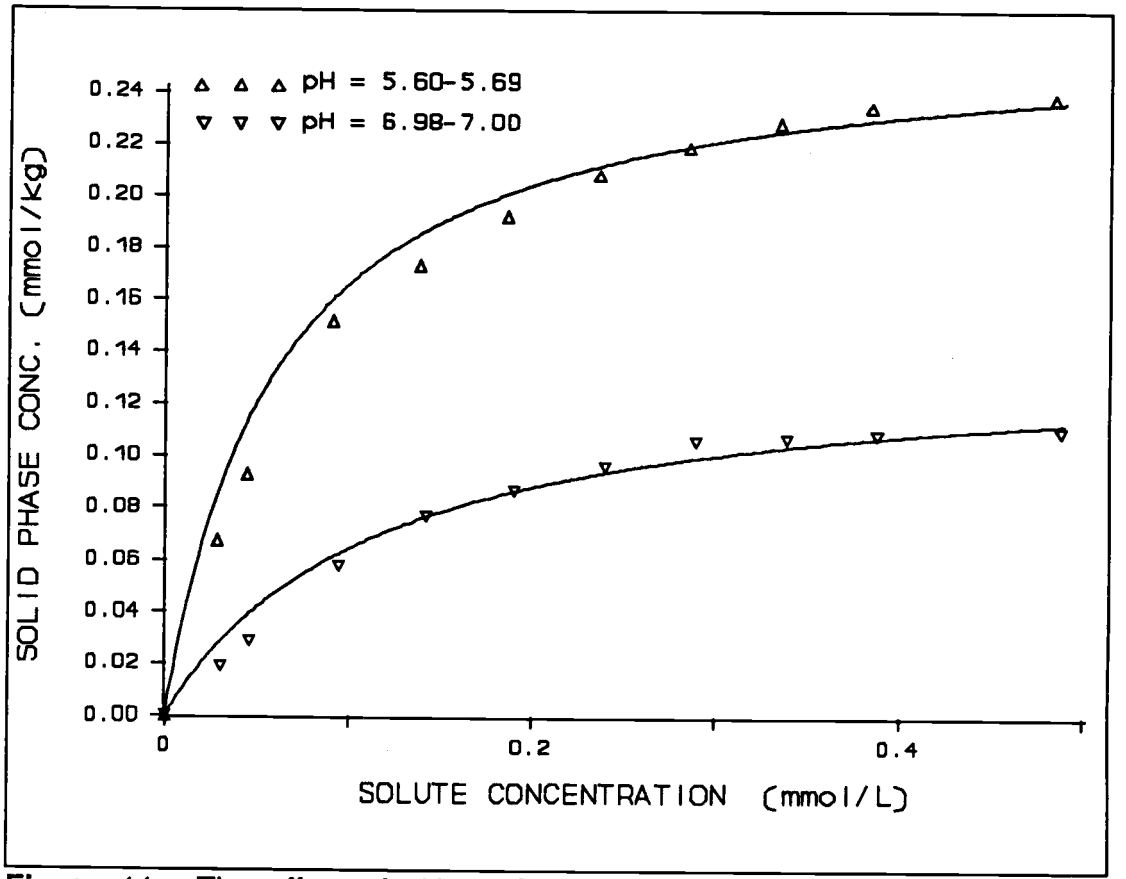

Figure 11: The effect of pH on Cr(VI) adsorption isotherm, 0.01 M NaCl electrolyte solution, 40 g/L soil. Solid lines represent fitted Langmuir equation.

5.2.3 *Effect of Background Electrolyte on Cr(VI) Adsorption.* The effects of changing electrolyte ionic strength on adsorption of Cr(VI) onto soil were examined in the adsorption isotherm experiments. The effect of background electrolyte concentration on Cr(VI) adsorption as a function of pH is shown in Figure 12. Cr(VI) adsorption in 0.01, 0.1 and 0.5 M NaCl electrolyte solutions indicated that higher ionic strength solution resulted in less Cr(VI) adsorption. Also clearly shown is the decrease in adsorption density as pH increases. The data for these experiments are listed in Tables 31–33 in Appendix 2.

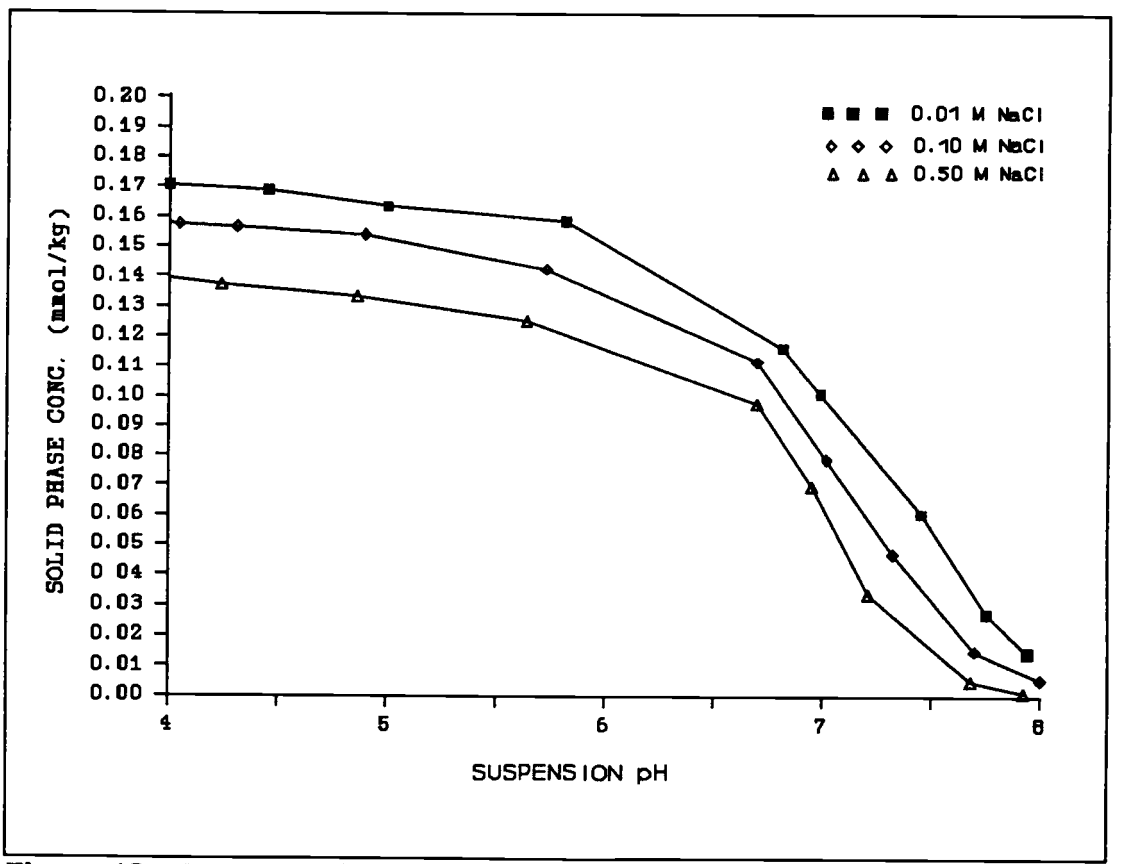

Figure 12: The effect of background electrolyte (NaCl) concentration on Cr(VI) adsorption as a function of pH, 0.1 mM Cr(VI), 40 g/L soil.

5.2.4 *Effects of Competing Oxyanions on Cr(VI) Adsorption.* The effects of the competing oxyanions sulfate (SO_4^-), phosphate ($H_2PO_4^-/HPO_4^{2-}$), bicarbonate (HCO_3^-), and nitrate (NO_3^-) were examined in equilibrium isotherm experiments. The effects of 0.01 M concentrations of these competing oxyanions are compared with 0.01 M chloride (as NaCl) in Figure 13. Phosphate caused the greatest decrease in chromate adsorption on the soil followed in order by sulfate, bicarbonate, nitrate, and chloride. Tables 34–37 in Appendix 2 report the data for these experiments.

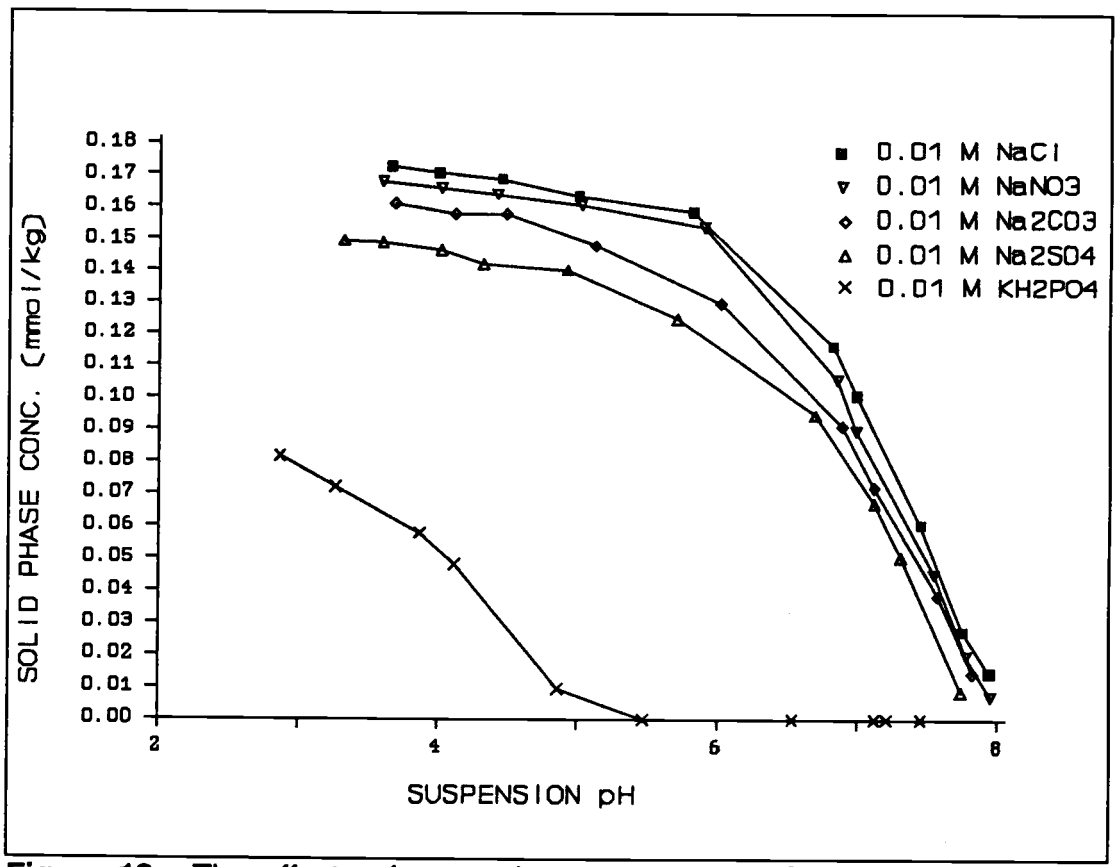

Figure 13: The effects of competing oxyanions on Cr(VI) adsorption as a function of pH, 0.1 mM Cr(VI), 40 g/L soil.

5.3 *Chromium Soil Column Experiments.* Adsorption and desorption of chromium were studied in packed soil columns to more closely simulate field conditions of continuous hydraulic flow through a stationary porous medium. Variables investigated included pH, ionic strength, and the addition of selected competitive oxyanions as desorption agents, while reduction of Cr(VI) was considered an important factor influencing chromium behavior and transport in the soil. General information about the columns is summarized in Table 3 (see section 3.2.10).

The following experiments were conducted in soil columns:

1. Determine Cr(VI) breakthrough curve and desorption as a function pH.
2. Determine effect of background electrolyte on Cr(VI) adsorption.
3. Determine effect of competing oxyanions on Cr(VI) desorption.
4. Determine effect of pH and background electrolyte on Cr(VI) reduction.

For column experiments, chromium (VI) was first adsorbed on the soil from an influent solution until equilibrium was approximately achieved between the soil column and applied chromium solution. These breakthrough curves were determined from Cr(VI) sorption on soil columns in 0.01 M NaCl background electrolyte solution. Then chromium was desorbed from the columns by application of various desorbing solutions. Desorption was achieved using 0.01 M NaCl background electrolyte or competitive oxyanions such as phosphate ($H_2PO_4^-/HPO_4^{2-}$) and sulfate (SO_4^{2-}) as the desorbing agents in the column influent. Columns 1–7 were packed with the upper silts samples (8.3–14.3) and

column # 8 was packed with the aquitard samples (18.6 –20.9 ft) from the deep aquifer (DW–12). Column # 8 had 50 percent less volume than those used in soil column experiments 1–7 (Tables 15–21 in Appendix 2). The specific conditions for the column experiments 1–8 are summarized in Table 11.

Sequential extractions were performed on soil column subsamples after column desorption with background electrolyte or competing oxyanion solutions. Reduced chromium in soil column experiments was determined by extraction using ammonium oxalate, dithionite–citrate–bicarbonate (DCB), and 1 M HCl solutions. Sequential extractions also differentiated between amorphous and crystalline solid phase forms of reduced chromium (see section 3.2.11). The results of sequential extractions on soil columns 1–8 are presented in Table 12.

Results of chromium(VI) adsorption, desorption, effluent pH, and flow rate changes in effluent solutions will be discussed in detail for columns # 1 and # 2. However, results of columns 3–8 are only briefly discussed below with emphasis on necessary information on Cr(VI) adsorption and desorption.

For soil column #1, the breakthrough and desorption curve for 0.2 mM Cr(VI) in 0.01 M NaCl as background electrolyte solution is shown in Figure 14. Column #1 was loaded with 0.2 mM Cr(VI) solution for 45 days. During this time 0.709 mmol Cr(VI) per kilogram soil was removed from solution by the soil within 109 pore volumes (Figure 14). The breakthrough occurred between 3 to 5 pore volumes of total flow through the column, followed by a rapid increase in the effluent Cr(VI) concentration (C_e) until maximum adsorption capacity of the soil for removing Cr(VI) was achieved. However, equilibrium (at C_e/C_o=1) was not

achieved even after 109 pore volumes. The pH of the effluent from the column was initially 7.91, but increased to 8.06 during the loading of the column with the Cr(VI) solution (Figure 30 in Appendix 1). The flow rate was about 10 ml/hr for the first 15 pore volumes, then gradually decreased to 3.8 ml/hr for the remainder of the loading period (Figure 31 in Appendix 1). Desorption (beginning at V_e/V_p = 109) with 0.01 M NaCl background electrolyte removed 0.326 mmol Cr(VI) per kilogram soil from the column within an additional 58 pore volumes. During this time the concentration of Cr(VI) decreased from 9.53 to 0.11 mg/L. The flow rate was relatively constant at 3.5 ml/hr during desorption with 0.01 M NaCl. The pH of the effluent from the column desorption decreased from 8.06 to 7.87.

Column #2 was loaded with 0.2 mM Cr(VI) in 0.5 M NaCl as electrolyte solution. The breakthrough occurred between 2 to 3 pore volumes of total flow through the column. Desorption conducted using 0.01 M NaCl electrolyte solution. The flow rate was 9.96 ml/hr, then gradually decreased to 5.28 ml/hr (Figure 33 in Appendix 1). The flow rate decreases in the column were caused by screen clogging at the top of the column. To clean screen clogging at the top of the column during desorption the column was shutdown for 58 hours. During this time the concentration of Cr(VI) in the effluent increased from 0.68 to 17.25 mg/L Cr(VI). Cr(VI) conentration then decreased to 0.35 mg/L Cr(VI) after 12 pore volumes additional flow (Figure 15). The pH of the effluent from the column during shutdown also increased from 8.05 to 9.60 (Figure 32 in Appendix 1). The increasing pH of the effluent solutions during shutdown of soil column # 2 can be attributed to the competition of H^+ in the extracting solution with cations (sodium)

for the adsorption sites. The increasing concentration of Cr(VI) immediately following start–up suggests that equilibrium has not been established in the column and that a kinetic reaction term should be taken into account.

Column # 3 was loaded with 0.2 mM Cr(VI) in 0.01 M NaCl as background electrolyte solution. Desorption was conducted using 0.01 M KH_2PO_4 at pH about 8. The concentration of Cr(VI) in the effluent increased from 9.20 to 23.19 mg/L Cr(VI) and then decreased to 0.13 mg/L Cr(VI) within 6 pore volumes (Figure 16). Column # 4 was loaded with 0.1 mM Cr(VI) in 0.01 M NaCl as electrolyte solution. Desorption was conducted using 0.01 M Na_2SO_4 solution. The concentration of Cr(VI) in the effluent solution increased from 4.58 to 7.41 mg/L Cr(VI) and then decreased to less than 0.01 mg/L Cr(VI) (IC detection limit) within 9 pore volumes (Figure 16).

Column # 4 was loaded with 0.1 mM Cr(VI) in 0.01 M NaCl as electrolyte solution. The breakthrough occurred between 3 to 5 pore volumes of total flow through the column. Desorption was conducted using 0.01 M Na_2SO_4 solution. The concentration of Cr(VI) in the effluent solution increased from 4.58 to 7.41 mg/L Cr(VI) and then decreased to less than 0.01 mg/L (Figure 17).

Column # 5 was loaded with 0.1 mM Cr(VI) in 0.1 M NaCl as electrolyte solution. The breakthrough occurred between 3 to 4 pore volumes of total flow through the column. Desorption was conducted using 0.01 M Na_2SO_4 solution. The concentration of Cr(VI) in the effluent solution increased from 4.58 to 8.72 mg/L Cr(VI) and then decreased to less than 0.01 mg/L (Figure 18).

Column # 6 was loaded with 0.1 mM Cr(VI) in 0.01 M NaCl and 12.5 ml/L

HCl (1 M) at pH about 2. The breakthrough did not occur even after 129 pore volumes. Desorption was conducted using 0.5 M phosphate solution at pH about 8. The concentration of Cr(VI) in the effluent solution increased from 2.18 to 15.00 mg/L Cr(VI) and then decreased to less than 0.01 mg/L Cr(VI) (Figure 19). The flow rate remained nearly constant when the top screen was eliminated for soil columns #4, #5, and #6 (Figures 37, 39, and 41 in Appendix 1).

Column # 7 was loaded with 0.1, 0.4, 1.0, and 10.0 mM Cr(VI) in 0.1 M NaCl and 12.5 ml/L HCl (1 M) at pH about 2. Desorption was conducted using 0.5 M phosphate at pH about 8.0. The concentration of Cr(VI) in the effluent solution increased from 500 to 660 mg/L Cr(VI) and then decreased to 0.79 mg/L Cr(VI) within 36 pore volumes (Figure 20).

Column # 8 was loaded with 10 mM Cr(VI) in 0.01 M NaCl. For this column, equilibrium (at C_e/C_o = 1) was achieved after 40 pore volumes. Desorption with 0.5 M phosphate at pH about 8.0 increased Cr(VI) concentration in the effluent solution from 411 to 965 mg/L Cr(VI) and then decreased to 0.30 mg/L Cr(VI) within 13.4 pore volumes (Figure 21). The flow rate decreases in soil column experiment #7 and #8 probably were caused by greater Cr(VI) reduction to Cr(III) at lower pH and precipitation onto the soil (Figures 43 and 45 in Appendix 1). A mass balance performed on chromium adsorption, desorption, and extraction on soil columns 1–8 is shown in Table 13. The data for soil columns 1–8 are listed in Tables 38–45 in Appendix 2.

Table 11: Chromium(VI) soil column experiments 1–8

Experiment No.	[a]ADS/ [b]DES	[c]V_p	[d]V_e/V_p	Influent solution	Background Elect. (M)	Initial pH	[e]Cr(VI) (mmol/kg)	Effluent pH	Effl. flow rate (ml/hr)
Column # 1	ADS	63.8	0–109	0.2 mM Cr(VI)	0.01 NaCl	6.30	0.709	7.91–8.06	10.3–3.80
	DES		109–167	0.01 M NaCl	0.01 NaCl	6.50	0.326	8.06–7.87	3.80–3.50
Column # 2	ADS	63.0	0–120	0.2 mM Cr(VI)	0.50 NaCl	5.07	0.371	7.78–8.05	9.96–5.28
	DES		120–133	0.01 M NaCl	0.01 NaCl	6.50	0.136	9.60–7.88	5.28–4.57
Column # 3	ADS	63.0	0–50.5	0.2 mM Cr(VI)	0.01 NaCl	6.21	0.501	7.80–7.92	5.71–4.76
	DES		50.5–56.6	0.01 M Phosphate	0.01 NaCl	7.21	0.240	7.92–7.80	4.76–4.48
Column # 4	ADS	57.5	0–31.8	0.1 mM Cr(VI)	0.01 NaCl	6.12	0.186	8.19–8.11	5.03–5.19
	DES		31.8–50	0.01 M Sulfate	0.01 NaCl	6.78	0.088	8.11–8.03	5.19–5.00
Column # 5	ADS	60.8	0–25.2	0.1 mM Cr(VI)	0.10 NaCl	5.87	0.138	8.15–7.90	6.53–6.50
	DES		25.2–29	0.01 M Sulfate	0.01 NaCl	7.23	0.064	7.90–7.97	6.50–6.21
Column # 6	ADS	62.5	0–129	0.1 mM Cr(VI) & HCl	0.01 NaCl	1.98	2.490	8.02–3.85	6.37–6.43
	DES		129–156	0.5 M Phosphate	0.01 NaCl	8.02	0.354	3.85–7.02	6.43–6.17
Column # 7	ADS	63.0	0–146	0.1 mM Cr(VI) & HCl	0.10 NaCl	1.98	4.91	8.05–3.69	6.30–6.58
	ADS		146–294	0.4 mM Cr(VI) & HCl	0.10 NaCl	1.87	10.76	3.69–3.12	6.58–6.24
	ADS		294–348	1.0 mM Cr(VI) & HCl	0.10 NaCl	1.86	10.77	3.12–3.39	6.24–6.13
	ADS		348–404	10.0 mM Cr(VI) & HCl	0.10 NaCl	1.89	30.09	3.39–2.75	6.13–6.04
	DES		404–440	0.5 M Phosphate	0.10 NaCl	8.02	12.94	2.75–7.71	6.04–5.25
Column # 8	ADS	28.7	0–50	10.0 mM Cr(VI)	0.01 NaCl	6.12	12.01	8.02–7.96	0.93–1.06
	ADS		50–118	10.0 mM Cr(VI) & HCl	0.01 NaCl	1.94	35.82	7.96–7.70	1.06–0.48
	DES		118–131	0.5 M Phosphate	0.01 NaCl	8.02	14.62	7.70–8.00	0.48–0.39

[a]ADS Adsorption, [b]DES Desorption, [c]V_p Pore Volume, [d]V_e Effluent Volume, [e]Cr(VI) removed from solution or desorbed

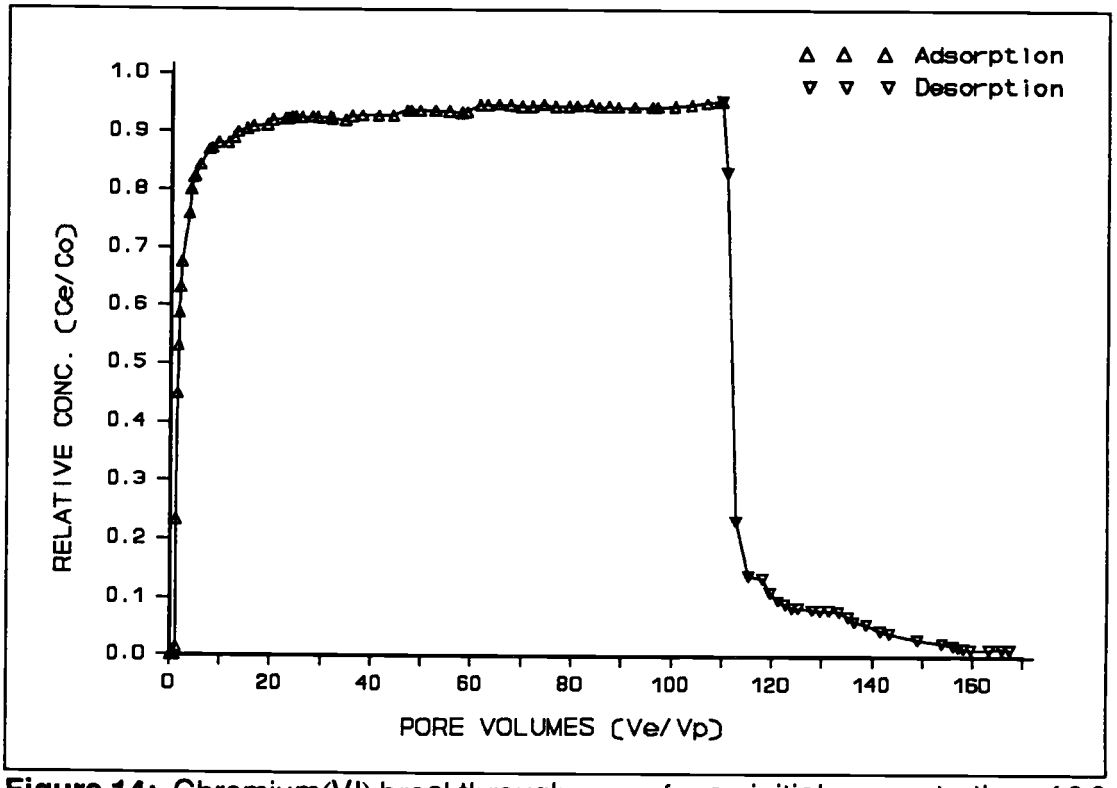

Figure 14: Chromium(VI) breakthrough curve for an initial concentration of 0.2 mM Cr(VI) in 0.01 M NaCl electrolyte solution. Desorption conducted using 0.01 M NaCl solution (column #1).

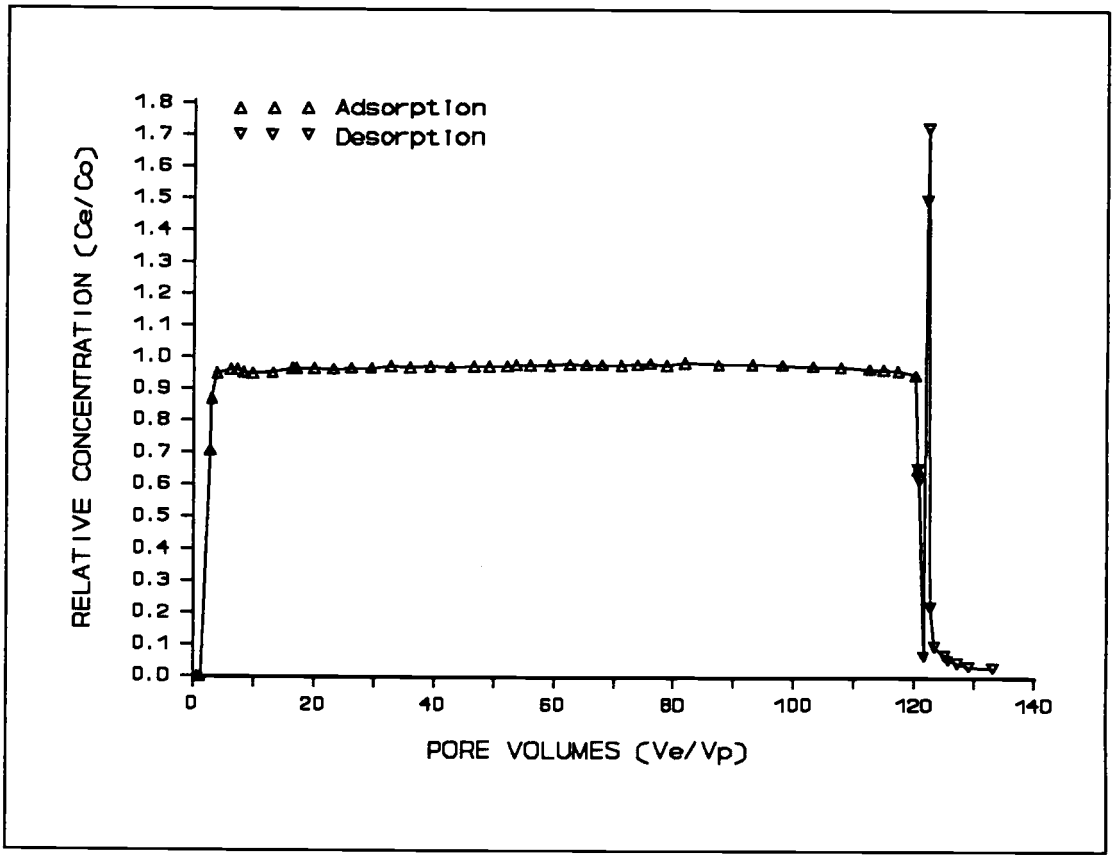

Figure 15: Chromium(VI) breakthrough curve for an initial concentration of 0.2 mM Cr(VI) in 0.5 M NaCl electrolyte solution. Desorption conducted using 0.01 M NaCl solution. Spike in desorption limb due to column shutdown (column #2).

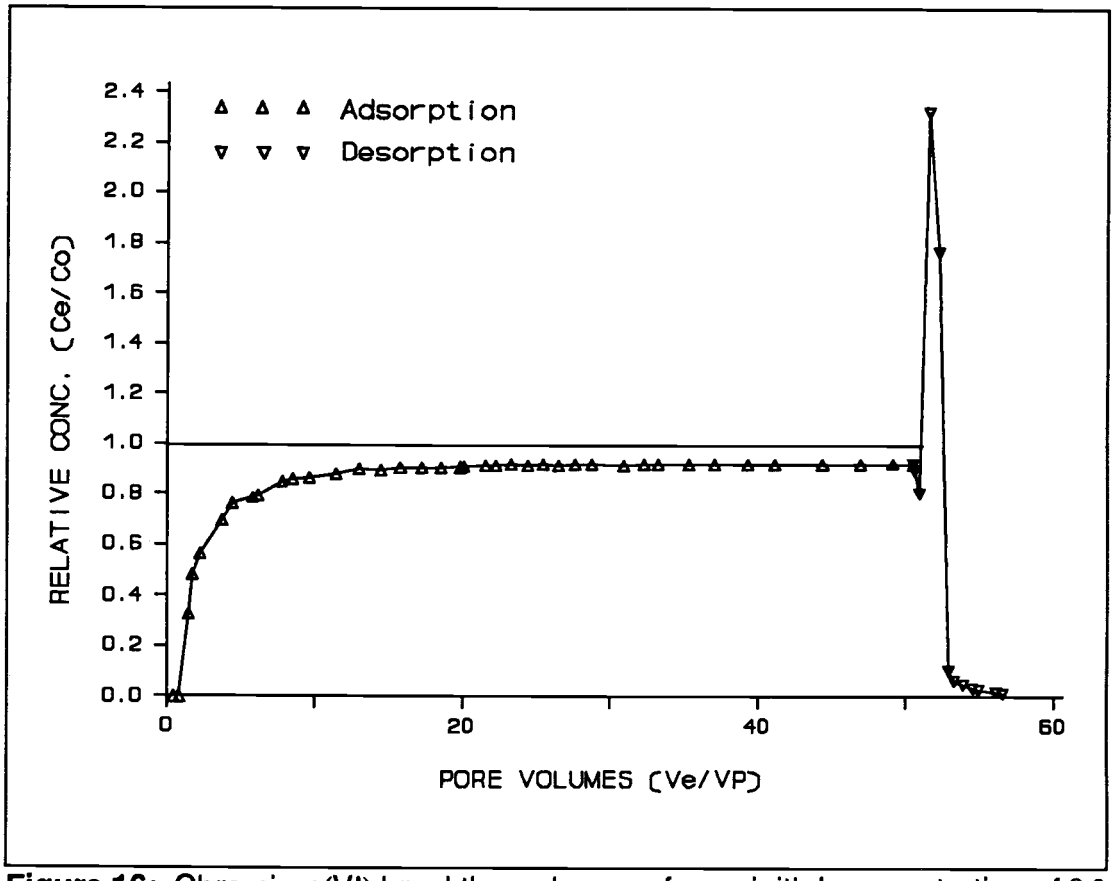

Figure 16: Chromium(VI) breakthrough curve for an initial concentration of 0.2 mM Cr(VI) in 0.01 M NaCl. Desorption conducted using 0.01 M phosphate solution at pH 7.21 (column #3).

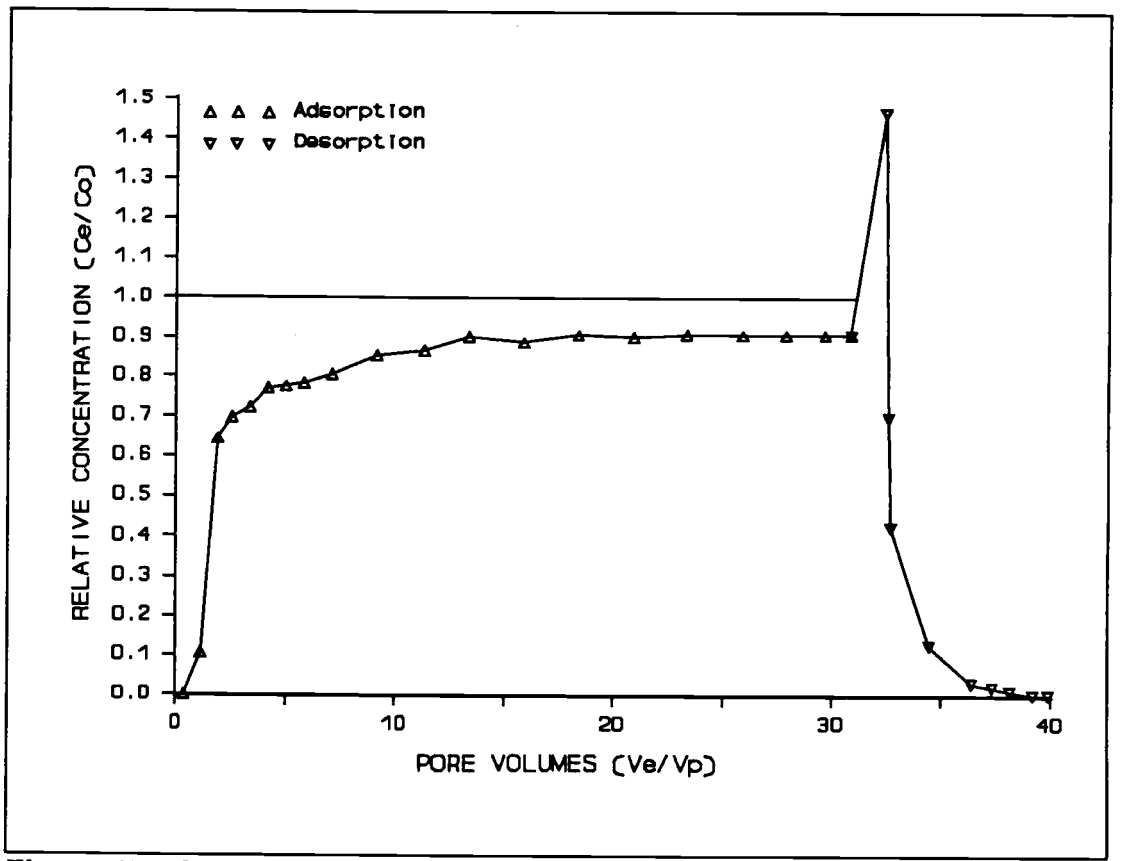

Figure 17: Chromium(VI) breakthrough curve for an initial concentration of 0.1 mM Cr(VI) in 0.01 M NaCl electrolyte solution. Desorption conducted using 0.01 M sulfate solution (column #4).

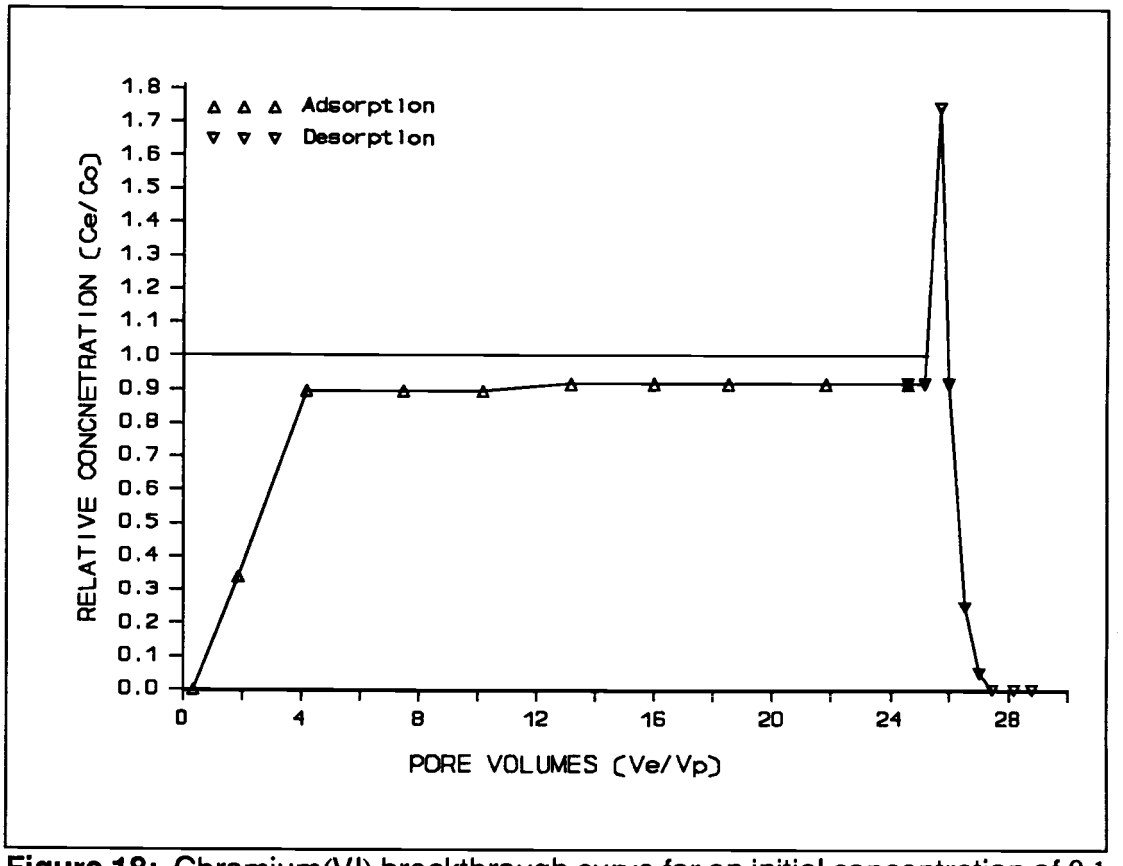

Figure 18: Chromium(VI) breakthrough curve for an initial concentration of 0.1 mM Cr(VI) in 0.1 M NaCl electrolyte solution. Desorption conducted using 0.01 M sulfate solution (column #5).

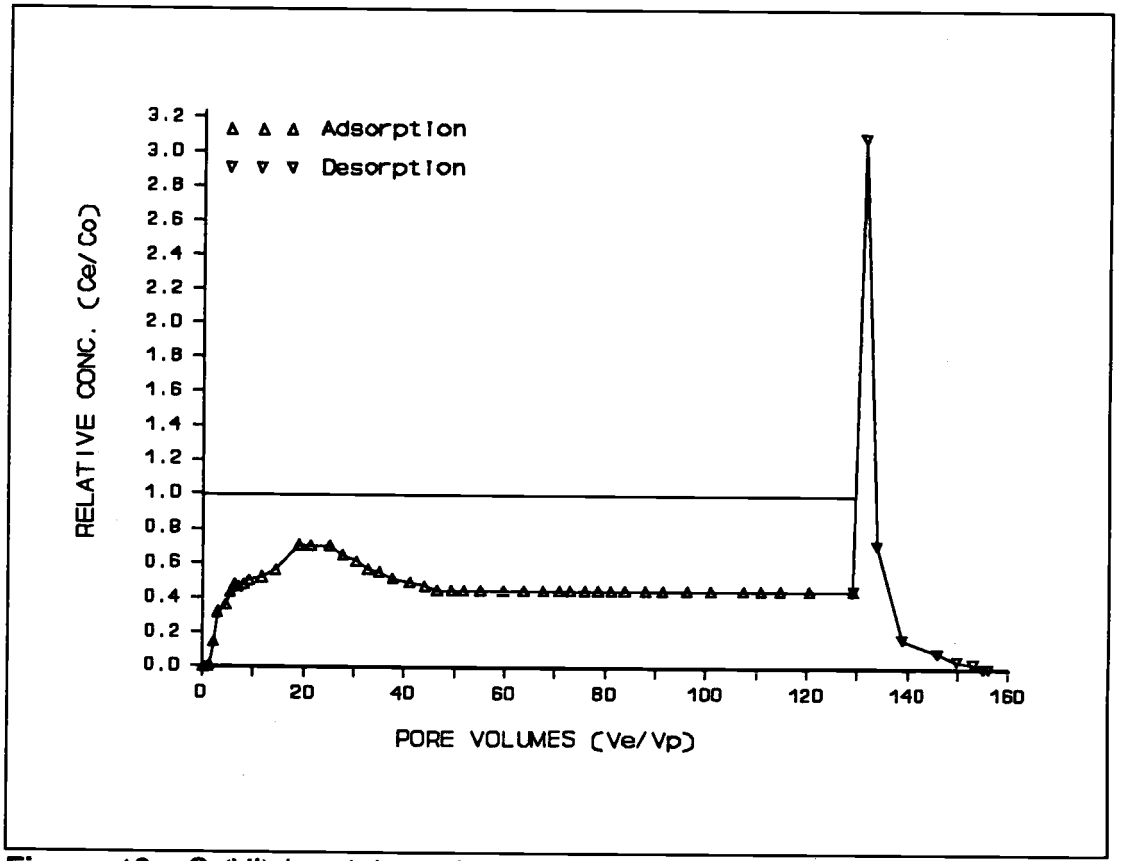

Figure 19: Cr(VI) breakthrough curve for an initial concentration of 0.1 mM Cr(VI) in 0.01 M NaCl at pH about 2. Desorption conducted using 0.5 M phosphate solution at pH = 8 (column #6).

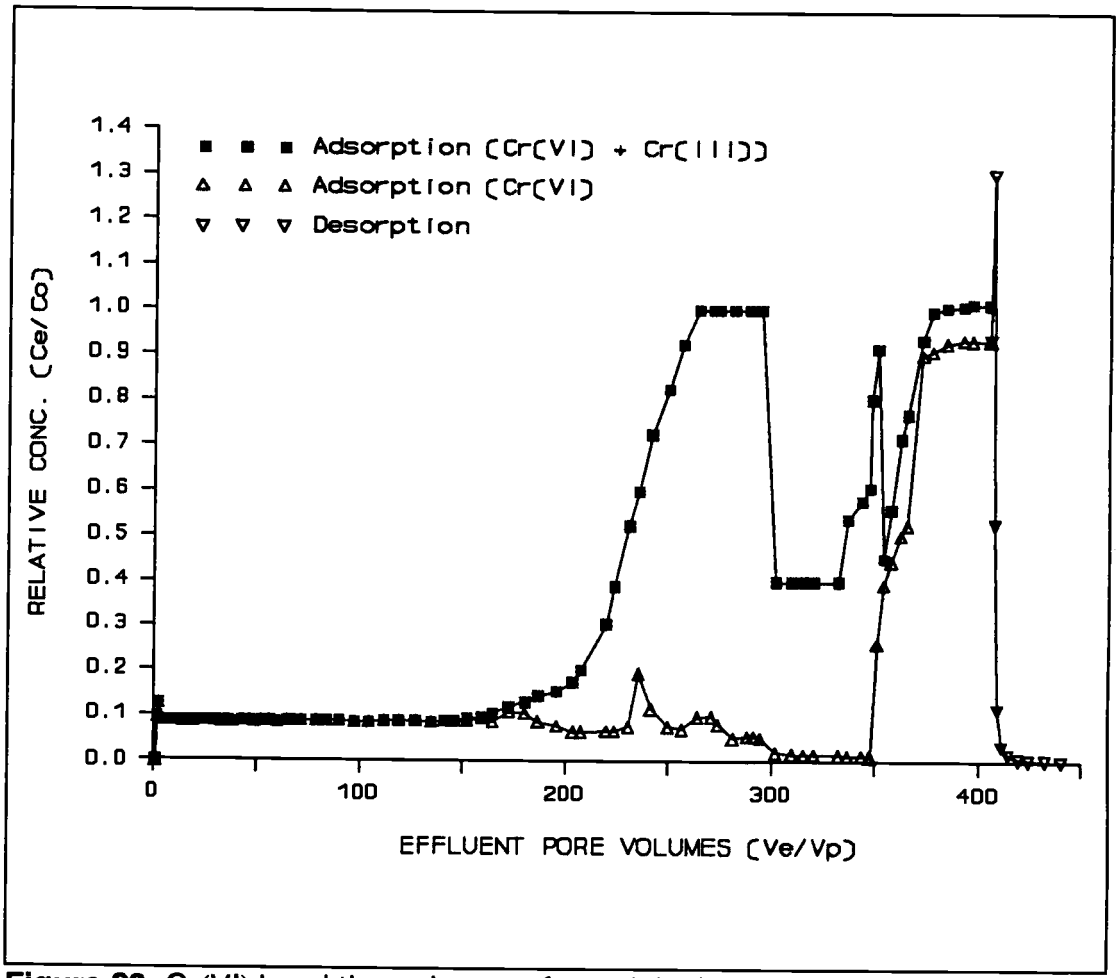

Figure 20: Cr(VI) breakthrough curve for an initial concentration of 0.1, 0.4, 1.0, and 10.0 mM Cr(VI) in 0.01 M NaCl at pH = 2. Desorption with 0.5 M phosphate solution at pH = 8 (column #7).

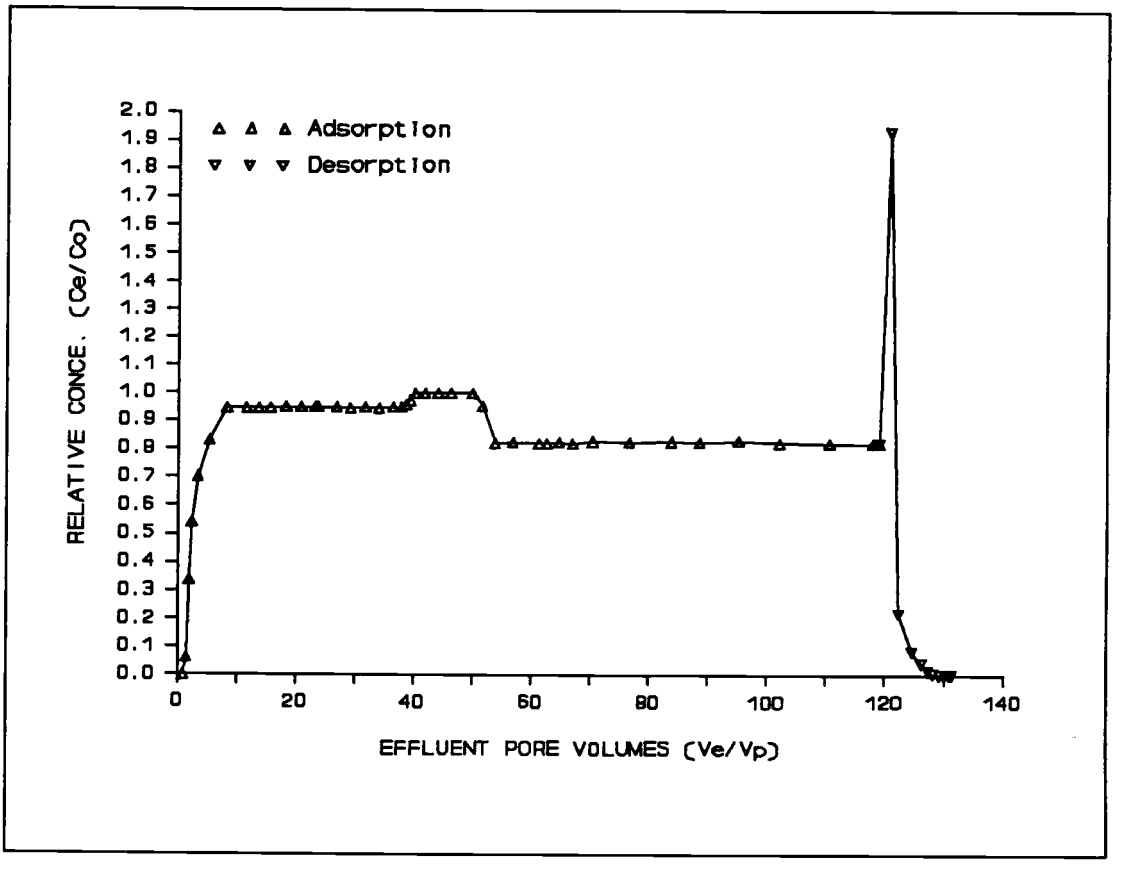

Figure 21: Cr(VI) breakthrough curve for an initial concentration of 10.0 mM Cr(VI) in 0.01 M NaCl. HCl added to the influent solution after 50 pore volumes at pH about 2. Desorption conducted using 0.5 M phosphate solution at pH about 8 (column #8).

Results of sequential batch extraction data for residual chromium from soil column experiments 1–8 are listed in Table 12. Distilled water extraction process was used to remove some readily desorbed Cr(VI) from the soil. Since only 13 pore volumes of 0.01 M NaCl was used to desorb Cr(VI) from the column # 2 (Table 11), distilled water extracted a small amount of Cr(VI) from this column.

Table 12: Sequential batch extraction data for residual chromium from soil column experiments.

Column no.	DDW (mmol/kg)	H_2PO_4/HPO_4[a] (mmol/kg)	Oxalate (mmol/kg)	DCB[b] (mmol/kg)	1 M HCl (mmol/kg)
1	0.0000	0.1500	0.0200	0.054	0.1441
2	0.0024	0.0098	0.0159	0.040	0.1663
3	0.0000	0.0000	0.0103	0.040	0.2044
4	0.0000	0.0000	0.0125	0.051	0.0302
5	0.0000	0.0000	0.0085	0.043	0.0196
6	0.0000	0.0000	0.1145	0.702	1.2504
7	0.0000	0.0000	0.2041	1.624	2.9759
8	0.0000	0.0000	1.4510	10.376	20.2510

[a]0.5 M phosphate at pH = 8, [b]Dithionite–citrate–bicarbonate

A phosphate extraction process was used to extract adsorbed Cr(VI) from the soil. Since phosphate or sulfate solutions were used to desorb Cr(VI) from the columns 3–8, the phosphate extraction did not remove Cr(VI) from these columns. The phosphate extraction yielded greater Cr(VI) from column # 1 compared with column # 2 because shutdown during desorption resulted in an increase in Cr(VI) removal from column # 2. Table 12 shows that small amounts of chromium were extracted by the ammonium oxalate extraction, while DCB extracted most of the

reduced chromium from the soil, indicating that it was predominantly in crystalline form. Total chromium extracted by 1 M HCl can be attributed to Cr(VI) minerals such as $BaCrO_4$ or chromite.

Results of a mass balance performed on soil column experiments 1–8 are listed in Table 13.

Table 13: Mass balance on Cr(VI) extraction from soil column experiments 1–8

Column no.	Cr(VI) REM[a] (mmol/kg)	Cr(VI) DES[b] (mmol/kg)	Cr(III) DES[c] (mmol/kg)	EXT[d] (mmol/kg)	RES[e] (mmol/kg)
1	0.709	0.326	0.00	0.368	0.015
2	0.371	0.136	0.00	0.226	0.009
3	0.501	0.240	0.00	0.248	0.013
4	0.186	0.088	0.00	0.094	0.004
5	0.138	0.064	0.00	0.071	0.003
6	2.490	0.354	0.00	2.067	0.069
7	56.300	12.940	37.38	4.804	1.176
8	47.83	14.630	0.00	32.078	1.132

[a]Cr(VI) removed from solution (adsorption and reduction), [b]Cr(VI) desorbed from the soil, [c]Cr(III) desorbed from the soil, [d]Total chromium extracted by sequential method, [e]Residual chromium in soil

As Table 13 shows, about 40–45 percent of total chromium removed from solution (REM) in columns 1–5 desorbed using either background electrolyte (NaCl) or competing oxyanion solutions. However only 14, 22, 30 percent of Cr(VI) removed from solution in columns # 6, # 7, and # 8 desorbed using phosphate solution, respectively. This can be explained by HCl addition to the influent solutions and increasing Cr(VI) reduction to Cr(III) which is not extractable with desorbing solution (phosphate). No Cr(III) was detected in effluent solutions from

the columns 1–6 and # 8, but 9.27, 8.63, and 19.48 mmol Cr(III)/kg per kilogram soil was removed from column # 7 when 0.4, 1.0, and 10 mM Cr(VI) at pH about 2 was added to the influent solution, respectively.

5.4 *Chromium(VI) Precipitation and Dissolution.* Thermodynamic calculations of the hexavalent chromium minerals $BaCrO_4$ and $BaSO_4$ are shown in Figure 22. Figure 22 shows the solubility diagram of $BaCrO_4$ and $BaSO_4$ in 0.01 M NaCl solution for the shallow wells (EW) at the United Chrome Sufperfund site. The data points in this plot were taken from a technical report (CH2M– Hill, 1990) and listed in Tables 46 and 47 in Appendix 2. As Figure 22 shows, $BaCrO_4$ may be present in the areas of EW–9, EW–16, EW–13, and EW–21 and $BaSO_4$ may be present in the areas of EW–8, EW–9, and EW–15, but all of the other groundwater samples are undersaturated with respect to $BaCrO_4$ and $BaSO_4$. CH2M–Hill report also listed 0.064 mmol/100 g of soil exchangeable Ba^{2+} and 0.23 mmol/100g of hydrochloric acid extractable Ba^{2+} in the upper silts. 1 M HCl–extractable chromium was assumed to be at least partially from $BaCrO_4$ precipitate. From the above results, it can be concluded that $BaCrO_4$ precipitation can be an important removal mechanism for chromium(VI) in soil and may be non–exchangeable with desorbing solutions. Further investigations are required to confirm this hypothesis.

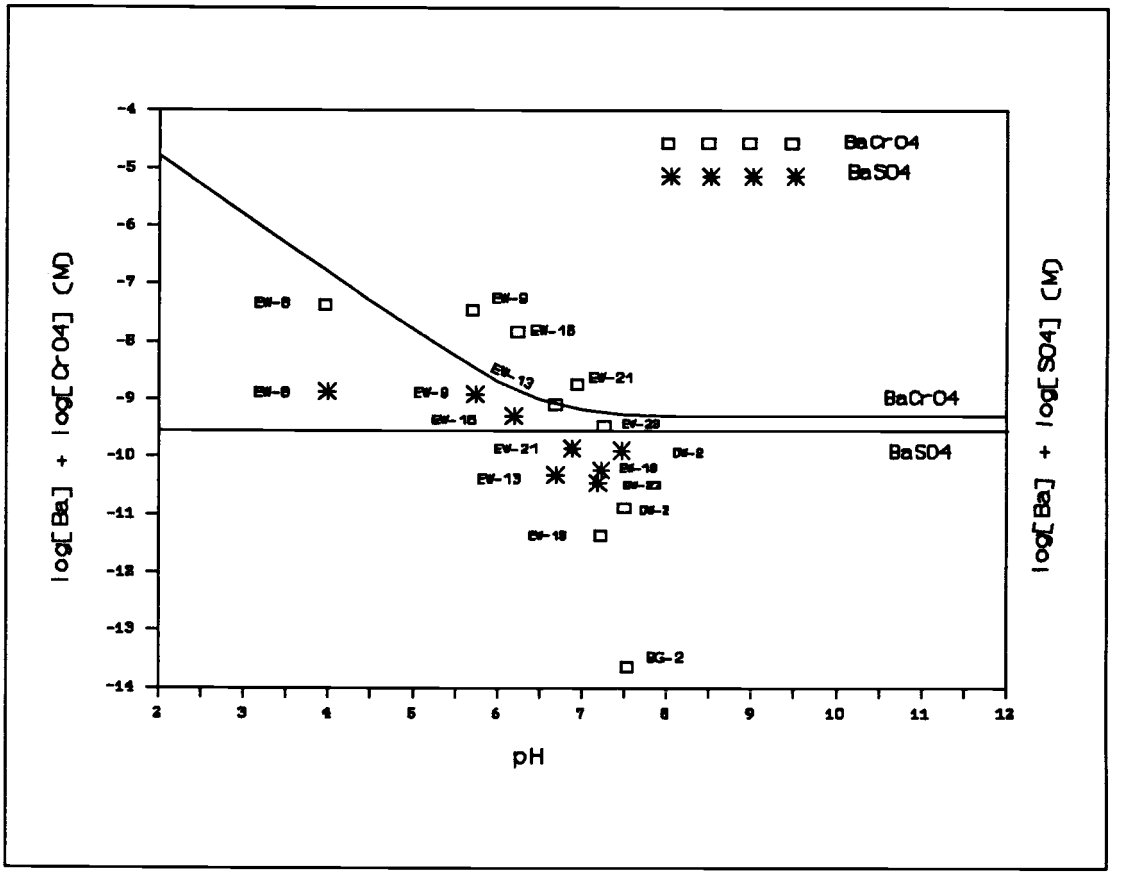

Figure 22: Solubility diagram of $BaCrO_4(s)$ and $BaSO_4(s)$ in 0.01 M NaCl solution versus pH at 25 °C for the shallow wells at the United Chrome Superfund site. Data points falling above the solubility lines indicate possible precipitation of solid phases.

5.5 Modeling Cr(VI) Adsorption in Batch Experiments

5.5.1 *Langmuir Model.* As shown in equations 36 and 41 (see section 4.1), the intrinsic equilibrium constants ($K^{int}_{SOH_2^+-CrO_4H^-}$ and $K^{int}_{SOH_2^+-CrO_4^{2-}}$) are related to the Langmiur adsorption constants (K_L and Γ_M), pH of the point–of–zero–charge (pH_{pzc}), dissociation constant of $HCrO_4^-$ (K_{a2}), and total chromate concentration. The intrinsic equilibrium constants obtained from the equilibrium isotherm experiments were log $K^{int}_{SOH_2^+-CrO_4H^-} = 8.95$ and log $K^{int}_{SOH_2^+-CrO_4^{2-}} = 16.5$.

5.5.2 *Triple Layer Model.* Surface complexation reactions of the CrO_4^{2-} and $HCrO_4^-$ ions were predicted by a triple–layer model (see section 4.2.2). The computer program FITEQL (Westall, 1982) with outer–sphere surface complexation reactions and two–site (FeOH and AlOH) modeling were used to simulate the chromate adsorption data. The constants for reactions 9 and 10 (section 4.2.6, Table 4) were calculated from data of 0.1 mM CrO_4^{2-} adsorption as a function of pH and at a soil concentration of 40 g/L, using the TLM and FITEQL. Convergence ($V_y = 5.2$) was obtained for adsorption edge data. The intrinsic equilibrium constants obtained were log $K^{int}_{FeOH_2^+-CrO_4H^-} = 10.37$ and log $K^{int}_{FeOH_2^+-CrO_4^{2-}} = 18.95$ and the estimated concentration of surface sites was 1.28×10^{-4} mol/L. Tables 49 and 50 in Appendix 3 report FITEQL input and output data for 0.1 mM Cr(VI) adsorption in 0.01 M NaCl solution and for varying pH, respectively.

Using the intrinsic equilibrium constants obtained from FITEQL along with surface area and inner–layer and outer–layer capacitances in the HYDRAQL

program (see section 4.3), we were able to simulate Cr(VI) sorption on the soil by potentiometric titrations. Figure 23 shows Cr(VI) adsorption experimental data and HYDRAQL simulation of 0.1 mM chromate adsorption as a function of pH. Tables 51 and 52 in Appendix 3 report HYDRAQL input and output data for 0.1 mM Cr(VI) adsorption in 0.01 M NaCl solution, respectively.

5.5.3 *Effect of Background Electrolyte on Cr(VI) Adsorption.* The effect of background electrolyte solution on Cr(VI) adsorption was described using the triple layer model and varying electrolyte solution concentration in the surface complexation model. Chromate adsorption as a function of pH and supporting electrolyte concentration (0.01 M, 0.1 M ,and 0.5 M NaCl) is shown in Figure 24. Tables 53–56 in Appendix 3 report HYDRAQL input and output data for 0.1 mM Cr(VI) adsorption in 0.1 and 0.5 M NaCl solution, respectively.

5.5.4 *Effects of Competing Oxyanions on Cr(VI) Adsorption.* Competing ion effects on Cr(VI) adsorption were described using the TLM and sulfate in the surface complexation model. The effect of 0.01 M sulfate ions on chromate adsorption as a function of pH is shown in Figure 25. Tables 57 and 58 in Appendix 3 report HYDRAQL input and output data for 0.1 mM Cr(VI) adsorption in 0.01 M sulfate solution.

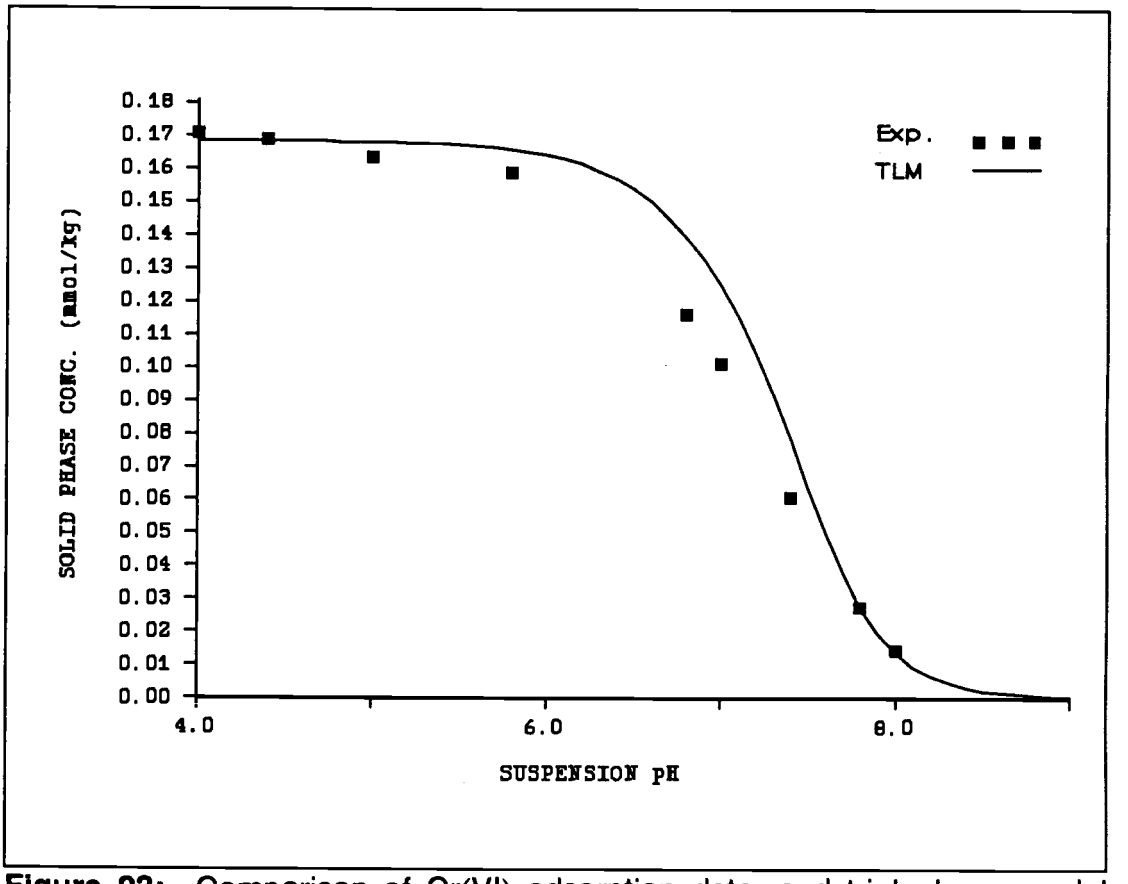

Figure 23: Comparison of Cr(VI) adsorption data, and triple–layer model (TLM) fit, as a function of pH, 0.1 mM Cr(VI) in 0.01 M NaCl electrolyte solution, 40 g/L soil.

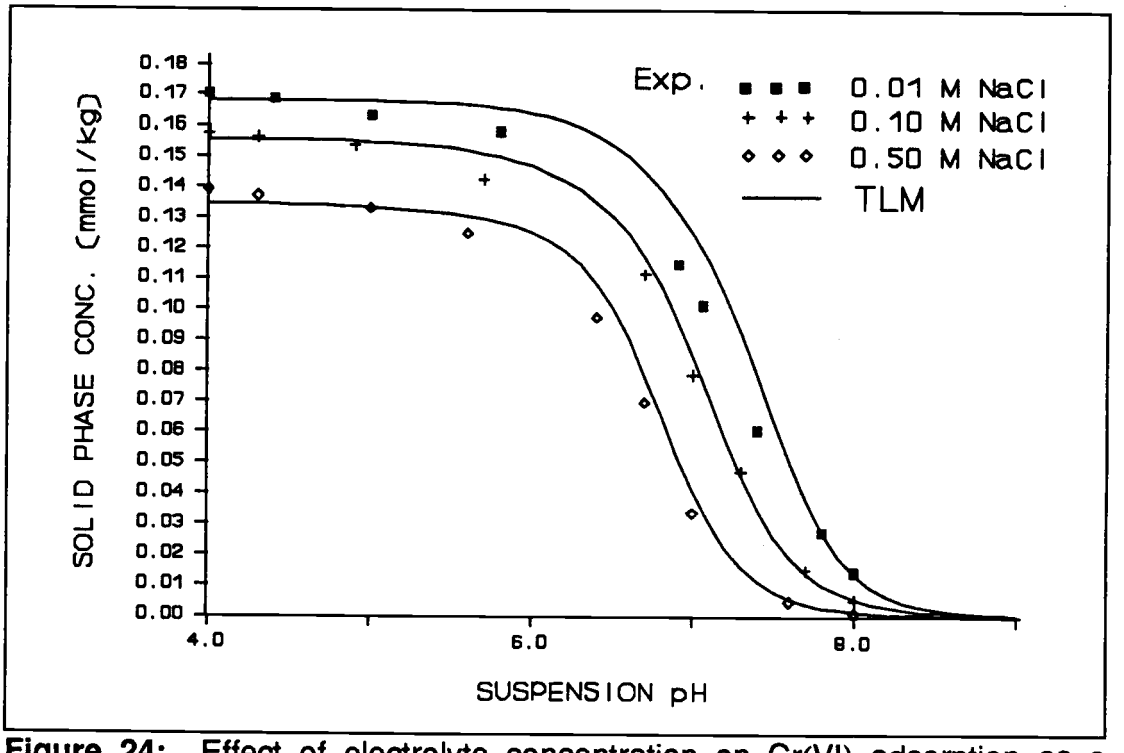

Figure 24: Effect of electrolyte concentration on Cr(VI) adsorption as a function of pH, and TLM fit, 0.1 mM Cr(VI), 40 g/L soil.

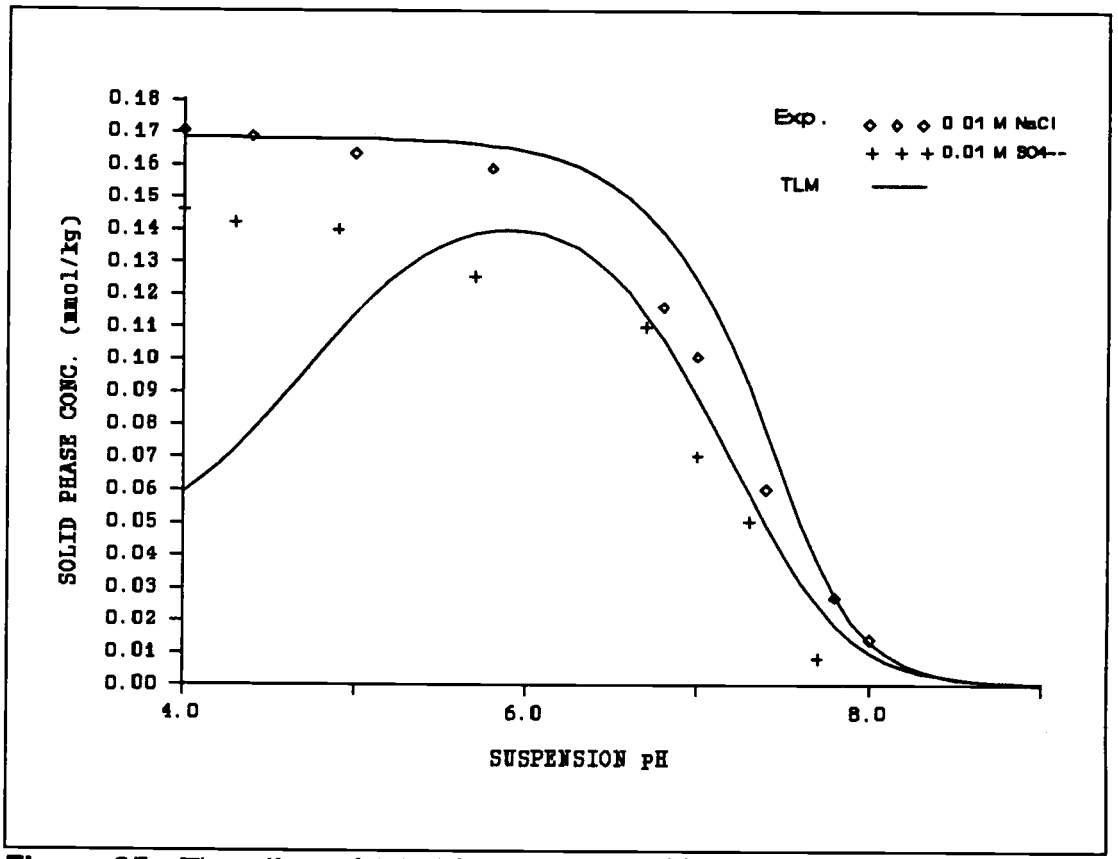

Figure 25: The effect of 0.01 M sulfate on Cr(VI) adsorption, and triple–layer model fit, as a function of pH, 0.1 mM Cr(VI), 40 g/l soil.

6. DISCUSSION OF THE RESULTS

6.1 *Chromium(VI) Reduction.* It was assumed that the soil was under oxidizing conditions since it was dried before usage. The average measured reduction capacities for the upper silts and aquitard soils ranged from 167 mM to 273 mM Cr(VI) reduced to Cr(III) per kilogram soil, respectively (Table 6). Palmer and Wittbrodt (1990) reported the reduction capacity of 163 mM Cr(VI) reduced to Cr(III) per kilogram in the upper silts for UCP soil. Chromium(VI) reduction by organic material most likely occurs under acidic conditions (Zachara et al., 1989), while the experimental soil was generally basic. The inorganic reduction capacities of the soil were higher than organic reduction capacities. This is understandable since our samples were relatively low in organic carbon (Table 10).

Magnetite (Fe_3O_4) is identified in both the upper silts and aquitard soil samples. The major peaks for the XRD pattern of magnetite are located between 30° and 60° 2Θ (Figures 26 and 27 in Appendix 1, Figures 28 and 29 also show the XRD pattern for pure magnetite). Since magnetite could not be perfectly isolated from the soil, quartz (SiO_2), anorthite ($CaAlSi_2O_8$), and muscovite ($KAl(Si_3Al)O_{10}(OHF)_2$ also appear in the pattern. Ilmenite ($FeTiO_3$), which is the another source of the ferrous iron, also appears in the pattern. The natural reducing ability of the soil can be quantitatively related to magnetite and the ferrous iron components (Tables 7 and 8). Eary and Rai (1989) concluded that chromate reduction with Fe^{2+} minerals occurs in the solution phase rather than

at the mineral surfaces. They also concluded that dissolution rates were more rapid in 0.01 M sulfate solutions than 0.01 M PO_4^{3-} because sulfate has greater affinity to complex with ferrous ions than phosphate. In agreement with the findings of Eary and Rai (1989), no Cr(III) was detected when phosphate was used as a competing oxyanion in Cr(VI) adsorption isotherms. But Cr(III) was detected (at pH 7.74 to 5.71), when sulfate was used instead of phosphate (Tables 36 and 37 in Appendix 2).

6.2 *Chromium(VI) Adsorption Kinetics.* The chromium(VI) removal process consists of an initial uptake followed by a slower, more time dependent removal. The kinetics of chromium removal from solution indicates that equilibrium was not achieved after 120 hours reaction time (Figure 6). Cameron and Klute (1983) explained such adsorption of solute to soils by a combination of equilibrium and kinetic models. These models incorporate a rapid reaction site which equilibrates instantaneously with adsorbate and a slow reaction site. Whether adsorption or possible reduction of Cr(VI) to Cr(III) was responsible for slow chromium uptake kinetics was not determined by Schroth (1989). He described such a removal process as a physical non–equilibrium phenomena. Our experiments showed that over the pH range considered, the Cr(VI) removal process exhibits a diphasic behavior with time (Figure 7). An initial, rapid, short–term uptake (phase I) of chromium(VI) is followed by a long–term, slower uptake (phase II). Reduction of Cr(VI) to Cr(III) was the suspected cause for slow Cr(VI) removal from solution and experimentally it was necessary to distinguish adsorption of Cr(VI) from Cr(VI) reduction to Cr(III). Phosphate (KH_2PO_4/K_2HPO_4) was found to be the best

extracting agent for adsorbed Cr(VI) in soils (Stollenwerk and Grove, 1985; Bartlett and Kimble, 1976; and James and Bartlett, 1983). In this study, Cr(VI) reduction to Cr(III) was the major cause of Cr(VI) removal by the soil. Chromium extracted from the soil by 0.5 M phosphate solution at pH about 8 was defined as the adsorbed fraction. Thus, any chromium that was not extracted was assumed to be reduced to Cr(III) which was immobile in the soil as a precipitated $Cr(OH)_3(s)$ phase. Cr(VI) adsorption was completed within 58 hours (Figure 7). Cr(VI) removal at longer reaction time (phase II) can be attributed to Cr(VI) reduction to Cr(III). It was concluded that phase I was largely due to diffusional transport and adsorption, as has been noted for the adsorption of chromium(VI) on soil (Zachara et al., 1989), while phase II was largely due to reduction of Cr(VI) to Cr(III).

6.2.1 *Effect of pH on Chromium(VI) Adsorption Kinetics.* Chromium(VI) adsorption kinetics increased with decreasing solution pH (Figure 8). In agreement with the findings of Griffin et. al., (1977), this can be explained by an increase in positive surface charges or electrostatic potential on soil particles with decreasing pH, resulting in more adsorption sites available for Cr(VI). Increasing adsorption sites increase Cr(VI) adsorption rate because the rate of reaction between the solution and adsorbent is proportional to the concentration of the reactants. Similar results were obtained by James and Bartlett (1983) for adsorption of Cr(VI) by various soils and $Fe(OH)_3$.

6.2.2 *Effect of Chromium(VI) Concentration on Adsorption Kinetics.* Chromium(VI) adsorption kinetics shows that adsorption rate increased with

increasing Cr(VI) concentration (Figure 9). Increased Cr(VI) uptake kinetics on the soil as Cr(VI) solution concentration increased is consistent with an adsorption removal mechanism because the rate of reaction is proportional to the concentration of the Cr(VI) solution.

6.3 *Adsorption and Desorption Kinetics in Soil Columns.* During the column experiments, the rate of Cr(VI) removal was high until the capacity of the soil for removing Cr(VI) was exhausted (within 3 to 5 pore volumes). Then removal decreased rapidly as reduction of Cr(VI) to Cr(III) began controlling the Cr(VI) removal rate (Figures 15–19). The difference between the rates of Cr(VI) desorption in column # 1 and column # 3, which were desorbed with 0.01 M NaCl and 0.01 M phosphate solutions, respectively, indicates that not reaction kinetics, but direct competition of phosphate with Cr(VI) for adsorption sites may be responsible for the difference between the two curves (compare Figures 14 and 16).

6.4 *Chromium(VI) Adsorption Isotherms.* Adsorption isotherms were developed for Cr(VI) adsorption on the experimental soil after 120 hours reaction time by excluding reduced Cr(III) from total chromium removal. Figure 11 shows that the equilibrium adsorption of Cr(VI) on a natural soil conformed well to the Langmuir isotherm at constant pH. Similar results have been noted by Griffin et al. (1977), Zachara et al. (1989), and Mesuere and Fish (1992) for the adsorption of chromate on clay minerals, natural soils, and goethite, respectively. The maximum sorption capacities at pH values of 5.65 and 7.00 were 2.6×10^{-4} and 1.4×10^{-4} mol Cr(VI)/kg soil, respectively. These values were lower than the

maximum adsorption capacities of 4.6 X 10^{-3} and 9.6 x 10^{-4} mol/kg at pH values of 5.33 and 6.94 for the adsorption of Cr(VI) on two soils reported by Zachara et al. (1989) for which no inorganic carbon was detected. This compares with 0.18 percent inorganic carbon content (Table 9) for the experimental soil in this study, which might be explained their lower adsorption capacities. Inorganic carbon (CO_3^{2-} and HCO_3^-) decreases chromate adsorption by competing for nonspecific adsorption sites (Davis and Leckie, 1980; and Zachara et al., 1987; and this study). Palmer and Wittbrodt (1990) showed that above pH 6.5 Cr(VI) adsorption on UPC soil was negligible. They also found that the adsorption data on UCP soil did not follow Langmuir isotherms very well. We assumed that reduction of Cr(VI) to Cr(III) was at least partially the reason for the poor fit of the adsorption data to the Langmuir model observed by Palmer and Wittbrodt (1990).

6.4.1 *Effect of Ionic Strength on Chromium(VI) Adsorption Isotherms.* Chromium(VI) adsorption edges in NaCl electrolyte solutions indicated that higher ionic strength resulted in less Cr(VI) adsorption. Less Cr(VI) was adsorbed (at adsorption equilibrium of column influent and effluent) when electrolyte concentration was increased in soil columns (Table 11). The effect of ionic strength is attributable to two effects: first, direct competition of Cl^- ion with Cr(VI) for oxyhydroxide surface sites (James and Bartlett, 1983) and second, decrease in the electrostatic potential near the surface sites (Davis and Leckie, 1980). The adsorption of Cr(VI) on hydrous Fe and Al oxides in the presence of Cl^- can be described by reactions 6 and 8 in Table 6. Cl^- adsorption on the soil reduces site density (see section 4.2.7), and consequently, reduces Cr(VI) adsorption. The

electrostatic potential effect of Cl^- on Cr(VI) adsorption can be attributed to the effect of the surface potential, ψ_β, on Cr(VI) surface complexation reactions (section 4.2.3, Eqs. 74 and 75). Increasing $[Cl^-]$ concentration decreases ψ_β and increases $\exp(F(\psi_o - \psi_\beta)/RT)$, and, consequently, decreases $[FeOH_2^+–HCrO_4^-]$ and $[FeOH_2^+–CrO_4^{2-}]$ concentrations, since $K^{int}_{FeOH_2^+–CrO_4H^-}$ and $K^{int}_{FeOH_2^+–CrO_4^{2-}}$ are constant.

6.4.2 *Effects of Competing Oxyanions on Chromium(VI) Adsorption Isotherms.* The effects of Cl^-, NO_3^-, HCO_3^-, and SO_4^{2-} on Cr(VI) adsorption are significantly less than that of $H_2PO_4^-/HPO_4^{2-}$ (Figure 13). Phosphate reduced Cr(VI) adsorption on the soil by nearly 100% at pH values greater than 5.5 and about 50 percent at pH 3. The smaller effects of Cl^-, NO_3^-, and HCO_3^- on Cr(VI) adsorption are nonspecific (Davis and Leckie, 1980), and can be attributed to decreased electrostatic potential near the particle surface. In contrast, phosphate and sulfate decreased Cr(VI) adsorption by direct competition for adsorption sites (Zachara et al., 1987 and Bartlett and Kimble, 1976). The greater influence of phosphate compared with sulfate may be related to the presence of H^+ and hydrogen bonding or precipitation of Fe phosphate minerals (Stollenwerk and Grove, 1985).

6.5 *Chromium(VI) Desorption in Soil Columns.* The extensive tailing of the Cr(VI) desorption limbs with NaCl solutions in soil columns # 1 and # 2 resulted from retarded Cr(VI) desorption (Figures 14 and 15). Similar results were obtained by Stollenwerk and Grove (1989) for desorption of Cr(VI) from soil column experiments. Schroth (1989) described such behavior by non–equilibrium conditions during desorption. The phosphate and sulfate addition in the columns

3–8 caused Cr(VI) spikes in the effluent, exceeding the initial influent Cr(VI) concentration (Figures 16–21). These spikes were followed by a steep decline of Cr(VI) concentration to almost zero. Little or no curve tailing was observed in the desorption limbs when phosphate or sulfate were used as desorption solutions. It is concluded that NaCl solution only slightly competes with Cr(VI) for sorption sites via a presumed outer–sphere complexation reaction, while phosphate and sulfate directly compete with Cr(VI) for adsorption sites.

6.6 *Chromium(VI) Reduction in Soil Columns.* Slight pH increases in effluent solutions from soil column experiments 1–3 can also be related to reduction of Cr(VI) to Cr(III) which consumed protons (Table 11). HCl addition to the influent solution increased Cr(VI) removal in soil columns 6–8 (Table 12). We attribute this to increased Cr(VI) reduction to Cr(III) (Table 12). In soil column experiments 1–7, equilibrium of soil column with influent chromium solution ($C_e/C_o = 1$) was not achieved even after 100 pore volumes of total flow through the column. This can be explained by a steady reduction of Cr(VI) to Cr(III) which is verified by Cr(III) extracted with oxalate and DCB (Table 12). In column # 8, equilibrium ($C_e/C_o = 1$) was achieved after 40 pore volumes, since the influent Cr(VI) concentration was high (500 mg/L Cr(VI)) and the reduction capacity of the soil due to magnetite was attained. Total chromium removed from soil column # 8 within 40 pore volumes was close to the magnetite reduction capacity of the aquitard soil (Table 7). Table 13 shows that the amount of residual chromium in the soil is fairly constant (about 2 %). The residual chromium could be due to Cr(III) ions which are substituted in the lattice structure of minerals such as natural α–Al_2O_3 and aluminosilicates.

6.7 Adsorption Modeling

6.7.1 *Triple Layer Model.* The triple layer modeling used in this study focused on the role of hydrous Fe and Al oxides, which were thought to dominate the adsorption of Cr(VI) on the soil (Zachara et al., 1989). A good agreement between the triple–layer model prediction and experimental data was observed for adsorption edges (Figures 23–25). Table 14 contains surface equilibrium constants of Cr(VI) adsorption determined in this study and elsewhere.

Table 14: Intrinsic surface complexation constants for Cr(VI) adsorption on amorphous oxyhydroxide and on natural soils

Material	Surface species	log K^{int}	Reference
Natural Soil	$FeOH_2^+$–$HCrO_4^-$ $FeOH_2^+$–CrO_4^{2-}	10.4 18.9	Figures 23–25 (this study)
Natural Soil	$FeOH_2^+$–$HCrO_4^-$ $FeOH_2^+$–CrO_4^{2-}	9.8 19.4	Zachara et al., 1989
$Fe_2O_3.H_2O$(am)	SOH_2^+–$HCrO_4^-$ SOH_2^+–CrO_4^{2-}	10.6 18.1	Davis and Leckie, 1980

Table 14 shows that the intrinsic equilibrium constants on natural soils and pure hydrous Fe oxide obtained from the TLM model are similar, which further verifies the hypothesized reaction mechanism (Table 4) in the experimental soil.

The triple layer model simulated well the effect of ionic strength on chromate adsorption (Figure 24). Raising the background electrolyte concentration from 0.01 M to 0.5 M NaCl reduced chromate adsorption. By

comparison, ionic strength effects were almost undetectable for strongly adsorbing anions such as selenite, whereas ionic strength had more effect on weakly adsorbing anions such as sulfate and selenate (Hayes et. al., 1987). Changing the background electrolyte concentration also influences adsorption by affecting the activity of adsorbing species (Hayes et. al., 1987). Outer–sphere surface complexes are more sensitive to ionic–strength variations than inner–sphere complexes, since electrolyte ions are placed in the same plane as the outer–sphere complexes (Davis et. al., 1978). It was concluded that chromate adsorption on the experimental soil can be explained by outer–sphere surface complexes.

The effects of competing oxyanions on chromate adsorption were also described using the triple–layer model. Attempts to use the TLM model to simulate chromate adsorption in the presence of 0.01 M phosphate ions failed, since there was very little or no Cr(VI) adsorption in 0.01 M phosphate solution. Competition with 0.01 M sulfate was modeled using previously derived binding constants for sulfate on ferrihydrite (Zachara et. al., 1987) (Figure 25). The model simulation matched the data closely in the pH range 6 to 8. Deviations of TLM calculations were observed for pH less than 6, where the model simulations underestimated Cr(VI) adsorption. Since the fit of model simulations to experimental data is dependent on the value of site density (see section 4.2.7), at lower pH values, actual sulfate adsorption probably exceeded the site density used in the model. Similar simulations for the effect of sulfate on Cr(VI) adsorption by the soil were presented by Zachara, et al. (1989).

6.7.2 *Langmuir Adsorption Model.* The Langmuir model was used to determine the intrinsic equilibrium constants of Cr(VI) adsorption reactions, using a single adsorbate (CrO_4^{2-} or $HCrO_4^-$ ions) and a single adsorbent (SOH). The concepts and assumptions used to relate the intrinsic equilibrium constant of Cr(VI) reactions on the soil surface to the Langmuir adsorption constants and chromate concentration at constant pH values were discussed in section 4.1. Attempts to use the intrinsic equilibrium constants obtained from an empirical expression to simulate chromate adsorption on the experimental soil failed, since there is about two log units difference between equilibrium constants obtained from the empirical expression (Langmuir model) and constants from triple–layer modeling approach. The dependence of adsorption equilibrium on pH is significant, and an empirical expression that is valid only for a constant pH value would be of limited use in modeling the migration of chromium(VI) in contaminated soils. However, if linked with geochemical aqueous speciation models (e.g. MINEQL; Westall et al., 1986), such generalized empirical expressions for adsorption could prove useful in complexation models. The differences between the intrinsic equilibrium constants obtained from the two–site (FeOH and AlOH) triple–layer–modeling and from the equilibrium isotherm experimental data, using single ideal oxide sites (SOH), can be accounted for by the electrical double layer properties of a mixture of mineral phases and their surface coatings. The determination of binding constants in laboratory experiments is complicated by variable solution compositions that may evolve from the dissolution of mineral phases and the

desorption of Cr(VI) ions. The surface complexation modeling approach has advantages over empirical ones (Langmuir model), since surface complexation models consider aqueous speciation and the sorption reactivity of all aqueous species (see Table 4).

7. SUMMARY AND CONCLUSIONS

Laboratory batch and column experiments were conducted to elucidate the chemical behavior of chromium in a natural soil. The results show that adsorption and reduction are major reactions accounting for removal of chromium (VI) from solution in a natural soil. While adsorption is low under the conditions present in this soil, reduction potential is high even at pH above 8.

Magnetite (identified in experimental soil by X–ray diffraction on magnetically enriched samples) is effective in the reduction of Cr(VI) to Cr(III) even in neutral to alkaline pH values. Ferrous ions contained in the soil cause the reduction of Cr(VI) to Cr(III), followed by precipitation of $Cr(OH)_{3(s)}$ or $(Cr, Fe)(OH)_{3(s)}$. The reduction process is highly time–dependent and continues until the reduction capacity of the soil is attained. It is concluded that chemical reactions such as reduction strongly influence chromium mobility in soil.

Adsorption kinetic experiments indicated that Cr(VI) removal from solution increased with increasing solute concentration and with decreasing solute pH. Adsorption reactions reached equilibrium within 58 hours in batch reactors. Increasing background electrolyte concentration (NaCl) decreased Cr(VI) adsorption on soil. The adsorption isotherm of Cr(VI) for this soil conforms well to the Langmuir isotherm at constant pH. Two Cr(VI) adsorption parameters, the maximum sorption capacity (Γ_M) and Langmuir adsorption constant (K_L), were determined in 120 hours isotherm experiments.

Results of soil column experiments were expressed using breakthrough and desorption curves which show that both retardation (adsorption) and loss of mass (reduction) processes occur in the experimental soil. Desorption with background electrolyte solution (NaCl) showed extensive tailing in desorption limb, while little or no tailing was observed when phosphate or sulfate were used as desorption solutions. However, only slightly more Cr(VI) could be recovered using the phosphate or sulfate solutions compared to background electrolyte solution, indicating that Cr(VI) adsorption is a reversible process.

Adsorption of CrO_4^{2-} and $HCrO_4^-$ can be explained by a positive net surface charge on the soil at the groundwater pH of 6.9. Outer–sphere surface complexation reactions and two–site (FeOH and AlOH) triple layer modeling were used to closely simulate adsorption of the chromate (CrO_4^{2-}) and bichromate ($HCrO_4^-$) ions on a natural soil. The results show the ability of two–site surface complexation model simulations to fit adsorption data in background electrolyte and competing oxyanion solutions.

The following specific conclusions are made based on the results of this research:

1. The rate of Cr(VI) removal from solution by a natural soil is influenced by both adsorption and reduction. Adsorption reactions reach equilibrium within 58 hours, while reduction reactions continue until the reduction capacity of the soil is attained.
2. The rate of Cr(VI) removal from solution increases strongly with

decreasing pH and increasing initial Cr(VI) concentration.

3. The equilibrium adsorption distribution of Cr(VI) on a natural soil conforms well to the Langmuir isotherm at constant pH.

4. Ferrous iron–containing minerals, particularly magnetite, reduce Cr(VI) to Cr(III) and contribute significantly to Cr(VI) removal from solution.

5. The equilibrium adsorption of Cr(VI) on a natural soil decreases with increasing background electrolyte concentration.

6. Oxyanions, particularly phosphate, compete effectively with chromate species for adsorption sites on a natural soil.

7. Outer sphere surface complexation reactions and two–site (FeOH and AlOH) modeling closely simulate adsorption of the chromate (CrO_4^{2-}) and bichromate ($HCrO_4^-$) ions on a natural soil.

8. ENGINEERING SIGNIFICANCE

The results of this study can be extended to the remediation of chromium–contaminated soils.

1. *Significance of chromium(VI) reduction, adsorption, desorption/extraction, and precipitation/dissolution for pump-and-treat method of soil remediation.*

Reduction. The presence of magnetite (Fe_3O_4) and other ferrous iron containing minerals in soils provides a measure of the amount of material readily available for the reduction of Cr(VI) to Cr(III). The residual ferrous ions in the soil can contribute to the long–term reduction capacity of the aquifer soil. This in combination with magnetite can be regarded to represent the maximum reduction capacity of the aquifer soil. The maximum reduction capacity of the soil can be used to estimate the maximum amount of chromium(III) that remains in the aquifer at the end of remediation.

Adsorption. The equilibrium adsorption of chromate on soils conforms to the Langmuir isotherm. The adsorption parameters obtained can be used in assessment models to predict adsorption capacity of the soil. The adsorption parameters can be used also in solute transport models that include adsorption. Intrinsic equilibrium constants for Cr(VI) adsorption on iron oxyhydroxide can be used to analyze adsorption data derived from more complicated systems in natural soils, such as surface competitive adsorption of inorganic oxyanions or organic acids.

Desorption/Extraction. Breakthrough and desorption curves generated in soil columns can be used in assessing the efficacy of soil remediation by desorption using pump–and–treat processes. Chemically–enhanced extraction (competitive anion addition) can be compared to background electrolyte solutions (e.g. groundwater) in the desorption limb to contrast desorption kinetics.

Chromium extractions by sequential extraction methods, using distilled water, phosphate, oxalate, and DCB, provide information about the amount of chromium that is easily removed and that more difficult to remove from the aquifer. This information is useful in making decisions about the amount of chromium in the soil that can be removed practically by pump–and–treat.

Precipitation/Dissolution. Chromium(VI) solid phases can influence remediation schemes. The potential of different Cr mineral phases to precipitate in the aquifer can be calculated if complete chemical analyses are available. Thermodynamic calculations showed that chromium(VI) minerals such as $BaCrO_4$ might be present in aquifer soils. The existence of such mineral phases can extend the time required to remediate the soil by extraction methods such as pump–and–treat.

2. *Mobilizing chromium(VI) by the effects of ionic strength and competing oxyanions for pump-and-treat method:*

Ionic Strength. High ionic strength solutions (0.1 to 0.5 M NaCl) were found to enhance the rate of Cr(VI) removal from the soil compared with low ionic strength solutions such as groundwater. The concomitant effect of pH decrease has to

be considered also, since high ionic strength (e.g. high Na^+ concentration) causes H^+ release into the solution through exchange of cation (Na^+) with hydrogen ions, which results in decreasing solution pH. Decreased pH could result in more Cr(VI) adsorption and reduction, and, consequently, in decreased chromium removal from the soil.

Competing Oxyanions. The effectiveness of competitive anions (0.01 M) in the decreasing of Cr(VI) adsorption was found to be in the order: phosphate > sulfate > bicarbonate > nitrate > chloride. A chemically–enhanced pump–and–treat process using phosphate solution for chromium(VI) removal from the soil would appear to be most effective. However, one must assess accurately the solution speciation to identify possible formation of phosphate solid phases (e.g. $Ca_5OH(PO_4)_3$). This may limit the applicability of this process in the soil. Some control of precipitation of suspected solid phases can be exerted through the controlling of ionic solution concentrations and solution pH.

3. *Immobilizing chromium(VI) by reduction to Cr(III) and precipitation onto the soil:*

Results of this study indicated that Cr(VI) is readily reduced to Cr(III) in the presence of ferrous–iron–containing minerals even at alkaline pH values. Reduction can be increased by decreasing soil solution pH (e.g. strong acid addition), enhancing Cr(VI) reduction to Cr(III) with subsequent precipitation as $Cr(OH)_3(s)$ or $(Cr, Fe)(OH)_3(s)$, thus immobilizing chromium in the soil. pH serves a dual function as a regulator of the rate of Cr(VI) reduction and as a regulator

of the solubility of Cr(III) solid phases. Based on our soil column experiments, a pH range of 4.0 to 6.0 is recommended for immobilization of chromium(III) in soil. At pH less than 6.0, the rate of Cr(VI) reduction increases, because any ferrous ions produced by dissolution will reduce Cr(VI) in solution. At pH less than 4.0, Cr(III) will stay in solution due to dissolution of Cr(III) solid phases if maximum capacity of soil to adsorb Cr(III) is attained. The solubility of the Cr(III) should be checked under the solution conditions expected, including the formation of soluble complexes with inorganic and organic ligands in the soil solution.

9. REFERENCES

1. Ainsworth, C. C., Grivin, D. C., Zachara, J. M., and Smith, S. C., "Chromate Adsorption on Goehtite: Effects of Aluminum Substitution," Soil Science Society of American Journal, Vol. 53, pp.411–418, March 1989.

2. Barcelona, M. J. and Holm, T. R., "Oxidation–Reduction Capacity of Aquifer Solids," Environmental Science and Technology, Vol. 25, No. 9, pp. 1565–1572, 1991.

3. Bartlett, R. J., and James B. J., "Behavior of Chromium in Soils: III. Oxidation", Journal of Environmental Quality, Vol. 8, No. 1, pp. 31–35, 1979.

4. Bartlett, R. J., and James B. J., "Mobility and Bioavailability of Chromium in Soils", in: Chromium in the Natural and Human Environments, Vol. 20 (Nriagu, J. O., and Nieboer, E.), pp. 267–304, 1988.

5. Bartlett, R. J., and Kimble, J. M., "Behavior of Chromium in Soils: I. Trivalent Forms", Journal of Environmental Quality, Vol. 5, No. 4, pp. 379–383, 1976.

6. Bartlett, R. J., and Kimble, J. M., "Behavior of Chromium in Soils: II. Hexavalent Forms," Journal of Environmental Quality, Vol. 5, No. 4, pp. 383–386, 1976.

7. Bean, G. R., "Adsorption of Hexavalent chromium to a Clay Silt Soil: Batch Kinetic and Equilibrium Studies," M. S. Thesis, Civil Engineering Department, Oregon State University, Corvallis, Oregon, 1989.

8. Begheijn, L. Th., "Determination of Iron(II) in Rock, Soil and Clay," Analyst, Vol. 104, pp. 1055–1061, 1979.

9. Beyer G. L. and Rieman W., "The Solubility Product of Barium Chromate at Various Iron Strengths," Journal of American Chemical Society, Vol. 65, pp. 971–973, 1943.

10. Brownawell, B. J., Chen Hua, Collier, J. M., and Westall, J. C., "Adsorption of Organic Cations to Natural Materials," Environmental Science and Technology, Vol. 24, No.8, pp. 1234–1241, 1990.

11. Bundy L. G. and Bremner J. M. "A Simple Titration Method for Determination of Inorganic Carbon in Soils," Soil Science Society of American Proceeding, Vol. 36, pp. 273–275, 1972.

12. Calder, L. M., "Chromium Contamination of Groundwater," in: Chromium in the Natural and Human Environments, Vol. 20 (Nriagu, J. O., and Nieboer, E.), pp. 215–229 (1988).

13. Cameron, D. R. and Klute, A., "Convection–Dispersion Solute Transport with a Combined Equilibrium and Kinetic Adsorption Model," Water Resources Research, Vol. 13, No. 1, pp. 183–188, 1977.

14. CH2M–Hill "Stage 2 Deep Aquifer Drilling Technical Report," United Chrome Products Site, Corvallis, Oregon, September 28, 1990.

15. Cotton , F. Albert, and Wilkinson, Geoffrey, Advanced Inorganic Chemistry: A Comprehensive Text, Wiley Interscience, New York, 1972.

16. Davies–Colley, R. J., Ph. D. Thesis, Oregon State University, Corvallis, Oregon, pp. 1–224, 1981.

17. Davis, J. A., and Leckie, J. O., "Surface Ionization and Complexation at the Oxide/water Interface 3. Adsorption of Anions," Journal of Colloid and Interface Science, Vol. 74, No. 1, pp. 32–43, 1980.

18. Davis, J. A., James, R. O., Leckie, J. O., "Surface Ionization and Complexation at the Oxide/water Interface 1. Computation of Electrical Double Layer Properties in Simple electrolytes," Journal of Colloid and Interface Science, Vol. 63, No. 3, pp. 480–499, 1978.

19. Davis, J. A., and Leckie, J. O., "Surface Ionization and Complexation at the Oxide/Water Interface," Journal of Colloid and Interface Science, Vol. 67, No. 1, pp. 90–107, 1978.

20. Dzombak, D. A., Morel, Francois, M. M., "Columbic Interactions and Activity Coefficients" in Surface Complexation Modeling, p. 34, 1990.

21. Eary, L. E., and Rai, D., "Kinetics of Chromium(III) Oxidation to Chromium(VI) by Reaction with Manganese Dioxide", Environmental Science and Technology, Vol. 2, pp. 1187–1193, 1987.

22. Eary, L. E., and Rai, D., "Kinetics of Chromate Reduction by Ferrous Ions Derived from Hematite and Biotite at 25 °C," American Journal of Science, Vol. 289, PP. 180–213, 1989.

23. Edzwald, J. K., Toensing, D. C., and Leung, M. C., "Phophate Adsorption Reactions with Clay Minerals," Environmental Science and Technology, Vol. 10, No. 5, pp. 485–490, 1976.

24. Fendorf, S. E., and Zasoki, R. J., "Chromium (III) Oxidation by β–MnO_2. 1. Characterization," Environmental Science and Technology, Vol. 26, No. 1, pp. 79–85, 1992.

25. Griffin, R. A., Au, A. K., and Frost, R. R., "Effect of pH on Adsorption of Chromium From Landfill–Leachate by Clay Minerals," Journal of Environmental Science and Health, A12(8), pp. 431–449, 1977.

26. Hayes, K. F., and Leckie, J. O., "Modeling Ionic Strength Effects on Cation Adsorption at Hydrous Oxide/Solution Interfaces," Journal of Colloid and Interface Science, Vol. 115, 564, 1987.

27. Hayes, K. F., Papelis, C., and Leckie, J. O., "Modeling Ionic Strength Effects on Anion Adsorption at Hydrous Oxide/Solution Interfaces," Journal of Colloid and Interface Science, Vol. 125, No. 2, pp. 717– 726, 1988.

28. Heilman, M. D., Carter, D. L., and Gonzalez, C. L., "The Ethylene Glycol Momethly Ether (EGME) Technique for Determination Soil–Surface Area," Soil Science, Vol. 100, No.6, pp. 409–413, 1965.

29. Hingston, F. R., Atkinson, R. J., Posner, A. M., and Qurik, J. P., "The Specific Adsorption of Anion", Nature Vol. 215, pp.1459–1461, 1967.

30. James, B. R. and Bartlett R. J. "Behavior of Chromium in Soils: VII. Adsorption and reduction of Hexavalent Forms," Journal of Environmental Quality, Vol. 12, No. 2, pp.177–181, 1983.

31. Mckeage, J. A. and Day, J. H., "Dithionite– and Xalate–Extractable Fe and Al as Aids in Differentiating Various Classes of Soils," Canadian Journal of Soil Science, Vol. 46, pp. 13–22, 1965.

32. Mehra, O. P., and Jackson, M. L., (1960), "Iron Oxide Removal from Soils and Clays by a Dithionite–Citrate System Buffered with Sodium Bicarbonate," *Clays and Clay Minerals*, Stucki, J. W., et al., Reidel Publishing Co. pp. 83–98, 1988.

33. Mesuere, K. and Fish, W., "Chromate and Oxalate Adsorption on Goethite. 1. Calibration of Surface Complexation Models," Environmental Sciences and Technology, Vol. 26, No. 12, pp. 2357–2364, 1992.

34. Nriegu, J. O., "Historical perspectives," in: Chromium in the Natural and Human Environments, Vol. 20, pp. 1–12, 1988.

35. Palmer, C. D. and Wittbrodt, P. R., "Geochemical characterization of the United Chrome Products site," Final Report, Environmental Science and Engineering, Oregon Graduate Institute, in: CH2M–Hill, Inc.: United Chrome Products Superfund site, phase II, 1990.

36. Parks G. A. and De Bruyn P. L. "The Zero Point of Charge of Oxides," Journal of Physical Chemistry, Vol. 66, pp. 967–973, 1962.

37. Papelis, C., Hayes, K. F., and Leckie J. O., "HYDRAQL: A Program for the Computation of Chemical Equilibrium Composition of Aqueous Batch Systems Including Surface–Complexation Modeling of Ion Adsorption at the Oxide/solution Interface," Environmental Engineering and Science, Department of Civil Engineering, Stanford University, Technical Report No. 306, September 1988.

38. Rai, D., Zachara, J. M., Schwab A. P., Schmidt R. L., Grivin D. C., Rogers J. E., "Chemical Attenuation Rates, Coefficients, and Constants in Leachate Migration," Electric Power Research Institute. EPRI EA–3356, Vol. 1, Project 21298–1, 1984.

39. Sabine, G., personal communication. USDA–ARS, U.S. Salinity Lab, Riverside, California, 925091.

40. Schroth, H. M., "A Kinetic Solute Transport Model for the Movement of Chromium(VI) Through Soils," Department of Civil Engineering, Oregon State University, Corvallis, Oregon, 1989.

41. Sengupta. A. K., and Clifford, D., "Important Process Variables in Chromate Ion Exchange," Environmental Science and Technology, Vol. 20, No. 2, pp. 149–155, 1986.

42. Snoeyink, V. L., and Jenkins, D., Water Chemistry, John Wiley and Sons, Inc., New York, 1980.

43. Sposito, Garrison, The Surface Chemistry of Soils, Oxford University Press, New York, 1984.

44. Sposito, Garrison, The Chemistry of Soils, Oxford Press, New York, 1989.

45. Stollenwerk, K. G., and Grove, D. B., "Adsorption and Desorption od Hexavalent Chromium in an Alluvial Aquifer Near Telluride, Colorado," Journal of Environmental Quality, Vol. 14, No. 1, pp. 150–155, 1985.

46. Stumm, W., and Morgan, J. J., Aquatic Chemistry: An Introduction Emphasizing Equilibria in Natural Waters, 2nd Ed., Wiley–Intersience, New York, 1981.

47. Trotman–Dickenson, A. F., Ed. Comprehensive Inorganic Chemistry, Pergamon Press, Oxford, Vol. 3, pp.691–700 (1973).

48. Van Dr Weijden, C. H. and Reith M. "Chromium(III)–Chromium(VI) Interconversions in Seawater," Marine Chemistry, No. 11 pp. 565–572, 1982.

49. Wang, P., Mori, T., Komori, K., Sastsu, M., Toda, K., and ohtake, H., "Isolation and Characterization of an Enterobacter Cloacae Strain that Reduces Hexavalent Chromium Under Anaerobic Conditions," Applied Environmental Microbial, 65, 1665–1669, 1989.

50. Westall, J. C., " FITEQL: A Computer Program for Determination of Chemical Equilibrium Constants from Equilibrium Data; Version 1.2. Report 82–01," Oregon State University, Corvallis, Oregon, 1982.

51. Westall, J. C. FITEQL: A Computer Program for Determination of Chemical Equilibrium Constants from Equilibrium Data; Version 2.0. Report 82–02; Oregon State University, Corvallis, Oregon, 1982.

52. Westall, J. C., Zachara, J. L., and Morel, F. M. M., "MINEQL: A Computer Program for the Calculation of the Chemical Equilibrium Composition of Aqueous Systems," Version 1.0, Report 86–01, 1986.

53. Zachara, J. M., Grivin, D. C., Schmidt R. L., and Resch, C., T., "Chromium Adsorption on Amorphous Iron Oxyhyroxide in the presence of Major Groundwater Ions," Environmental Science and Technology, Vol. 21, No. 6, pp.589–594, 1987.

54. Zachara, J. M., Ainsworth, C. C., Cowan, C. E., Resch, C. T., "Adsorption of Chromium by Subsurface Soil Horizons," Soil Science Society of American Journal, Vol. 53, pp.418–428, 1989.

APPENDICES

APPENDIX 1

X–ray Diffraction (XRD) Curves of the Soil and pH and flow rate curves of soil column experiments.

This appendix contains the X–ray diffraction (XRD) of magnetically separated sample from a natural soil and pure magnetite. It also contains the pH and flow rate curves of soil column experiments.

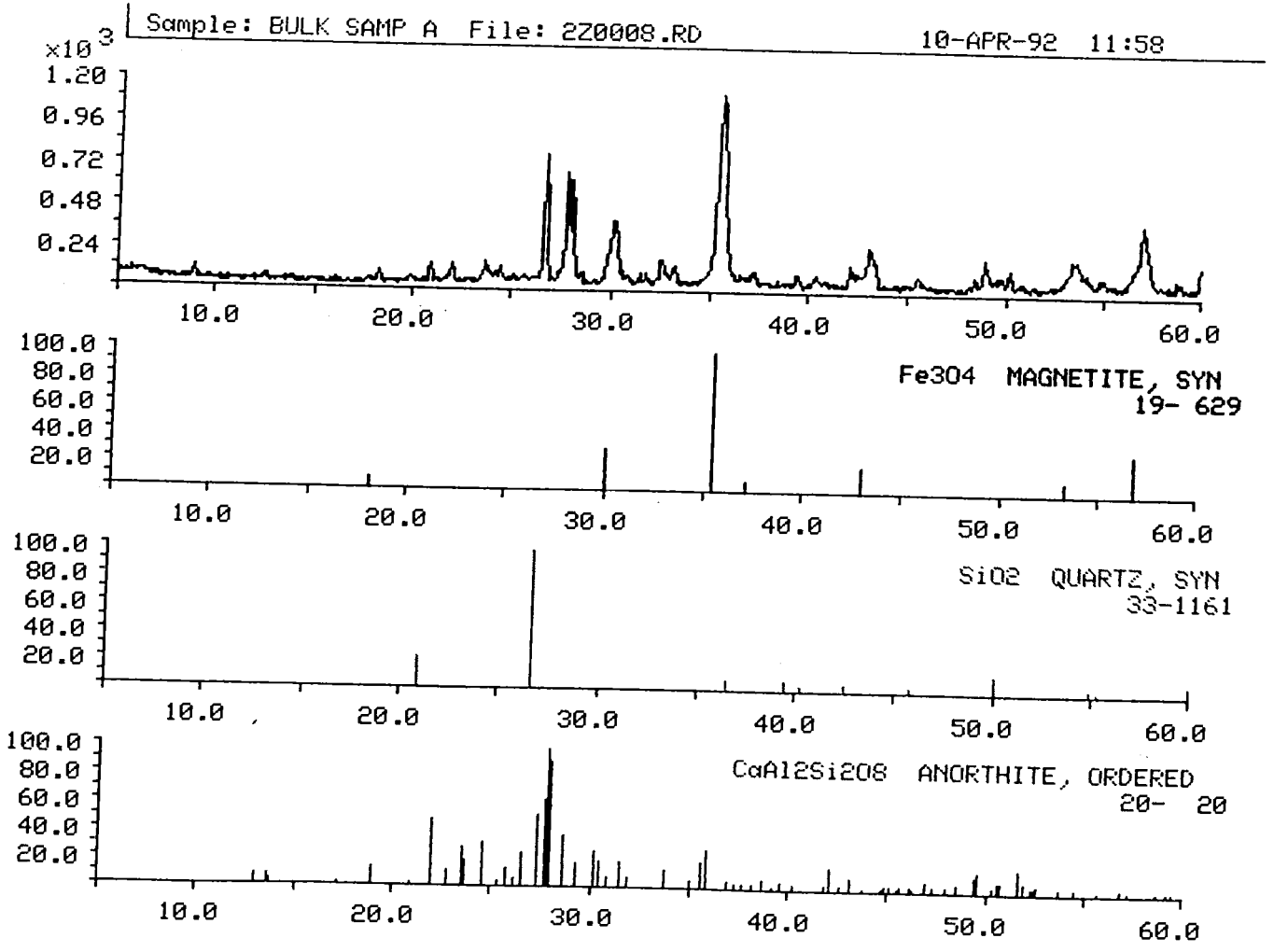

Figure 26: X–ray diffraction pattern of magnetically separated sample from a natural soil (#1).

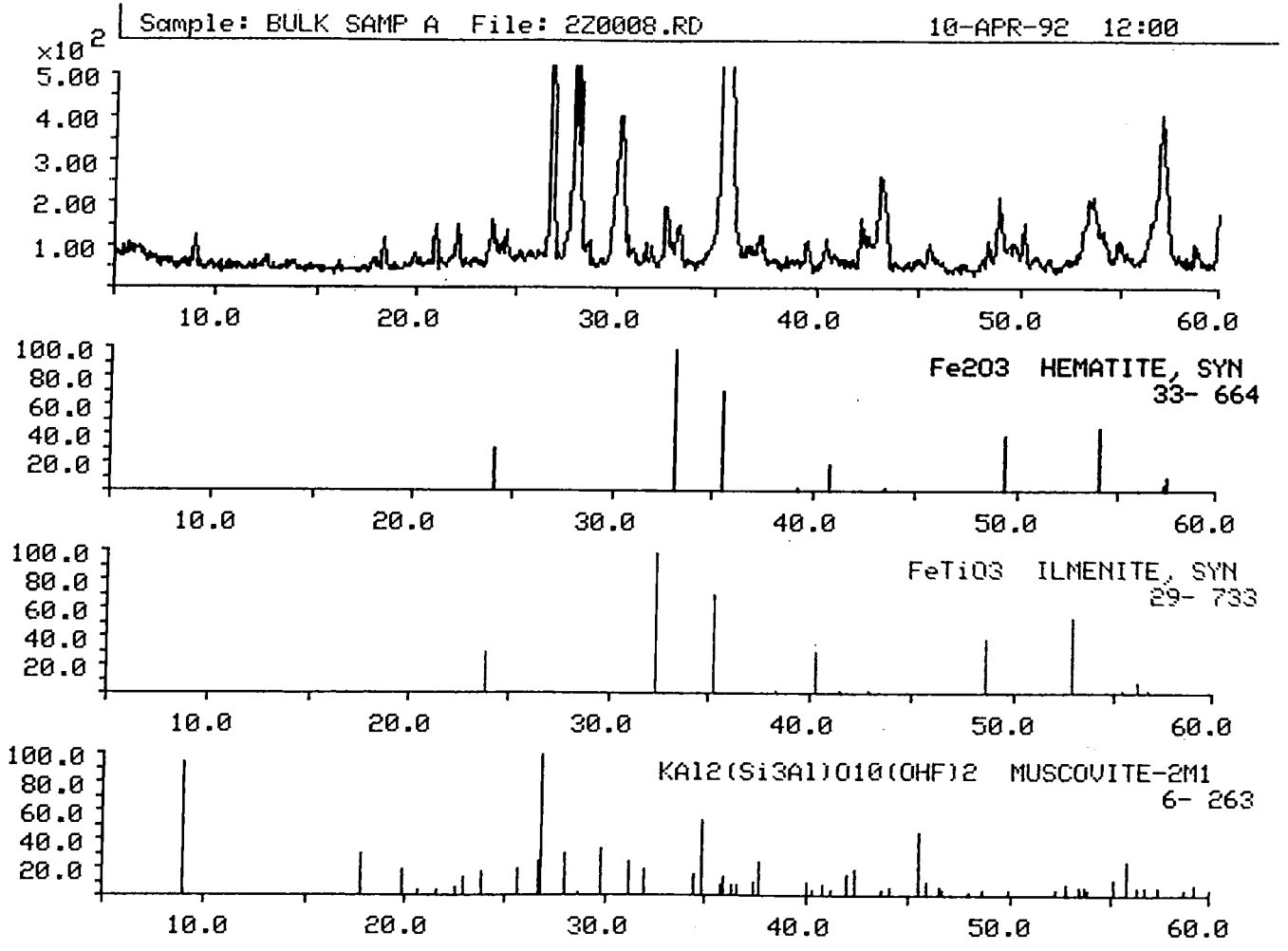

Figure 27: X–ray diffraction pattern of magnetically separated sample from a natural soil (#2).

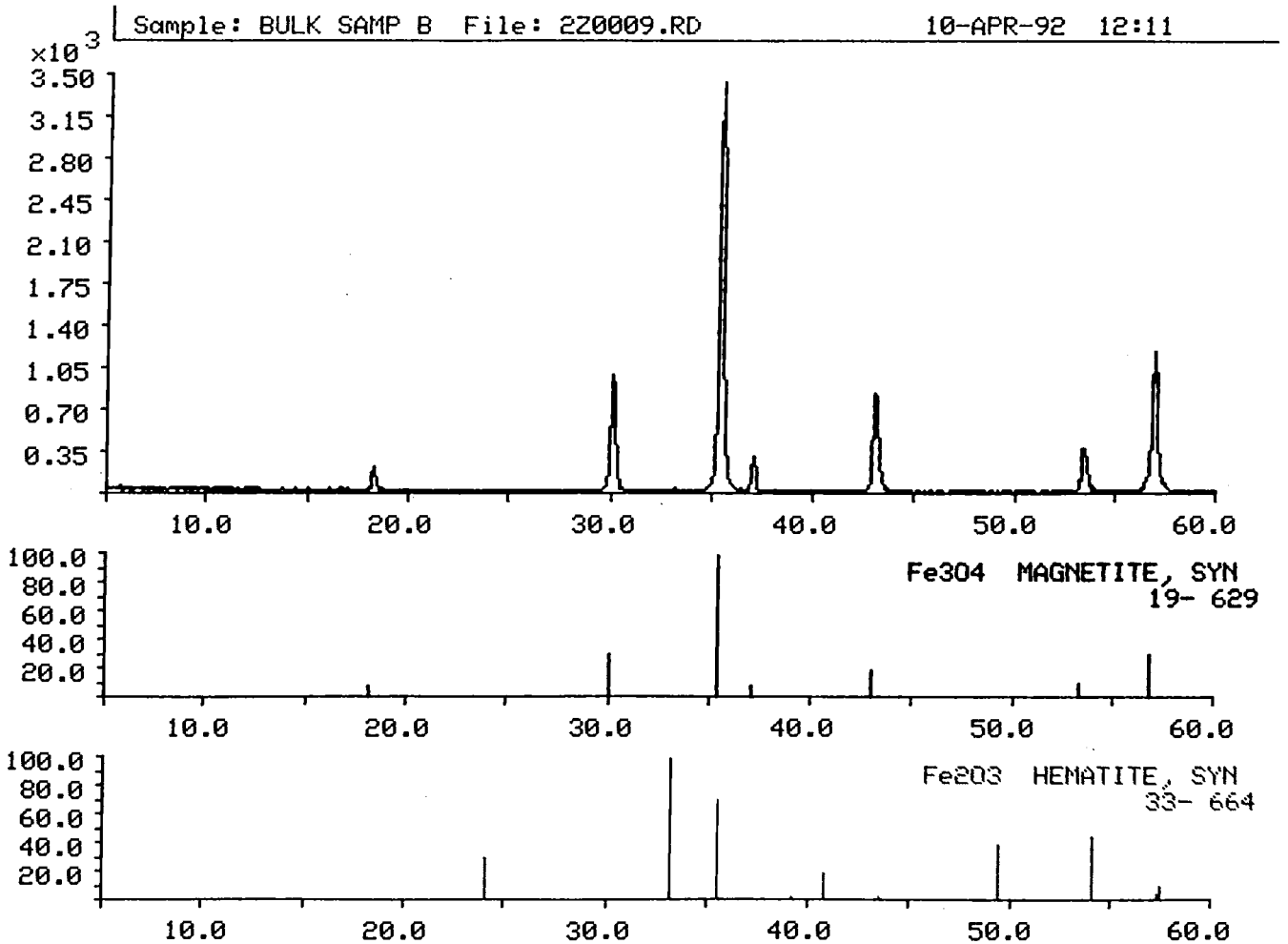

Figure 28: X–ray diffraction pattern of the pure magnetite (#1).

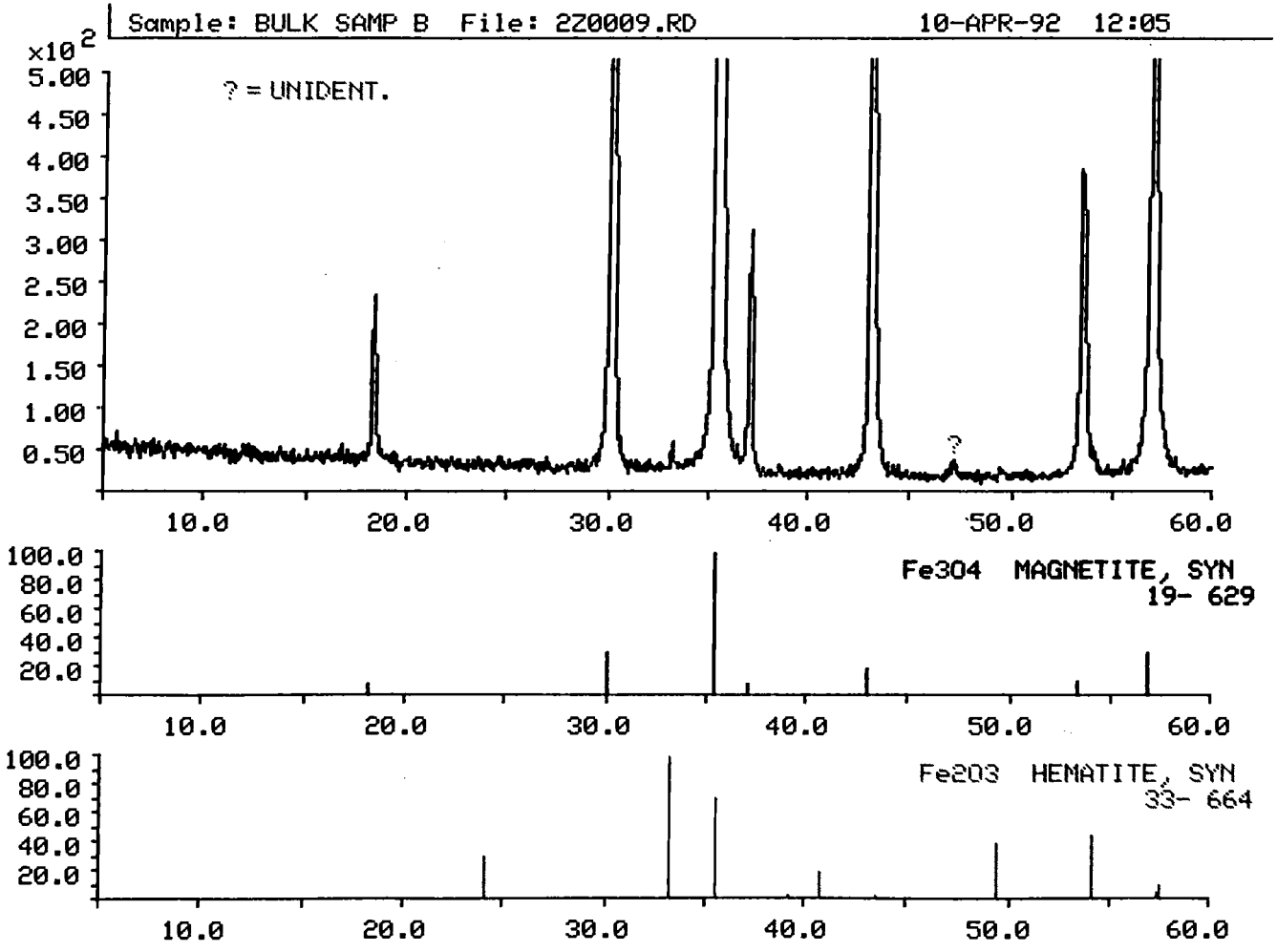

Figure 29: X–ray diffraction pattern of the pure magnetite (#2).

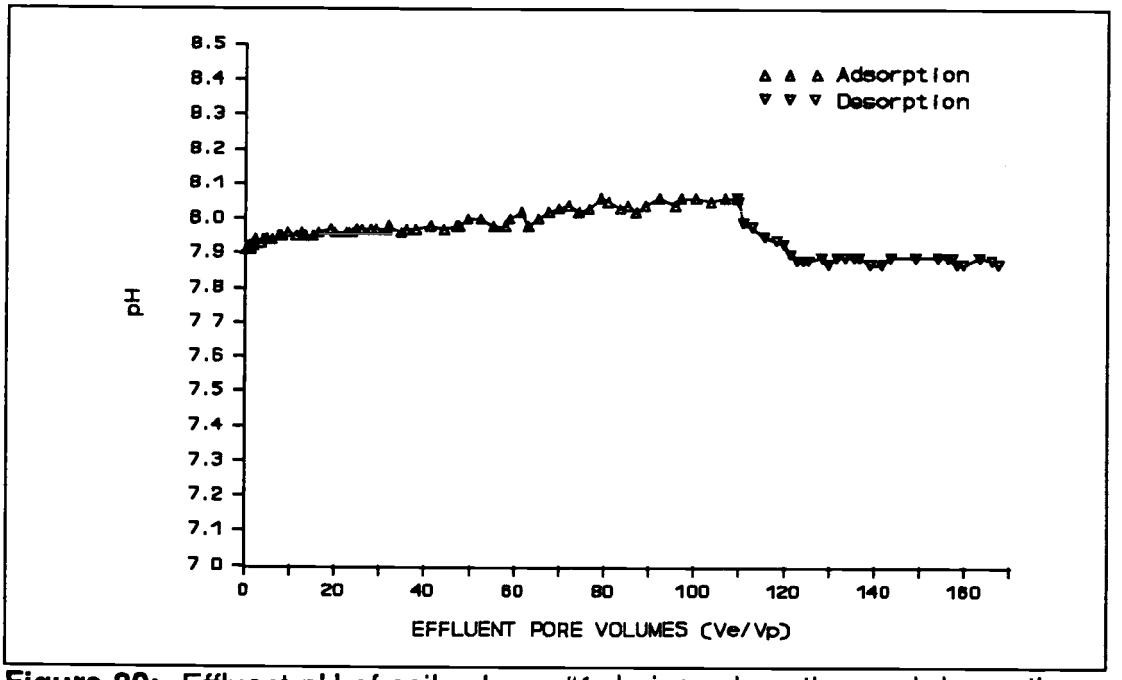

Figure 30: Effluent pH of soil column #1 during adsorption and desorption.

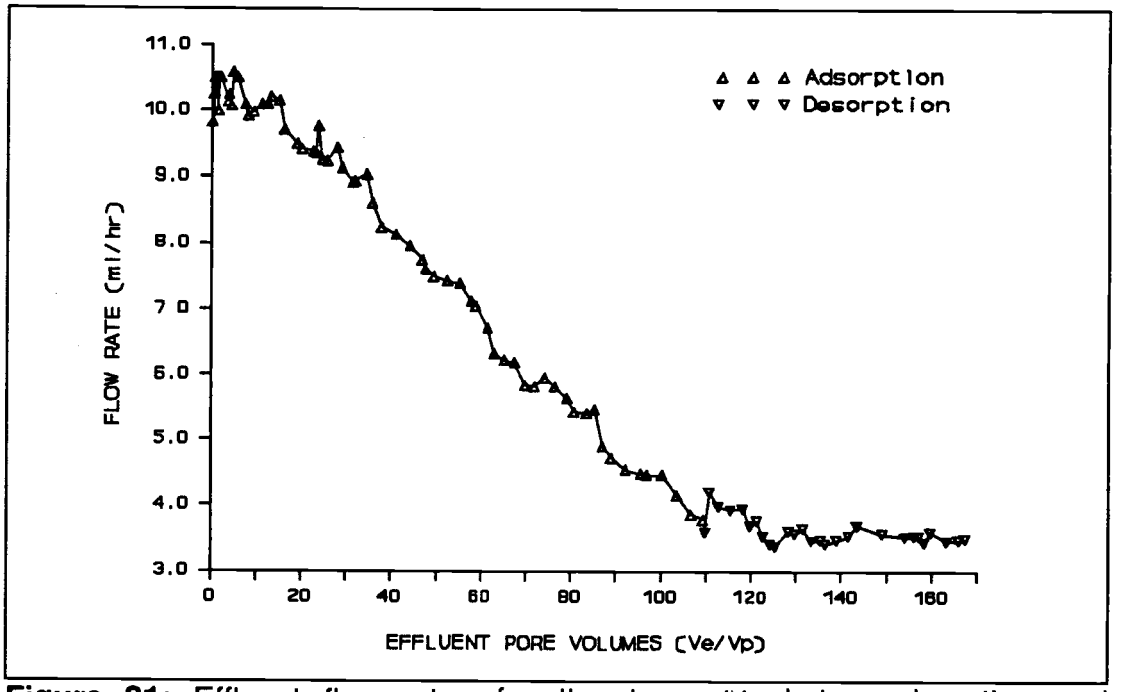

Figure 31: Effluent flow rate of soil column #1 during adsorption and desroption.

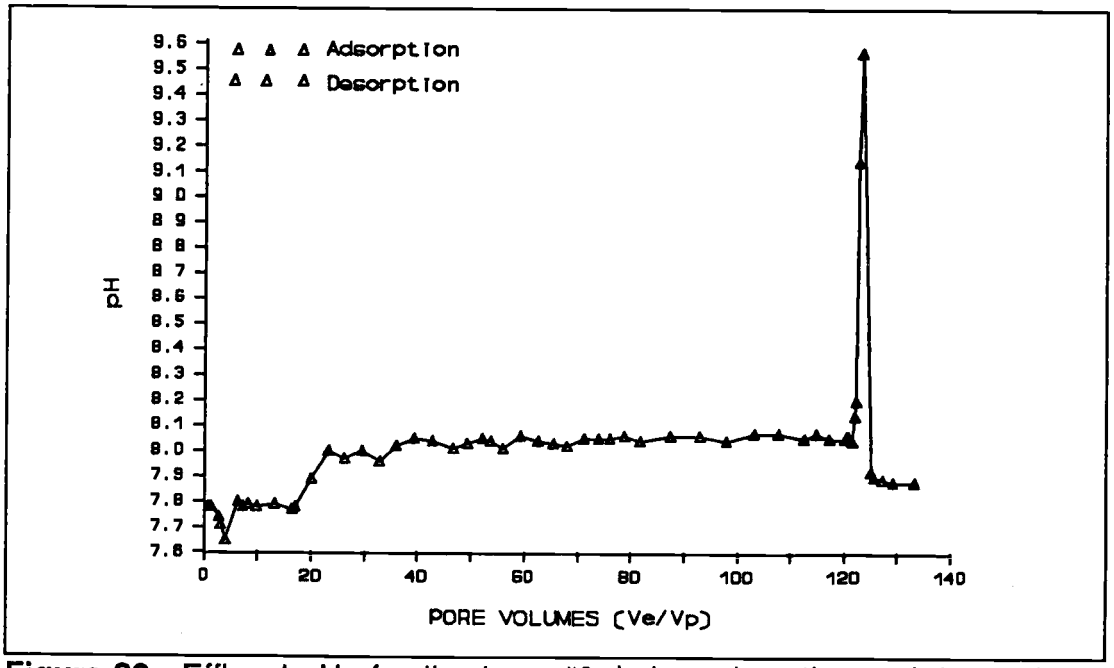

Figure 32: Effluent pH of soil column #2 during adsorption and desorption.

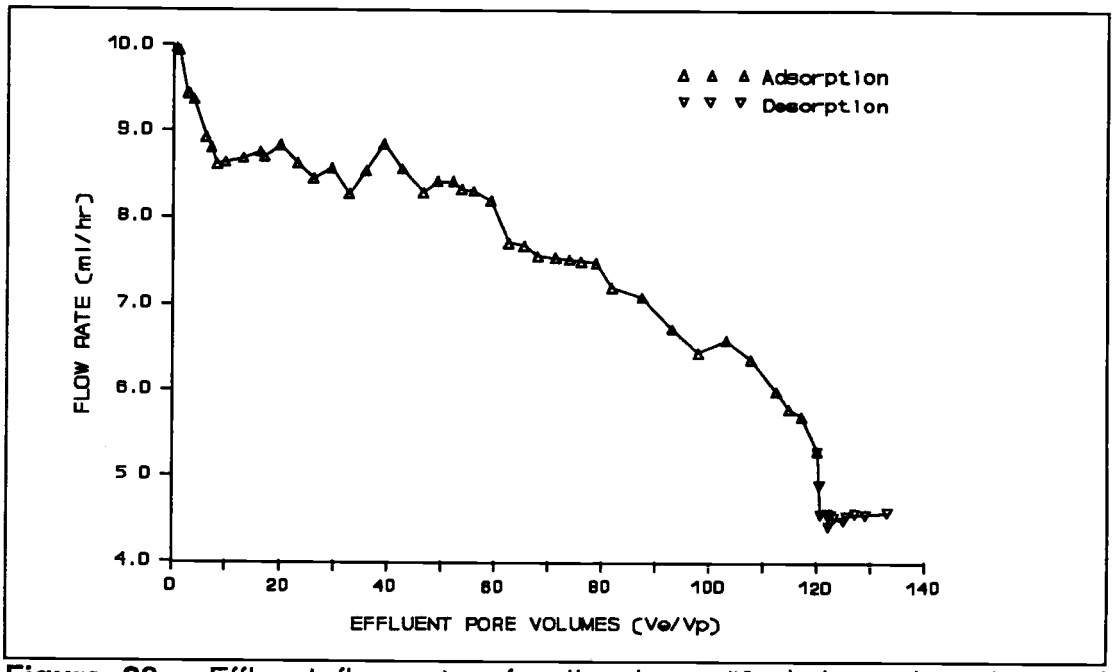

Figure 33: Effluent flow rate of soil column #2 during adsorption and desorption.

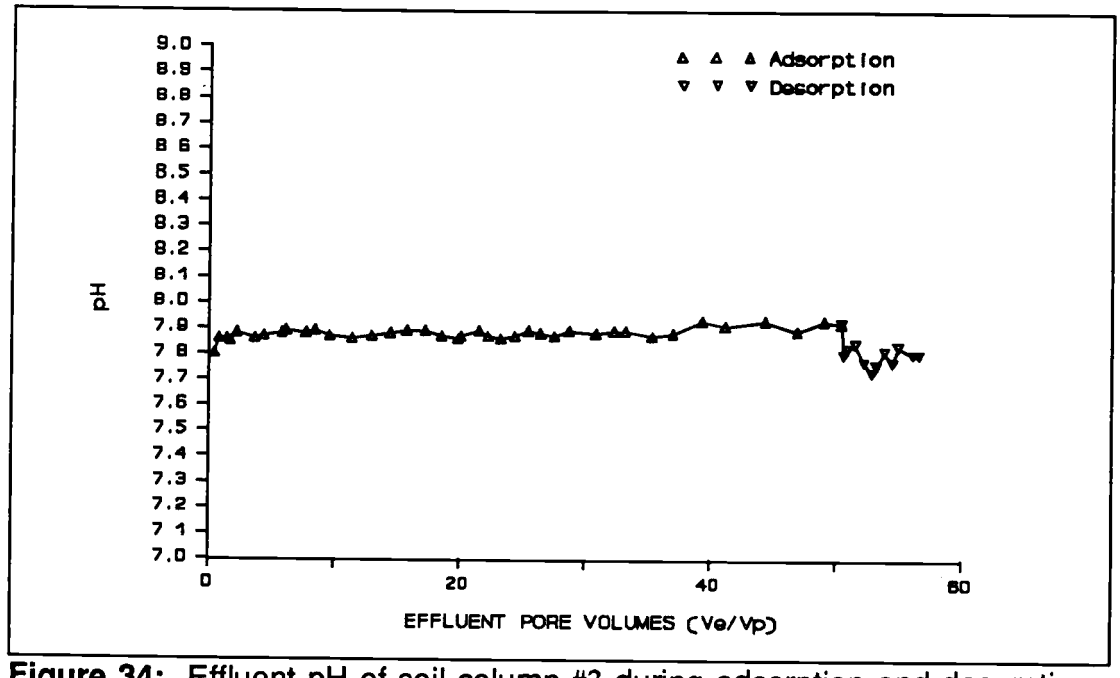

Figure 34: Effluent pH of soil column #3 during adsorption and desorption.

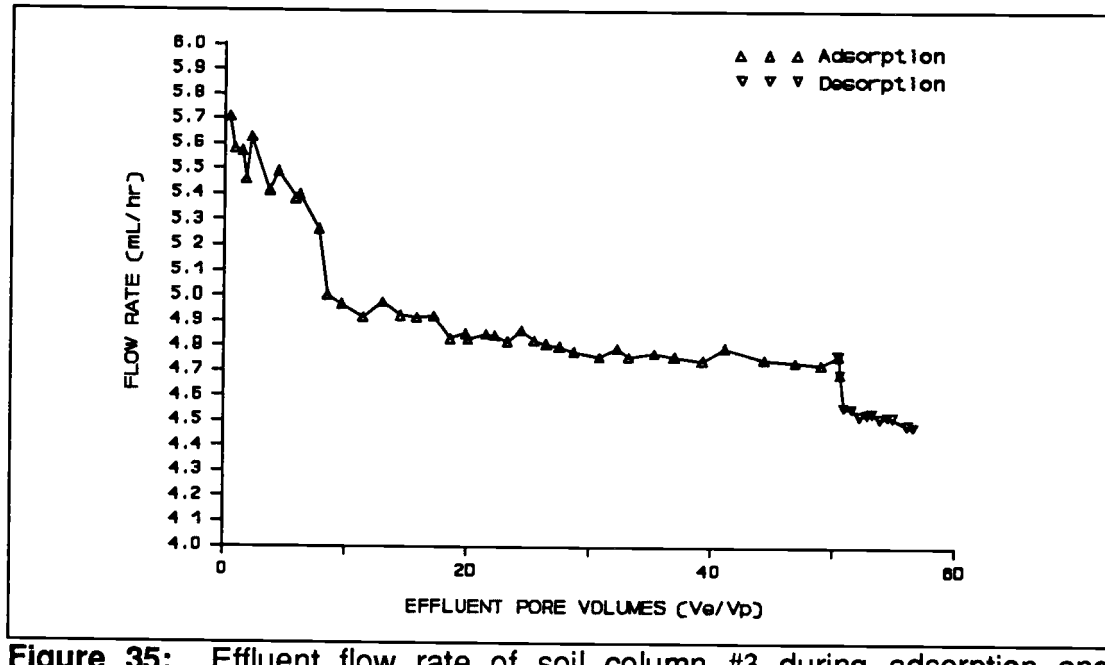

Figure 35: Effluent flow rate of soil column #3 during adsorption and desorption.

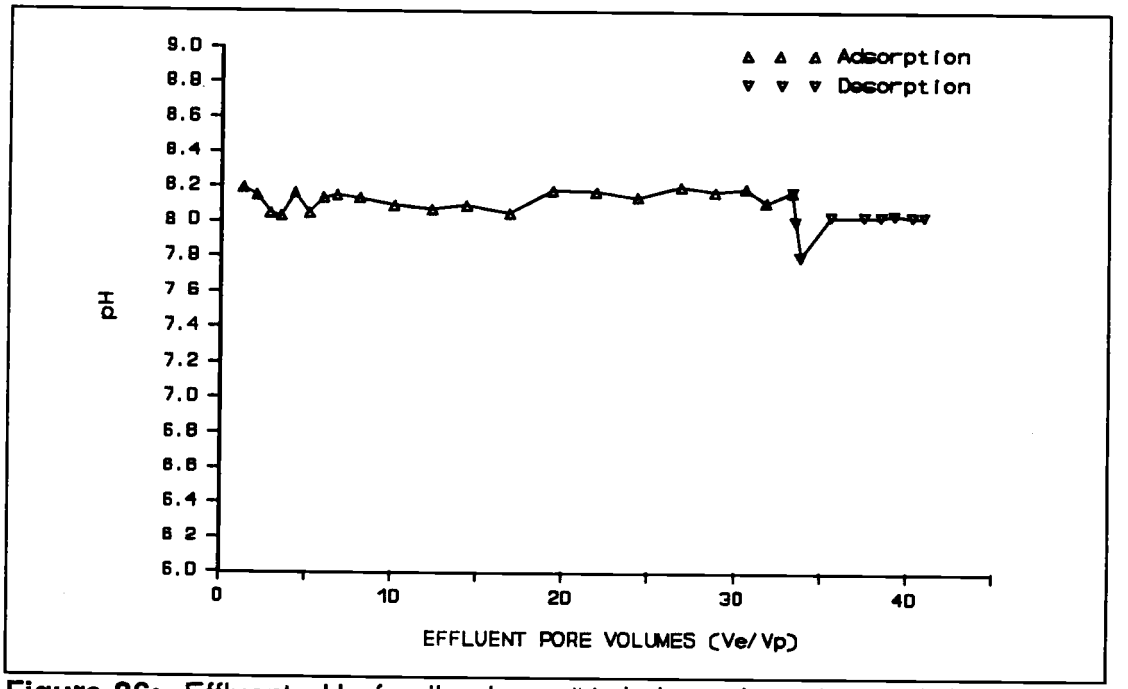

Figure 36: Effluent pH of soil column #4 during adsorption and desorption.

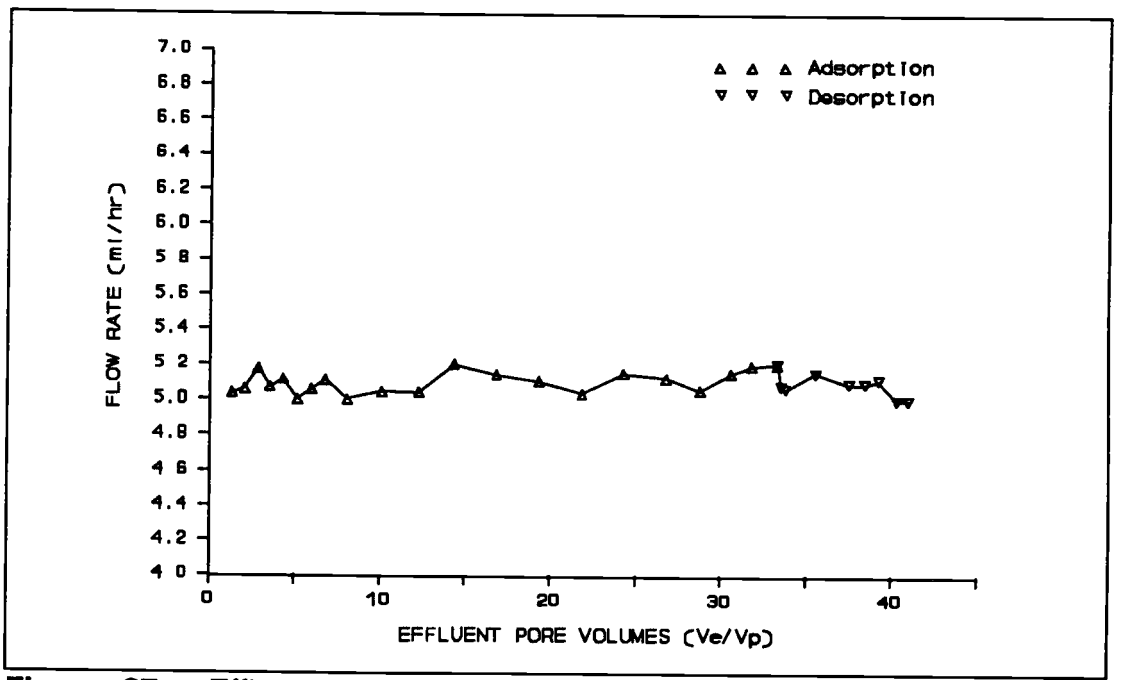

Figure 37: Effluent flow rate of soil column #4 during adsorption and desorption.

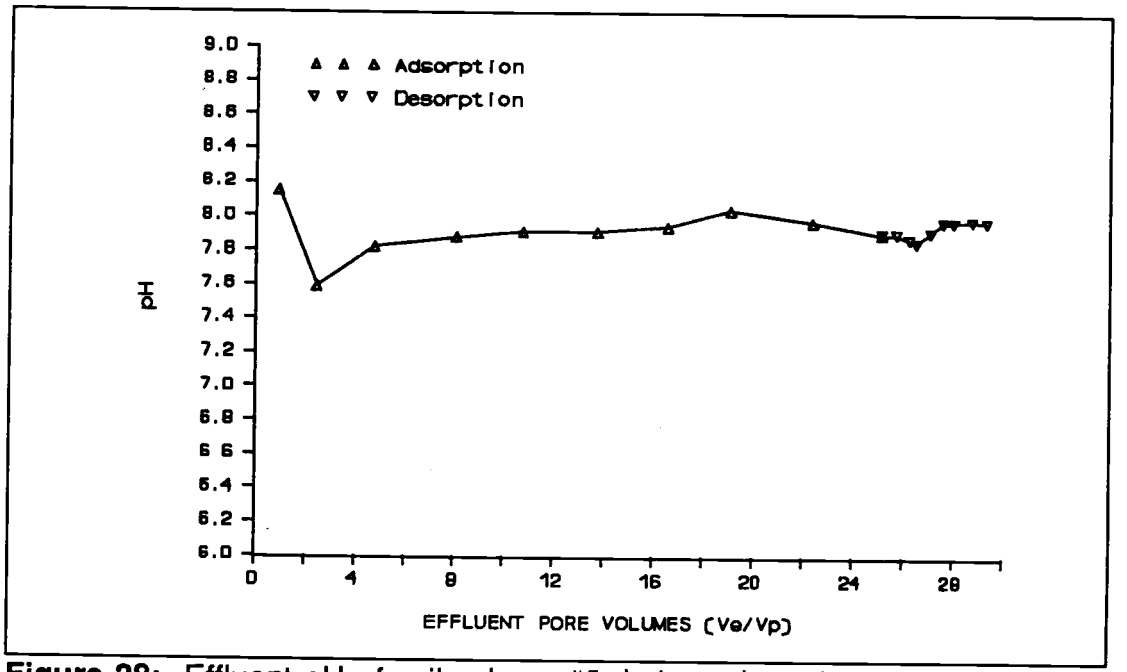

Figure 38: Effluent pH of soil column #5 during adsorption and desorption.

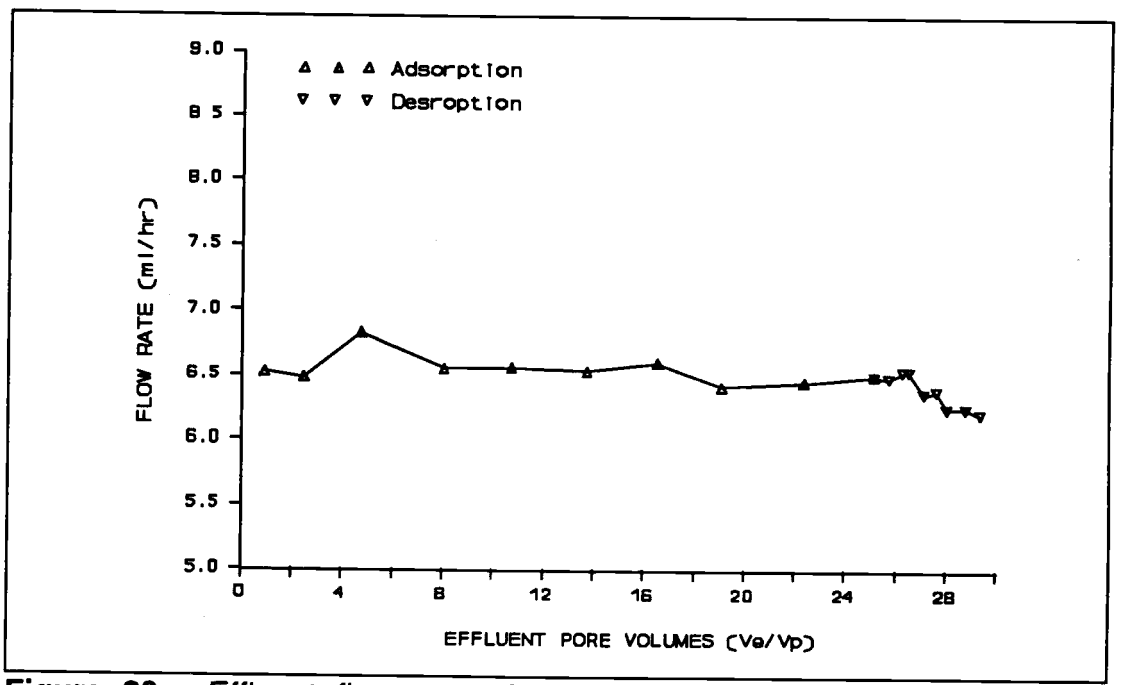

Figure 39: Effluent flow rate of soil column #5 during adsorption and desorption.

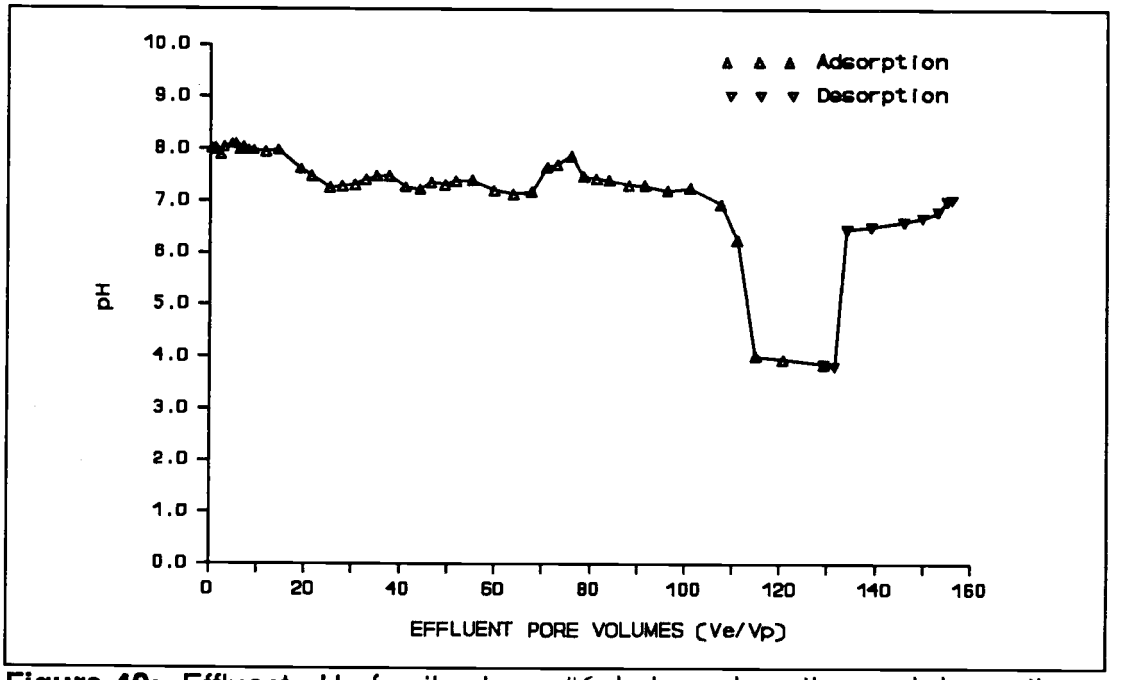

Figure 40: Effluent pH of soil column #6 during adsorption and desorption.

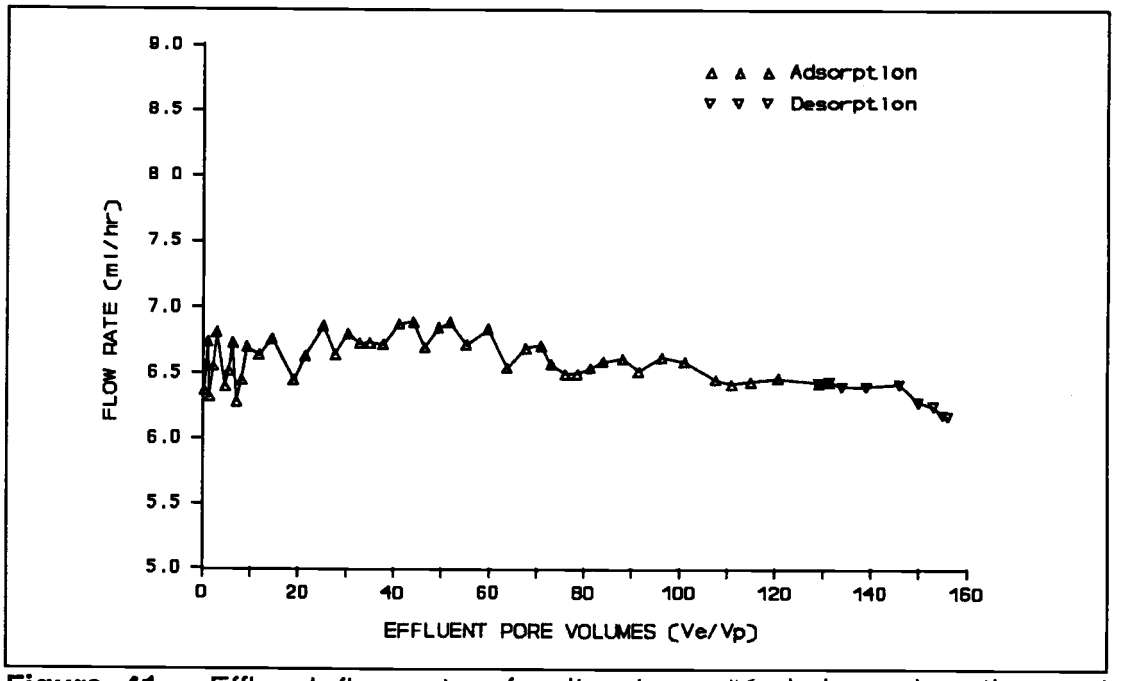

Figure 41: Effluent flow rate of soil column #6 during adsorption and desorption.

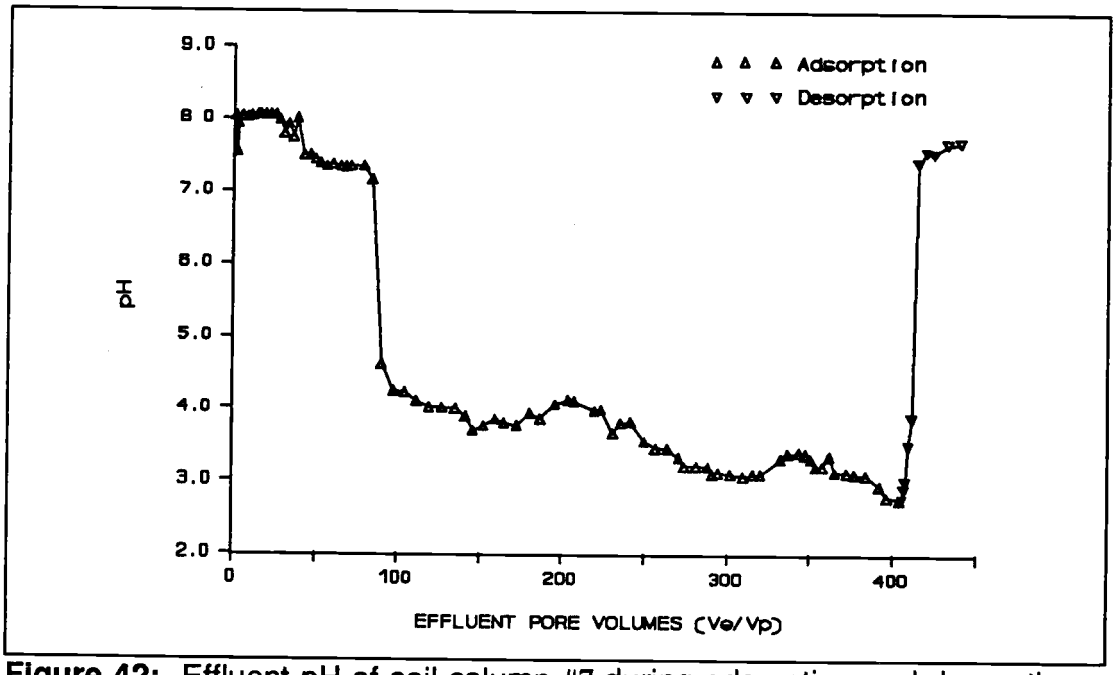

Figure 42: Effluent pH of soil column #7 during adsorption and desorption.

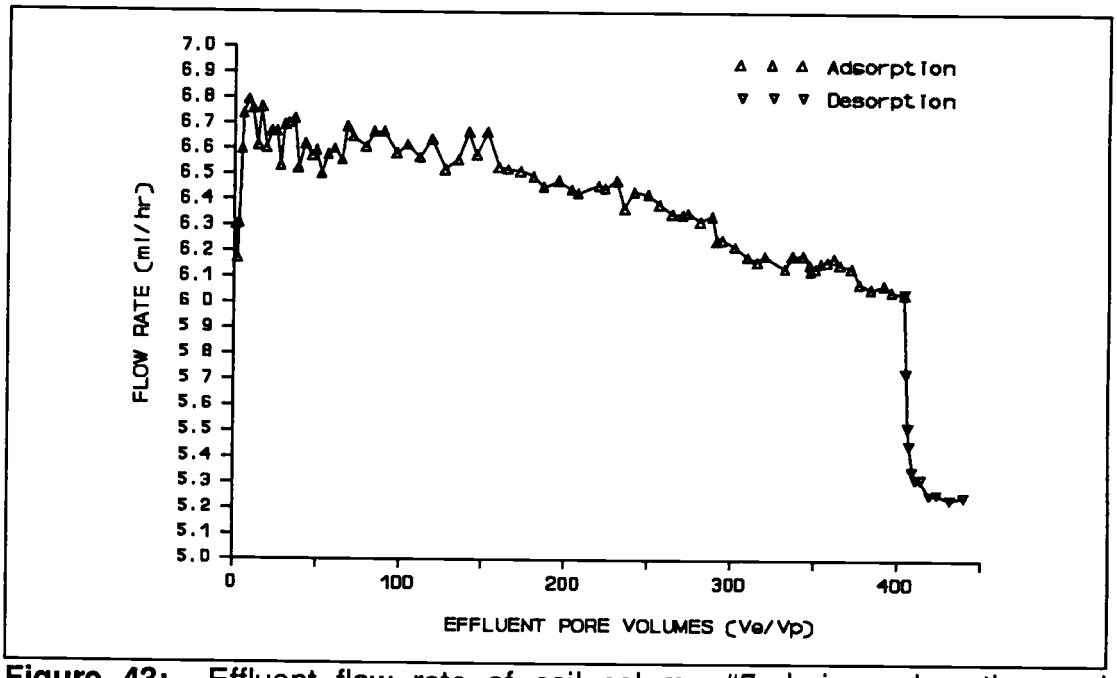

Figure 43: Effluent flow rate of soil column #7 during adsorption and desorption.

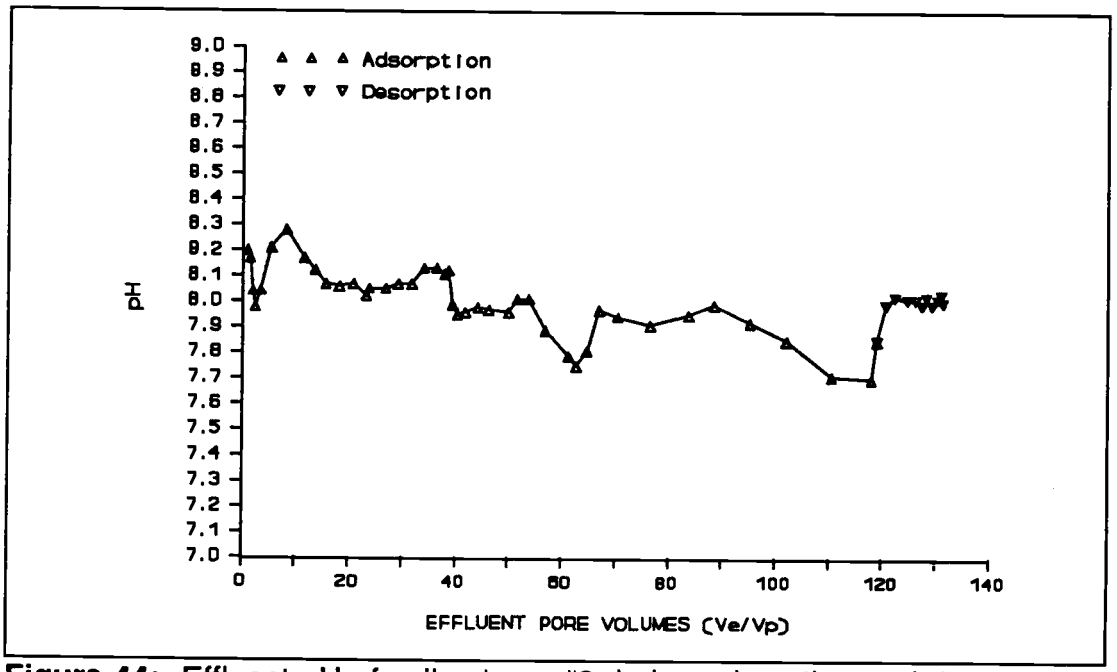

Figure 44: Effluent pH of soil column #8 during adsorption and desorption.

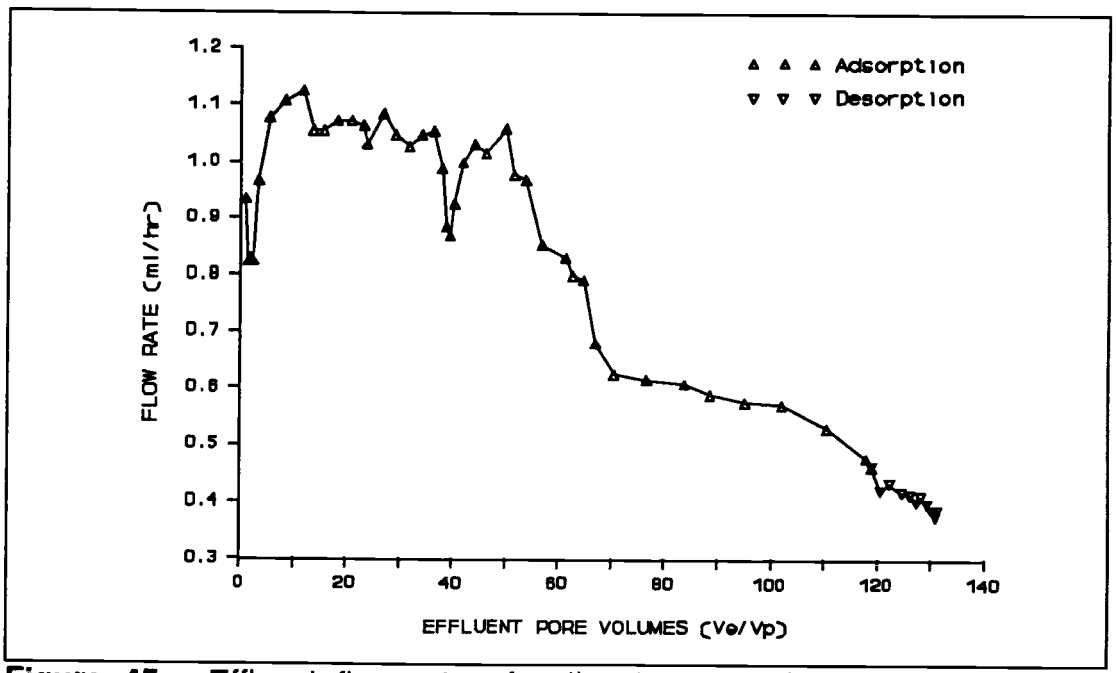

Figure 45: Effluent flow rate of soil column #8 during adsorption and desorption.

APPENDIX 2

Batch and Soil Column Experiment Tables

This appendix contains tables with experimental data for chromium batch and column experiments.

Table 15: Description of the soil column experiment # 1

Column Length, L	25.5	(cm)
Column Diameter, D	2.5	(cm)
Column Volume, V_t	125.1	(cm^3)
Pore Volume, V_p	63.8	(cm^3)
Mass of Soil, M_s	162.4	(g)
Porosity, η	51	(%)
Particle Density, ρ_s	2.65	(g/cm^3)
Influent Cr(VI) Conc., C_o	10.0	(mg/L)
Background Electrolyte, NaCl	0.01	(M)
Desorption with NaCl	0.01	(M)

Table 16: Description of the soil column experiment # 2

Column Length, L	25.5	(cm)
Column Diameter, D	2.5	(cm)
Column Volume, V_t	125.1	(cm^3)
Pore Volume, V_p	63.0	(cm^3)
Mass of Soil, M_s	164.5	(g)
Porosity, η	50	(%)
Particle Density, ρ_s	2.65	(g/cm^3)
Influent Cr(VI) Conc., C_o	10.0	(mg/L)
Background Electrolyte, NaCl	0.5	(M)
Desorption with NaCl	0.01	(M)

Table 17: Description of the soil column experiment # 4

Column Length, L	25.5	(cm)
Column Diameter, D	2.5	(cm)
Column Volume, V_t	125.1	(cm^3)
Pore Volume, V_p	57.5	(cm^3)
Mass of Soil, M_s	179.3	(g)
Porosity, η	46	(%)
Particle Density, ρ_s	2.65	(g/cm^3)
Influent Cr(VI) Conc., C_o	10.0	(mg/L)
Background Electrolyte, NaCl	0.01	(M)
Desorption with sulfate	0.01	(M)

Table 18: Description of the soil column experiment # 5

Column Length, L	25.5	(cm)
Column Diameter, D	2.5	(cm)
Column Volume, V_t	125.1	(cm^3)
Pore Volume, V_p	60.8	(cm^3)
Mass of Soil, M_s	170.3	(g)
Porosity, η	49	(%)
Particle Density, ρ_s	2.65	(g/cm^3)
Influent Cr(VI) Conc., C_o	5.0	(mg/L)
Background Electrolyte, NaCl	0.1	(M)
Desorption with sulfate	0.01	(M)

Table 19: Description of the soil column experiment # 6

Column Length, L	25.5	(cm)
Column Diameter, D	2.5	(cm)
Column Volume, V_t	125.1	(cm^3)
Pore Volume, V_p	62.5	(cm^3)
Mass of Soil, M_s	165.8	(g)
Porosity, η	50	(%)
Particle Density, ρ_s	2.65	(g/cm^3)
Influent Cr(VI) Conc., C_o	5.0	(mg/L)
Background Electrolyte, NaCl	0.01	(M)
Desorption with phosphate	0.5	(M)

Table 20: Description of the soil column experiment # 7

Column Length, L	25.5	(cm)
Column Diameter, D	2.5	(cm)
Column Volume, V_t	125.1	(cm^3)
Pore Volume, V_p	63.0	(cm^3)
Mass of Soil, M_s	164.5	(g)
Porosity, η	50	(%)
Particle Density, ρ_s	2.65	(g/cm^3)
Influent Cr(VI) Conc., C_o	5.0	(mg/L)
Background Electrolyte, NaCl	0.01	(M)
Desorption with phosphate	0.5	(M)

Table 21: Description of the soil column experiment # 8

Column Length, L	12.75	(cm)
Column Diameter, D	2.5	(cm)
Column Volume, V_t	62.5	(cm^3)
Pore Volume, V_p	28.7	(cm^3)
Mass of Soil, M_s	89.8	(g)
Porosity, η	46	(%)
Particle Density, ρ_s	2.65	(g/cm^3)
Influent Cr(VI) Conc., C_o	5.0	(mg/L)
Background Electrolyte, NaCl	0.01	(M)
Desorption with phosphate	0.5	(M)

Table 22: Soil titration with 1.0 M HCl in H_2O

Reading No.	Time (sec.)	Volume (uL)	E (mv)	pH	HCl (mol)	Cumu. HCl (mol)
10	5401	0	0.2180	8.968	0.0000	0.0000
20	11401	200	0.1889	8.462	0.0004	0.0004
30	17402	400	0.1617	7.990	0.0008	0.0012
40	23402	900	0.1209	7.281	0.0018	0.0030
50	29403	1400	0.0974	6.873	0.0028	0.0058
60	35404	1900	0.0779	6.535	0.0038	0.0096
70	41404	2400	0.0562	6.158	0.0048	0.0144
80	47405	2900	0.0350	5.790	0.0058	0.0202
90	53405	3400	0.0071	5.305	0.0068	0.0270
100	59406	3900	-0.0209	4.819	0.0078	0.0348
110	65407	4400	-0.0482	4.345	0.0088	0.0436
120	71407	4900	-0.0805	3.784	0.0098	0.0534
130	77408	5900	-0.1161	3.166	0.0118	0.0652
140	83408	6900	-0.1368	2.806	0.0138	0.0790

Table 23: Soil titration with 1.0 M HCl in 0.01 M NaCl

Reading No.	Time (sec.)	Volume (uL)	E (mv)	pH	HCl (mol)	Cumu. HCl (mol)
10	5401	0	0.2090	8.811	0.0000	0.0000
20	11401	200	0.1808	8.322	0.0004	0.0004
30	17402	400	0.1615	7.986	0.0008	0.0012
40	23402	900	0.1169	7.212	0.0018	0.0030
50	29403	1400	0.0939	6.812	0.0028	0.0058
60	35404	1900	0.0743	6.472	0.0038	0.0096
70	41404	2400	0.0561	6.156	0.0048	0.0144
80	47405	2900	0.0310	5.720	0.0058	0.0202
90	53405	3400	0.0036	5.244	0.0068	0.0270
100	59406	3900	-0.0237	4.770	0.0078	0.0348
110	65407	4400	-0.0554	4.220	0.0088	0.0436
120	71407	4900	-0.0849	3.707	0.0098	0.0534
130	77408	5900	-0.1173	3.145	0.0118	0.0652
140	83409	6900	-0.1339	2.856	0.0138	0.0790

Table 24: Soil titration with 1.0 M HCl in 0.10 M NaCl

Reading No.	Time (sec.)	Volume (uL)	E (mv)	pH	HCl (mol)	Cumu. HCl (mol)
10	5401	0	0.2046	8.735	0.0000	0.0000
20	11401	200	0.1822	8.345	0.0004	0.0004
30	17402	200	0.1621	7.997	0.0004	0.0008
40	23402	500	0.1259	7.368	0.0010	0.0018
50	29403	500	0.1040	6.988	0.0010	0.0028
60	35404	500	0.0819	6.603	0.0010	0.0038
70	41404	500	0.0575	6.180	0.0010	0.0048
80	47405	500	0.0295	5.694	0.0010	0.0058
90	53405	500	0.0007	5.194	0.0010	0.0068
100	59406	500	-0.0231	4.781	0.0010	0.0078
110	65407	500	-0.0555	4.218	0.0010	0.0088
120	71407	500	-0.0856	3.695	0.0010	0.0098
130	77408	1000	-0.1196	3.105	0.0020	0.0118
140	83408	1000	-0.1377	2.790	0.0020	0.0138

Table 25: Soil titration with 1.0 M HCl in 1.0 M NaCl

Reading No.	Time (sec.)	Volume (uL)	E (mv)	pH	HCl (mol)	Cumu. HCl (mol)
10	5401	0	0.1905	8.490	0.0000	0.0000
20	11401	200	0.1781	8.274	0.0004	0.0004
30	17402	400	0.1626	8.005	0.0008	0.0012
40	23402	900	0.1364	7.550	0.0018	0.0030
50	29403	1400	0.1151	7.180	0.0028	0.0058
60	35404	1900	0.0922	6.783	0.0038	0.0096
70	41404	2400	0.0586	6.199	0.0048	0.0144
80	47405	2900	0.0162	5.462	0.0058	0.0202
90	53405	3400	-0.0099	5.010	0.0068	0.0270
100	59406	3900	-0.0348	4.577	0.0078	0.0348
110	65407	4400	-0.0725	3.923	0.0088	0.0436
120	71407	4900	-0.1039	3.377	0.0098	0.0534
130	77408	5900	-0.1364	2.813	0.0118	0.0652
140	83408	6900	-0.1516	2.549	0.0138	0.0790

Table 26: 0.1 mM Cr(VI) adsorption kinetic in 0.01 M NaCl, pH =6.5

Sample no.	Initial Cr(VI) mg/L	pH	ADS[a] Cr(VI) mg/L	ADS Cr(VI) mmol/kg	DES[b] Cr(VI) mg/L	Net ADS Cr(VI) mmol/kg	RED[c] Cr(VI) mmol/kg	Rxn time hr	Cumu. time hr
K0	5.20	6.35	5.20	0.0000	5.20	0.0000	0.0000	0.0	0.0
K1	5.20	6.36	5.15	0.0264	5.18	0.0168	0.0096	5.0	5.0
K2	5.20	6.27	5.11	0.0433	5.17	0.0288	0.0144	4.0	9.0
K3	5.20	6.30	5.06	0.0683	5.17	0.0524	0.0159	12.0	21.0
K4	5.20	6.33	5.03	0.0803	5.16	0.0615	0.0188	12.5	33.5
K5	5.20	6.35	5.05	0.0846	5.16	0.0649	0.0197	24.0	57.5
K6	5.20	6.41	5.02	0.0861	5.16	0.0659	0.0202	19.0	76.5
K7	5.20	6.55	5.02	0.0889	5.15	0.0668	0.0221	23.5	100.0
K8	5.20	6.65	5.01	0.0914	5.15	0.0673	0.0240	24.0	124.0

ADS[a] Equilibrium adsorption concentration
DES[b] Equilibrium desorption concentration
RED[c] Reduced chromium (VI) concentration

Table 27: 0.1 mM Cr(VI) adsorption kinetic in 0.01 M NaCl, pH 5.25

Sample no.	Initial Cr(VI) mg/L	pH	ADS[a] Cr(VI) mg/L	ADS Cr(VI) mmol/kg	DES[b] Cr(VI) mg/L	Net ADS Cr(VI) mmol/kg	RED[c] Cr(VI) mmol/kg	Rxn time hr	Cumu. time hr
K0	5.20	6.35	5.20	0.0000	5.20	0.0000	0.0000	0.0	0.0
K1	5.20	5.02	4.90	0.1442	4.99	0.0433	0.1010	5.0	5.0
K2	5.20	5.10	4.85	0.1683	4.98	0.0625	0.1058	4.0	9.0
K3	5.20	5.08	4.75	0.2164	4.97	0.1058	0.1106	12.0	21.0
K4	5.20	5.12	4.65	0.2644	4.94	0.1418	0.1226	12.5	33.5
K5	5.20	5.24	4.64	0.2712	4.96	0.1582	0.1130	24.0	57.5
K6	5.20	5.23	4.62	0.2789	4.95	0.1587	0.1202	19.0	76.5
K7	5.20	5.24	4.60	0.2885	4.93	0.1563	0.1322	23.5	100.0
K8	5.20	5.26	4.58	0.2981	4.91	0.1587	0.1394	24.0	124.0

ADS[a] Equilibrium adsorption concentration
DES[b] Equilibrium desorption concentration
RED[c] Reduced chromium (VI) concentration

Table 28: 0.2 mM Cr(VI) adsorption kinetic in 0.01 M NaCl, pH=6.5

Sample No.	Initial Cr(VI) mg/L	pH	ADS[a] Cr(VI) mg/L	ADS Cr(VI) mmol/kg	DES[b] Cr(VI) mg/L	Net ADS Cr(VI) mmol/kg	RED[c] Cr(VI) mmol/kg	Rxn time hr	Cumu. time hr
K0	10.40	6.35	10.40	0.0000	10.40	0.0000	0.0000	0.0	0.0
K1	10.40	6.36	10.24	0.0769	10.29	0.0240	0.0529	5.0	5.0
K2	10.40	6.27	10.21	0.0914	10.28	0.0337	0.0577	4.0	9.0
K3	10.40	6.30	10.14	0.1250	10.28	0.0659	0.0591	12.0	21.0
K4	10.40	6.33	10.11	0.1394	10.27	0.0793	0.0601	12.5	33.5
K5	10.40	6.35	10.10	0.1442	10.28	0.0889	0.0553	24.0	57.5
K6	10.40	6.41	10.09	0.1490	10.28	0.0904	0.0587	19.0	76.5
K7	10.40	6.55	10.07	0.1587	10.26	0.0933	0.0654	23.5	100.0
K8	10.40	6.65	10.06	0.1635	10.26	0.0942	0.0692	24.0	124.0

ADS[a] Equilibrium adsorption concentration
DES[b] Equilibrium desorption concentration
RED[c] Reduced chromium (VI) concentration

Table 29: Chromium(VI) adsorption isotherm in 0.01 M NaCl, pH=5.65

Sample No.	Initial Cr(VI) mg/L	pH	ADS[a] Cr(VI) mg/L	ADS Cr(VI) mmol/L	ADS Cr(VI) mmol/kg	DES[b] Cr(VI) mg/L	Net ADS Cr(VI) mmol/kg	RED[c] Cr(VI) mmol/kg
I1	1.56	5.68	1.39	0.0267	0.0817	1.53	0.0673	0.0144
I2	2.60	5.67	2.24	0.0431	0.1731	2.43	0.0928	0.0803
I3	5.20	5.65	4.70	0.0903	0.2428	5.01	0.1515	0.0914
I4	7.80	5.64	7.15	0.1375	0.3125	7.51	0.1731	0.1394
I5	10.40	5.69	9.67	0.1860	0.3510	10.07	0.1923	0.1587
I6	13.00	5.64	12.26	0.2358	0.3558	12.69	0.2082	0.1476
I7	15.60	5.63	14.83	0.2852	0.3702	15.29	0.2188	0.1515
I8	18.20	5.62	17.41	0.3348	0.3798	17.89	0.2284	0.1515
I9	20.80	5.60	19.99	0.3845	0.3885	20.48	0.2346	0.1539
I10	26.00	5.60	25.18	0.4843	0.3943	25.68	0.2380	0.1563

ADS[a] Equilibrium adsorption concentration
DES[b] Equilibrium desorption concentration
RED[c] Reduced chromium (VI) concentration

Table 30: Chromium(VI) adsorption isotherm in 0.01 M NaCl, pH=7.0

Sample No.	Initial Cr(VI) mg/L	pH	ADS[a] Cr(VI) mg/L	ADS Cr(VI) mmol/L	ADS Cr(VI) mmol/kg	DES[b] Cr(VI) mg/L	Net ADS Cr(VI) mmol/kg	RED[c] Cr(VI) mmol/kg
I1	1.56	7.00	1.51	0.0290	0.0240	1.55	0.0192	0.0048
I2	2.60	7.00	2.44	0.0469	0.0769	2.50	0.0288	0.0481
I3	5.20	7.00	4.87	0.0937	0.1587	4.99	0.0577	0.1010
I4	7.80	7.00	7.34	0.1412	0.2212	7.50	0.0769	0.1442
I5	10.40	7.00	9.90	0.1904	0.2404	10.08	0.0865	0.1539
I6	13.00	7.00	12.45	0.2394	0.2644	12.65	0.0962	0.1683
I7	15.60	7.00	15.03	0.2891	0.2741	15.25	0.1058	0.1683
I8	18.20	6.99	17.60	0.3385	0.2885	17.82	0.1067	0.1817
I9	20.80	6.99	20.20	0.3884	0.2909	20.42	0.1082	0.1827
I10	26.00	6.98	25.39	0.4883	0.2923	25.62	0.1096	0.1827

ADS[a] Equilibrium adsorption concentration
DES[b] Equilibrium desorption concentration
RED[c] Reduced chromium (VI) concentration

Table 31: 0.1 mM Cr(VI) adsorption in 0.01 M NaCl for varying pH

Sample No.	Initial Cr(VI (mg/L)	pH	Equil. Cr(VI) (mg/L)	ADS[a] Cr(VI) (mmol/kg)	DES[b] Cr(VI) (mg/L)	Net ADS Cr(VI) (mmol/kg)	RED[c] Cr(VI) (mmol/kg)
AD1	5.20	7.94	5.13	0.0337	5.16	0.0144	0.0192
AD2	5.20	7.75	5.05	0.0721	5.11	0.0274	0.0447
AD3	5.20	7.45	4.80	0.1923	4.93	0.0606	0.1317
AD4	5.20	6.99	4.74	0.2212	4.95	0.1009	0.1203
AD5	5.20	6.82	4.70	0.2404	4.94	0.1163	0.1241
AD6	5.20	5.82	4.65	0.2644	4.98	0.1587	0.1058
AD7	5.20	5.00	4.64	0.2693	4.98	0.1635	0.1058
AD8	5.20	4.45	4.60	0.2885	4.95	0.1683	0.1202
AD9	5.20	4.00	4.59	0.2933	4.95	0.1731	0.1202
AD10	5.20	3.66	4.58	0.2981	4.94	0.1741	0.1240
AD11	5.20	3.45	4.36	0.4039	4.73	0.1779	0.2260
AD12	5.20	3.00	4.11	0.5241	4.52	0.1971	0.3269

DAS[a] Equilibrium adsorption concentration
DES[b] Equilibrium desorption concentration
RED[c] Reduced chromium (VI) concentration

Table 32: 0.1 mM Cr(VI) adsorption in 0.1 M NaCl for varying pH

Sample No.	Initial Cr(VI (mg/L)	pH	Equil. Cr(VI) (mg/L)	ADS[a] Cr(VI) (mmol/kg)	DES[b] Cr(VI) (mg/L)	Net ADS Cr(VI) (mmol/kg)	RED[c] Cr(VI) (mmol/kg)
AD1	5.20	8.00	5.15	0.0240	5.16	0.0053	0.0188
AD2	5.20	7.71	5.10	0.0481	5.13	0.0149	0.0332
AD3	5.20	7.32	4.85	0.1683	4.95	0.0471	0.1212
AD4	5.20	7.00	4.80	0.1923	4.96	0.0789	0.1135
AD5	5.20	6.71	4.76	0.2116	4.99	0.1115	0.1000
AD6	5.20	5.70	4.69	0.2452	4.99	0.1428	0.1024
AD7	5.20	4.90	4.66	0.2596	4.98	0.1539	0.1058
AD8	5.20	4.31	4.66	0.2596	4.99	0.1563	0.1034
AD9	5.20	4.00	4.62	0.2789	4.95	0.1572	0.1216
AD10	5.20	3.62	4.60	0.2885	4.93	0.1587	0.1298
AD11	5.20	3.30	4.59	0.2933	4.93	0.1644	0.1289
AD12	5.20	3.25	4.38	0.3943	4.73	0.1683	0.2260

DAS[a] Equilibrium adsorption concentration
DES[b] Equilibrium desorption concentration
RED[c] Reduced chromium (VI) concentration

Table 33: 0.1 mM Cr(VI) adsorption in 0.5 M NaCl for varying pH

Sample No.	Initial Cr(VI (mg/L)	pH	Equil. Cr(VI) (mg/L)	ADS* Cr(VI) (mmol/kg)	DES* Cr(VI) (mg/L)	Net ADS Cr(VI) (mmol/kg)	RED* Cr(VI) (mmol/kg)
AD1	5.20	7.88	5.16	0.0192	5.17	0.0024	0.0168
AD2	5.20	7.62	5.12	0.0385	5.13	0.0048	0.0337
AD3	5.20	7.03	4.87	0.1587	4.94	0.0337	0.1250
AD4	5.20	6.73	4.83	0.1779	4.97	0.0697	0.1082
AD5	5.20	6.42	4.77	0.2067	4.97	0.0976	0.1091
AD6	5.20	5.64	4.72	0.2308	4.98	0.1250	0.1058
AD7	5.20	5.03	4.69	0.2452	4.96	0.1332	0.1120
AD8	5.20	4.30	4.71	0.2356	4.99	0.1370	0.0986
AD9	5.20	4.00	4.73	0.2260	5.02	0.1394	0.0865
AD10	5.20	3.60	4.65	0.2644	4.94	0.1404	0.1240
AD11	5.20	3.30	4.60	0.2885	4.90	0.1442	0.1442
AD12	5.20	3.25	4.38	0.3943	4.73	0.1683	0.2260

DAS[a] Equilibrium adsorption concentration
DES[b] Equilibrium desorption concentration
RED[c] Reduced chromium (VI) concentration

Table 34: 0.1 mM Cr(VI) adsorption in 0.01 M $NaNO_3$ for varying pH

Sample No.	Initial Cr(VI (mg/L)	pH	Equil. Cr(VI) (mg/L)	ADS[a] Cr(VI) (mmol/kg)	DES[b] Cr(VI) (mg/L)	Net ADS Cr(VI) (mmol/kg)	RED[c] Cr(VI) (mmol/kg)
AD1	5.20	7.95	5.14	0.0288	5.16	0.0096	0.0192
AD2	5.20	7.78	5.07	0.0625	5.11	0.0178	0.0447
AD3	5.20	7.55	4.82	0.1827	4.93	0.0510	0.1317
AD4	5.20	6.99	4.77	0.2067	4.95	0.0864	0.1203
AD5	5.20	6.85	4.73	0.2260	4.94	0.1019	0.1241
AD6	5.20	5.90	4.66	0.2596	4.98	0.1539	0.1058
AD7	5.20	5.02	4.64	0.2693	4.97	0.1587	0.1106
AD8	5.20	4.42	4.61	0.2837	4.95	0.1635	0.1202
AD9	5.20	4.02	4.60	0.2885	4.95	0.1683	0.1202
AD10	5.20	3.60	4.59	0.2933	4.94	0.1683	0.1250

ADS[a] Equilibrium adsorption concentration
DES[b] Equilibrium desorption concentration
RED[c] Reduced chromium (VI) concentration

Table 35: 0.1 mM Cr(VI) adsorption in 0.01 M $NaHCO_3$ for varying pH

Sample No.	Initial Cr(VI (mg/L)	pH	Equil. Cr(VI) (mg/L)	ADS[a] Cr(VI) (mmol/kg)	DES[b] Cr(VI) (mg/L)	Net ADS Cr(VI) (mmol/kg)	RED[c] Cr(VI) (mmol/kg)
AD1	5.20	8.24	5.15	0.0240	5.16	0.0048	0.0192
AD2	5.20	7.82	5.09	0.0529	5.10	0.0058	0.0471
AD3	5.20	7.57	4.84	0.1731	4.92	0.0385	0.1346
AD4	5.20	7.12	4.79	0.1971	4.94	0.0721	0.1250
AD5	5.20	6.89	4.74	0.2212	4.93	0.0914	0.1298
AD6	5.20	6.02	4.68	0.2500	4.95	0.1298	0.1202
AD7	5.20	5.12	4.66	0.2596	4.97	0.1490	0.1106
AD8	5.20	4.48	4.63	0.2741	4.96	0.1587	0.1154
AD9	5.20	4.12	4.62	0.2789	4.95	0.1587	0.1202
AD10	5.20	3.69	4.61	0.2837	4.95	0.1635	0.1202

DAS[a] Equilibrium adsorption concentration
DES[b] Equilibrium desorption concentration
RED[c] Reduced chromium (VI) concentration

Table 36: 0.1 mM Cr(VI) adsorption in 0.01 M Na_2SO_3 for varying pH

Sample No.	Initial Cr(VI (mg/L)	pH	Equil. Cr(VI) (mg/L)	ADS[a] Cr(VI) (mmol/kg)	DES[b] Cr(VI) (mg/L)	Net ADS Cr(VI) (mmol/kg)	RED[c] Cr(VI) (mmol/kg)
AD1	5.20	7.74	5.14	0.0288	5.16	0.0096	0.0192
AD2	5.20	7.31	5.01	0.0914	5.12	0.0529	0.0385
AD3	5.20	7.12	4.83	0.1779	4.97	0.0673	0.1106
AD4	5.20	6.70	4.79	0.1971	4.99	0.0962	0.1010
AD5	5.20	5.71	4.72	0.2308	4.98	0.1250	0.1058
AD6	5.20	4.92	4.65	0.2644	4.94	0.1394	0.1250
AD7	5.20	4.32	4.64	0.2693	4.94	0.1442	0.1250
AD8	5.20	4.02	4.63	0.2741	4.94	0.1490	0.1250
AD9	5.20	3.60	4.61	0.2837	4.93	0.1539	0.1298
AD10	5.20	3.32	4.58	0.2981	4.91	0.1587	0.1394

DAS[a] Equilibrium adsorption concentration
DES[b] Equilibrium desorption concentration
RED[c] Reduced chromium (VI) concentration

Table 37: 0.1 mM Cr(VI) adsorption in 0.01 M KH_2PO_4 for varying pH

Sample No.	Initial Cr(VI (mg/L)	pH	Equil. Cr(VI) (mg/L)	ADS[a] Cr(VI) (mmol/kg)	DES[b] Cr(VI) (mg/L)	Net ADS Cr(VI) (mmol/kg)	RED[c] Cr(VI) (mmol/kg)
AD1	5.20	7.45	5.20	0.0000	5.20	0.0000	0.0000
AD2	5.20	7.21	5.20	0.0000	5.20	0.0000	0.0000
AD3	5.20	7.12	5.20	0.0000	5.20	0.0000	0.0000
AD4	5.20	6.54	5.20	0.0000	5.20	0.0000	0.0000
AD5	5.20	5.47	5.20	0.0000	5.20	0.0000	0.0000
AD6	5.20	4.86	5.15	0.0240	5.17	0.0096	0.0144
AD7	5.20	4.12	4.96	0.1154	5.06	0.0481	0.0673
AD8	5.20	3.87	4.63	0.2741	4.75	0.0577	0.2164
AD9	5.20	3.27	4.58	0.2981	4.73	0.0721	0.2260
AD10	5.20	2.87	4.21	0.4760	4.38	0.0817	0.3943

DAS[a] Equilibrium adsorption concentration
DES[b] Equilibrium desorption concentration
RED[c] Reduced chromium (VI) concentration

Table 38: Soil column experiment # 1

Sample no.	time (hr)	Sample vol. (ml)	Cumu. vol. (ml)	Cumu. pore (vol.)	Flow rate (ml/hr)	pH	Specific conduct. (umho/cm)	Cr(VI) conc. (mg/L)	Cr(VI) adsorb. (mmol/kg)
A1	1.6	15.5	15.5	0.2	9.8	7.91		0.00	0.018
A2	2.0	20.5	36.0	0.6	10.3	7.91	1080	0.00	0.043
A3	1.3	14.0	50.0	0.8	10.5	7.92	1076	0.00	0.059
A4	1.3	13.0	63.0	1.0	10.4	7.91	1059	0.00	0.075
A5	1.0	10.5	73.5	1.2	10.5	7.92	1080	0.14	0.087
A6	1.0	10.5	84.0	1.3	10.5	7.91	1080	2.32	0.096
A7	1.1	11.0	95.0	1.5	10.0	7.92	1100	4.48	0.104
A8	1.1	11.0	106.0	1.7	10.0	7.93	1080	5.31	0.110
A9	1.0	10.5	116.5	1.8	10.5	7.92	1080	5.87	0.115
A10	1.0	10.5	127.0	2.0	10.5	7.92	1100	6.32	0.119
A11	1.0	10.5	137.5	2.2	10.5	7.94	1124	6.76	0.123
A12	9.7	98.0	235.5	3.7	10.1	7.93	1180	7.59	0.151
A13	2.0	20.5	256.0	4.0	10.3	7.94		8.00	0.156
A14	3.0	30.2	286.2	4.5	10.1	7.94		8.21	0.163
A15	2.2	23.5	309.7	4.9	10.6	7.94		8.23	0.168
A16	6.3	66.5	376.2	5.9	10.5	7.94		8.43	0.180
A17	10.3	103.5	479.7	7.5	10.1	7.95	1180	8.69	0.196
A18	3.8	38.0	517.7	8.1	9.9	7.95		8.71	0.202
A19	8.2	81.5	599.2	9.4	10.0	7.96	1188	8.80	0.213
A20	12.0	121.0	720.2	11.3	10.1	7.95	1180	8.81	0.231
A21	7.8	79.0	799.2	12.5	10.1	7.96	1080	8.90	0.241
A22	4.6	46.8	846.0	13.3	10.2	7.95		9.00	0.246
A23	11.8	120.0	966.0	15.1	10.1	7.95		9.05	0.260
A24	7.6	73.5	1039.5	16.3	9.7	7.96		9.09	0.268
A25	18.3	173.0	1212.5	19.0	9.5	7.97	1025	9.11	0.286
A26	6.8	63.5	1276.0	20.0	9.4	7.96		9.21	0.292
A27	17.5	164.0	1440.0	22.6	9.4	7.96		9.22	0.307
A28	4.2	39.0	1479.0	23.2	9.4	7.96		9.23	0.311
A29	4.1	40.0	1519.0	23.8	9.8	7.96		9.25	0.314
A30	6.0	55.5	1574.5	24.7	9.3	7.97	1025	9.25	0.319
A31	7.8	72.0	1646.5	25.8	9.2	7.97		9.25	0.326
A32	15.0	141.5	1788.0	28.0	9.4	7.97		9.26	0.338
A33	7.7	70.0	1858.0	29.1	9.1	7.97		9.24	0.344
A34	16.6	148.0	2006.0	31.4	8.9	7.97		9.24	0.358
A35	4.1	36.5	2042.5	32.0	8.9	7.98	1180	9.22	0.361
A36	18.4	166.5	2209.0	34.6	9.0	7.96	1184	9.21	0.377
A37	9.0	77.0	2286.0	35.8	8.6	7.97	1180	9.27	0.383
A38	15.8	130.0	2416.0	37.9	8.2	7.97	1188	9.28	0.394
A39	25.7	209.0	2625.0	41.1	8.1	7.98		9.28	0.412
A40	24.0	191.0	2816.0	44.1	8.0	7.97	1180	9.28	0.428
A41	23.1	179.0	2995.0	46.9	7.8	7.98	1100	9.37	0.442
A42	5.9	45.0	3040.0	47.6	7.6	7.98		9.37	0.445
A43	16.1	121.0	3161.0	49.5	7.5	8.00		9.37	0.454
A44	25.0	185.5	3346.5	52.4	7.4	8.00	1100	9.37	0.468
A45	24.1	178.0	3524.5	55.2	7.4	7.98		9.36	0.482
A46	23.7	168.5	3693.0	57.9	7.1	7.98	1050	9.34	0.495
A47	8.6	60.5	3753.5	58.8	7.0	8.00	1055	9.35	0.499
A48	25.2	169.0	3922.5	61.5	6.7	8.02	1050	9.46	0.510
A49	15.4	97.0	4019.5	63.0	6.3	7.98	1057	9.47	0.516
A50	22.6	140.5	4160.0	65.2	6.2	8.00	1050	9.48	0.525
A51	24.3	150.0	4310.0	67.5	6.2	8.02		9.46	0.534
A52	25.0	146.0	4456.0	69.8	5.8	8.03		9.44	0.544

A53	23.4	136.0	4592.0	71.9	5.8	8.04		9.45	0.553
A54	23.5	140.0	4732.0	74.1	6.0	8.02		9.48	0.562
A55	25.7	149.0	4881.0	76.5	5.8	8.03	1065	9.45	0.571
A56	29.7	167.5	5048.5	79.1	5.6	8.06	1215	9.44	0.582
A57	19.3	105.0	5153.5	80.7	5.4	8.05	1218	9.45	0.589
A58	32.7	176.5	5330.0	83.5	5.4	8.03		9.46	0.600
A59	19.6	107.0	5437.0	85.2	5.5	8.04	1220	9.43	0.608
A60	24.2	118.5	5555.5	87.0	4.9	8.02	1228	9.45	0.615
A61	26.0	123.0	5678.5	89.0	4.7	8.04	1220	9.43	0.624
A62	44.3	201.0	5879.5	92.1	4.5	8.06		9.43	0.637
A63	50.4	226.0	6105.5	95.7	4.5	8.04		9.43	0.653
A64	18.2	81.0	6186.5	96.9	4.5	8.06	1220	9.43	0.658
A65	47.8	213.0	6399.5	100.3	4.5	8.06		9.44	0.672
A66	50.3	209.5	6609.0	103.5	4.2	8.05		9.46	0.685
A67	52.2	202.0	6811.0	106.7	3.9	8.06	1229	9.50	0.697
A68	44.1	167.0	6978.0	109.3	3.8	8.06	1275	9.52	0.707
AD1*	7.9	28.5	7006.5	109.8	3.6	8.05		9.53	0.709
AD2*	15.0	63.0	7069.5	110.8	4.2	7.99	1200	8.30	0.062
AD3*	32.7	130.0	7199.5	112.8	4.0	7.98	1206	2.32	0.098
AD4*	42.0	165.0	7364.5	115.4	3.9	7.95	1200	1.38	0.125
AD5*	46.0	181.5	7546.0	118.2	3.9	7.94	1207	1.34	0.153
AD6*	27.6	101.5	7647.5	119.8	3.7	7.93		1.11	0.167
AD7*	26.4	99.5	7747.0	121.4	3.8	7.90	1245	0.96	0.178
AD8*	23.8	84.0	7831.0	122.7	3.5	7.88	1240	0.91	0.187
AD9*	26.9	92.0	7923.0	124.1	3.4	7.88		0.84	0.196
AD10*	21.0	71.0	7994.0	125.2	3.4	7.88	1240	0.83	0.203
AD11*	53.0	191.0	8185.0	128.2	3.6	7.89		0.81	0.222
AD12*	25.0	89.0	8274.0	129.6	3.6	7.87	1223	0.80	0.230
AD13*	32.0	116.5	8390.5	131.5	3.6	7.89	1220	0.79	0.241
AD14*	35.0	121.2	8511.7	133.4	3.5	7.89	1224	0.78	0.252
AD15*	36.0	125.0	8636.7	135.3	3.5	7.89	1220	0.69	0.262
AD16*	22.0	75.0	8711.7	136.5	3.4	7.89	1220	0.60	0.268
AD17*	45.0	156.0	8867.7	138.9	3.5	7.87		0.55	0.278
AD18*	47.0	166.0	9033.7	141.5	3.5	7.87		0.45	0.287
AD19*	34.0	125.5	9159.2	143.5	3.7	7.89		0.41	0.293
AD20*	98.0	350.0	9509.2	149.0	3.6	7.89	1180	0.29	0.305
AD21*	90.0	317.0	9826.2	154.0	3.5	7.89	1180	0.22	0.313
AD22*	40.0	141.0	9967.2	156.2	3.5	7.89	1160	0.19	0.316
AD23	17.0	60.0	10027.2	157.1	3.5	7.89		0.15	0.317
AD24	20.0	68.5	10095.7	158.2	3.4	7.87	4000	0.14	0.318
AD25	25.0	90.0	10185.7	159.6	3.6	7.87	4600	0.12	0.320
AD26	66.5	230.0	10415.7	163.2	3.5	7.89	4600	0.11	0.323
AD27	49.0	170.0	10585.7	165.9	3.5	7.88	4650	0.13	0.325
AD28	27.5	96.0	10681.7	167.4	3.5	7.87	4600	0.11	0.326

AD1* Desorption with 0.01 M NaCl

Table 39: Soil column experiment # 2

Sample no.	time (hr)	Sample vol. (ml)	Cumu. pore (vol)	Flow rate (ml/hr)	pH	Specific conduct. (umho/cm)	Cr(VI) conc. (mg/L)	Cr(VI) adsorb. (mmol/kg)
A1	4.9	49.0	0.8	9.96	7.78	1230	0.00	0.057
A2	2.9	29.0	1.2	9.93	7.78		0.00	0.091
A3	10.0	94.0	2.7	9.45	7.74	3750	7.06	0.124
A4	2.12	20.0	3.0	9.43	7.71		8.70	0.127
A5	6.1	57.0	4.0	9.38	7.65	3900	9.50	0.130
A6	16.1	143.5	6.2	8.93	7.80	3500	9.62	0.136
A7	7.2	63.0	7.2	8.81	7.78	3700	9.61	0.139
A8	7.4	63.5	8.2	8.62	7.79	3700	9.54	0.143
A9	11.6	100.0	9.8	8.64	7.78	3700	9.51	0.148
A10	24.1	209.0	13.1	8.68	7.79		9.52	0.160
A11	23.4	205.0	16.4	8.75	7.77	3700	9.65	0.168
A12	4.6	40.0	17.0	8.70	7.78		9.65	0.170
A13	21.2	187.5	20.0	8.83	7.89		9.66	0.177
A14	23.6	203.5	23.2	8.63	8.00		9.63	0.186
A15	22.5	190.0	26.2	8.44	7.97		9.67	0.194
A15	24.3	208.5	29.5	8.57	8.00		9.67	0.202
A16	24.9	206.0	32.8	8.27	7.96		9.72	0.208
A17	23.4	200.0	36.0	8.54	8.02		9.70	0.215
A18	23.5	208.0	39.3	8.85	8.05		9.73	0.222
A19	25.7	220.0	42.8	8.56	8.04		9.71	0.229
A20	29.8	247.0	46.7	8.29	8.01	3850	9.72	0.238
A21	19.3	162.0	49.3	8.42	8.03	4100	9.73	0.243
A22	21.9	184.0	52.2	8.41	8.05	4450	9.74	0.248
A23	11.9	99.0	53.8	8.33	8.04	4250	9.78	0.251
A24	16.9	140.0	56.0	8.31	8.01		9.78	0.254
A25	25.4	208.0	59.3	8.19	8.06	4250	9.78	0.260
A26	27.5	212.0	62.6	7.71	8.04	4252	9.80	0.265
A27	22.8	175.0	65.4	7.68	8.03	4250	9.79	0.269
A28	21.7	164.0	68.0	7.56	8.02	4251	9.79	0.273
A29	27.1	204.5	71.3	7.54	8.05		9.78	0.278
A30	22.3	168.0	73.9	7.52	8.05		9.80	0.282
A31	17.9	134.5	76.1	7.50	8.05	4200	9.83	0.285
A32	23.1	173.0	78.8	7.48	8.06		9.78	0.289
A33	24.2	187.0	81.8	7.20	8.04	4400	9.84	0.293
A34	50.5	357.5	87.4	7.08	8.06		9.80	0.301
A35	52.3	351.0	93.0	6.71	8.06		9.82	0.309
A36	48.3	311.0	97.9	6.44	8.04		9.79	0.316
A37	49.4	325.0	103.1	6.58	8.07	4400	9.75	0.326
A38	45.6	290.0	107.7	6.37	8.07	4445	9.72	0.335
A39	50.6	303.0	112.5	5.99	8.05	4400	9.67	0.347
A40	25.6	148.0	114.9	5.79	8.07	4405	9.65	0.353
A41	26.3	150.0	117.2	5.70	8.05	4400	9.61	0.360
A42	35.4	187.0	120.2	5.28	8.05	4410	9.48	0.371
AD1*	4.6	22.5	120.6	4.89	8.06		6.54	0.017
AD2*	2.2	10.0	120.7	4.55	8.06	4450	6.16	0.024
AD3		50.0	121.5		8.04		0.68	0.028
AD4*	6.8	31.0	122.0	4.56	8.14	4450	14.98	0.083
AD5	3.4	15.0	122.2	4.41	8.20	4490	17.25	0.113
AD6	6.7	30.5	122.7	4.55	9.14	4500	2.19	0.121
AD7	8.2	37.0	123.3	4.51	9.57	4570	0.98	0.125
AD8	24.0	107.5	125.0	4.48	7.92	4600	0.69	0.134
AD9	7.5	34.0	125.6	4.53	7.90	4650	0.56	0.136

AD10	21.5	98.0	127.1	4.56	7.89	4650	0.48	0.141
AD11	27.5	125.0	129.1	4.55	7.88	4650	0.37	0.147
AD12	56	256.0	133.2	4.57	7.88	4650	0.35	0.157

AD1* Desorption with 0.01 M NaCl
AD3 Desorption stopped for 138 hours

Table 40: Soil column experiment # 3

Sample no.	time (hr)	Sample vol. (ml)	Cumu. pore vol.	Flow rate (ml/hr)	pH	Specific conduct. (umho/cm)	Cr(VI) conc. (mg/L)	Cr(VI) adsorb. (mmol/kg)
A1	5.2	29.5	0.46	5.71	7.80		0.00	0.035
A2	4.3	24.0	0.84	5.58	7.86	1080	0.00	0.063
A3	7.0	39.0	1.46	5.57	7.86		3.26	0.094
A4	3.3	18.0	1.74	5.45	7.85	1080	4.82	0.105
A5	5.6	31.5	2.23	5.63	7.88		5.65	0.121
A6	17.0	92.0	3.68	5.41	7.86		6.95	0.154
A7	8.2	45.0	4.39	5.49	7.87		7.63	0.167
A8	17.0	91.5	5.83	5.38	7.88	1040	7.85	0.190
A9	4.2	22.5	6.18	5.40	7.89		7.93	0.196
A10	19.0	100.0	7.76	5.26	7.88	1060	8.50	0.213
A11	9.0	45.0	8.46	5.00	7.89		8.60	0.221
A12	15.0	74.5	9.64	4.97	7.87		8.62	0.233
A13	23.0	113.0	11.41	4.91	7.86		8.79	0.249
A14	20.5	102.0	13.02	4.98	7.87	1040	8.97	0.261
A15	19.0	93.5	14.49	4.92	7.88	1060	8.93	0.273
A16	17.2	84.5	15.82	4.91	7.89		9.02	0.283
A17	18.5	91.0	17.25	4.92	7.89	1070	9.05	0.293
A18	17.6	85.0	18.59	4.83	7.87		9.04	0.303
A19	16.7	81.0	19.86	4.85	7.86	1080	9.06	0.312
A20	2.9	14.0	20.08	4.83	7.87		9.09	0.313
A21	19.5	94.5	21.57	4.85	7.89		9.12	0.323
A22	9.5	46.0	22.29	4.84	7.87		9.14	0.328
A23	13.7	66.0	23.33	4.82	7.86	1080	9.17	0.334
A24	14.5	70.5	24.44	4.86	7.87		9.16	0.341
A25	14.0	67.5	25.50	4.82	7.89		9.18	0.348
A26	13.0	62.5	26.49	4.81	7.88		9.15	0.354
A27	14.8	71.0	27.60	4.80	7.87		9.17	0.361
A28	15.7	75.0	28.78	4.78	7.89		9.18	0.368
A29	28.4	135.0	30.91	4.75	7.88	1120	9.15	0.382
A30	19.0	91.0	32.34	4.79	7.89		9.17	0.390
A31	12.2	58.0	33.25	4.75	7.89	1230	9.20	0.396
A32	28.3	135.0	35.37	4.77	7.87		9.18	0.409
A33	22.6	107.5	37.07	4.76	7.88		9.18	0.419
A34	31.0	147.0	39.38	4.74	7.93	1230	9.20	0.433
A35	24.0	115.0	41.19	4.79	7.91		9.19	0.444
A36	43.0	204.0	44.40	4.74	7.93		9.18	0.464
A37	34.0	161.0	46.93	4.74	7.89	1300	9.18	0.480
A38	29.0	137.0	49.09	4.72	7.93		9.21	0.492
A39	18.9	90.0	50.50	4.76	7.92	1300	9.20	0.501
AP1*	1.6	7.5	50.62	4.69	7.80	1300	8.91	0.008
AP2*	4.5	20.5	50.94	4.56	7.82	1300	8.03	0.027
AP3*	8.9	40.5	51.58	4.55	7.84	1300	23.19	0.138
AP4*	9.4	42.5	52.25	4.52	7.77	1300	17.62	0.226
AP5*	9.1	41.0	52.89	4.53	7.73		1.05	0.231
AP6*	4.9	22.0	53.24	4.54	7.76		0.65	0.233
AP7*	9.2	41.5	53.89	4.51	7.81		0.48	0.235
AP8*	8.9	40.0	54.52	4.52	7.77		0.32	0.237
AP9*	6.2	28.0	54.96	4.52	7.83	1200	0.28	0.238
AP10*	16.5	74.0	56.13	4.48	7.80	1200	0.19	0.240
AP11*	6.7	30.0	56.60	4.48	7.80	1200	0.13	0.240

AP* Desorption with 0.01 M $H_2PO_4^-/HPO_4^-$ at pH = 7.00

Table 41: Soil column experiment # 4

Sample no.	time (hr)	Sample vol. (ml)	Cumu. pore vol.	Flow rate (ml/hr)	pH	Specific conduct. (umho/cm)	Cr(VI) conc. (mg/L)	Cr(VI) adsorb. (mmol/kg)
B1	15.0	75.5	1.31	5.03	8.19	1375	0.00	0.041
B2	8.7	44.0	2.08	5.06	8.15	1375	0.54	0.062
B3	8.6	44.5	2.85	5.17	8.05	1375	3.25	0.071
B4	7.5	38.0	3.52	5.07	8.03	1375	3.53	0.077
B5	9.0	46.0	4.32	5.11	8.16	1375	3.65	0.084
B6	9.4	47.0	5.13	5.00	8.05	1375	3.89	0.090
B7	9.3	47.0	5.95	5.05	8.13	1375	3.91	0.096
B8	9.2	47.0	6.77	5.11	8.15	1375	3.95	0.101
B9	15.0	75.0	8.08	5.00	8.13	1375	4.07	0.109
B10	23.0	116.0	10.10	5.04	8.09	1375	4.32	0.118
B11	25.0	126.0	12.29	5.04	8.07	1375	4.37	0.127
B12	22.5	117.0	14.33	5.20	8.09	1320	4.55	0.134
B13	28.0	144.0	16.83	5.14	8.05	1320	4.48	0.142
B14	28.2	144.0	19.34	5.11	8.18	1375	4.58	0.150
B15	29.0	146.0	21.88	5.03	8.17	1375	4.55	0.157
B16	27.0	139.0	24.30	5.15	8.14	1375	4.58	0.164
B17	28.3	145.0	26.82	5.12	8.20	1375	4.58	0.172
B18	22.8	115.0	28.83	5.05	8.17	1375	4.58	0.177
B19	20.0	103.0	30.62	5.15	8.19	1375	4.58	0.183
B20	13.0	67.5	31.79	5.19	8.11	1450	4.58	0.186
BS1*	17.1	89.0	33.34	5.20	8.17	1500	7.41	0.071
BS2*	2.0	10.0	33.52	5.08	8.00	1800	3.52	0.075
BS3*	3.4	17.0	33.81	5.06	7.80	2000	2.14	0.078
BS4*	19.4	100.0	35.55	5.15	8.03	2000	0.63	0.085
BS5*	22.0	112.0	37.50	5.09	8.03	2150	0.15	0.087
BS6*	10.8	55.0	38.46	5.09	8.03	2200	0.10	0.088
BS7*	8.8	45.0	39.24	5.11	8.04	2200	0.05	0.088
BS8*	12.0	60.0	40.29	5.00	8.03	2200	0.00	0.088
BS9*	8.0	40.0	40.98	5.00	8.03	2200	0.00	0.088

BS1* Desorption with 0.01 M Na_2SO_4

Table 42: Soil column experiment # 5

Sample no.	time (hr)	Sample vol. (ml)	Cumu. pore vol.	Flow rate (ml/hr)	pH	Specific conduct. (umho/cm)	Cr(VI) conc. (mg/L)	Cr(VI) adsorb. (mmol/kg)
E1	8.6	56.0	0.92	6.53	8.15	1500	0.00	0.032
E2	14.5	94.0	2.47	6.48	7.59	1800	1.70	0.067
E3	20.5	140.0	4.77	6.83	7.82	10800	4.48	0.075
E4	30.5	200.0	8.05	6.56	7.88	11000	4.48	0.087
E5	25.0	164.0	10.75	6.56	7.91	11000	4.48	0.096
E6	28.0	183.0	13.76	6.54	7.91	11200	4.58	0.105
E7	25.9	171.0	16.57	6.60	7.94	11200	4.58	0.113
E8	24.0	154.0	19.10	6.42	8.04	11200	4.58	0.120
E9	31.0	200.0	22.38	6.45	7.97	11000	4.58	0.130
E10	26.0	169.0	25.16	6.50	7.90	10800	4.58	0.138
ES1*	5.4	35.0	25.74	6.48	7.90	10800	4.58	0.018
ES2*	4.9	32.0	26.26	6.53	7.87	9700	8.72	0.050
ES3*	2.6	17.0	26.54	6.54	7.85	9500	4.58	0.058
ES4*	5.5	35.0	27.12	6.36	7.91	9400	1.25	0.063
ES5*	4.7	30.0	27.61	6.38	7.97	9300	0.25	0.064
ES6*	4.0	25.0	28.02	6.25	7.97	9100	0.00	0.064
ES7*	7.2	45.0	28.76	6.25	7.98	9100	0.00	0.064
ES8*	5.8	36.0	29.35	6.21	7.97	9100	0.00	0.064

ES1* Desorption with 0.01 M Na_2SO_4 at pH = 6.0

Table 43: Soil column experiment # 6

Sample no.	time (hr)	Sample vol. (ml)	Cumu. pore vol.	Flow rate (ml/hr)	pH	Specific conduct. (umho/cm)	Cr(VI) conc. (mg/L)	Cr(VI) adsorb. (mmol/kg)
A1	3.3	21.0	0.34	6.36	8.02		0.00	0.012
A2	6.8	45.5	1.06	6.74	8.03	3100	0.00	0.039
A3	3.8	24.0	1.45	6.32	8.00	3200	0.06	0.052
A4	7.1	46.5	2.19	6.55	7.88	3000	0.74	0.075
A5	7.2	49.0	2.97	6.81	8.05	3000	1.59	0.095
A6	16.3	104.5	4.64	6.40	8.10	3150	1.79	0.134
A7	7.8	51.0	5.46	6.51	8.10	3150	2.15	0.150
A8	7.8	52.5	6.30	6.73	8.00	3100	2.37	0.166
A9	7.8	49.0	7.08	6.28	8.05	3100	2.31	0.182
A10	10.0	64.5	8.11	6.45	7.98	3100	2.39	0.201
A11	10.0	67.0	9.19	6.70	7.98		2.49	0.221
A12	23.5	156.0	11.68	6.64	7.95	3100	2.58	0.265
A13	25.0	169.0	14.38	6.76	7.98	3200	2.79	0.308
A14	45.0	290.0	19.02	6.44	7.61	3000	3.50	0.358
A15	22.0	146.0	21.35	6.64	7.48	3000	3.47	0.384
A16	35.0	240.0	25.19	6.86	7.25	3150	3.41	0.428
A17	24.0	159.5	27.74	6.65	7.28	3100	3.15	0.463
A18	25.0	170.0	30.46	6.80	7.31	3200	3.00	0.502
A19	22.0	148.0	32.83	6.73	7.41	3000	2.76	0.541
A20	20.5	138.0	35.03	6.73	7.47	3000	2.69	0.577
A21	25.0	168.0	37.72	6.72	7.48	3150	2.52	0.626
A22	31.0	213.0	41.12	6.87	7.27	3100	2.40	0.690
A23	27.0	186.0	44.10	6.89	7.22	3200	2.31	0.748
A24	22.7	152.0	46.53	6.70	7.36	3000	2.18	0.798
A25	26.0	178.0	49.37	6.85	7.31	3000	2.18	0.856
A26	21.5	148.0	51.74	6.88	7.38	3150	2.18	0.904
A27	32.0	215.0	55.18	6.72	7.40	3100	2.18	0.975
A28	42.0	287.0	59.77	6.83	7.21	3100	2.18	1.069
A29	39.0	255.0	63.84	6.54	7.14	3100	2.18	1.152
A30	36.0	241.0	67.70	6.69	7.18	3150	2.18	1.231
A31	29.8	200.0	70.89	6.71	7.65	3100	2.18	1.296
A32	21.0	138.0	73.10	6.57	7.71	3100	2.18	1.342
A33	28.0	182.0	76.01	6.50	7.87	3100	2.18	1.401
A34	24.0	156.0	78.51	6.50	7.47	3100	2.18	1.452
A35	26.0	170.0	81.22	6.54	7.43	3100	2.18	1.508
A36	25.5	168.0	83.91	6.59	7.40	3100	2.18	1.563
A37	39.0	258.0	88.03	6.62	7.31	3000	2.18	1.647
A38	33.0	215.0	91.47	6.52	7.30	3000	2.18	1.717
A39	45.0	298.0	96.24	6.62	7.20	3000	2.18	1.815
A40	45.5	300.0	101.03	6.59	7.25	2800	2.18	1.913
A41	62.0	400.0	107.43	6.45	6.94	2600	2.18	2.044
A42	33.5	215.0	110.87	6.42	6.24	3000	2.18	2.114
A43	38.5	248.0	114.83	6.44	4.01	3000	2.18	2.195
A44	56.0	362.0	120.62	6.46	3.95	3000	2.18	2.314
A45	84.0	540.0	129.25	6.43	3.85	3000	2.18	2.490
AP46*	20.5	132.0	131.36	6.44	3.81	3000	15.00	0.230
AP47	25.0	160.0	133.92	6.40	6.45	3600	3.45	0.294
AP48	50.0	320.0	139.04	6.40	6.50		0.82	0.324
AP49	67.0	430.0	145.91	6.42	6.60		0.44	0.346
AP50	39.0	245.0	149.83	6.28	6.68	4200	0.21	0.352

AP51	32.0	200.0	153.03	6.25	6.78	4200	0.10	0.354
AP52	19.4	120.0	154.95	6.19	6.99	4200	0.00	0.354
AP53	10.7	66.0	156.00	6.17	7.02		0.00	0.354

AP46* Desorption with 0.5 M phosphate solution at pH = 8.0

Table 44: Soil column experiment # 7

Sample no.	time (hr)	Sample vol. (ml)	Cumu. pore (vol)	Flow rate (ml/hr)	pH	Specific conduct. (umho/cm)	Cr(VI) conc. (mg/L)	Cr(VI) adsorb. (mmol/kg
D1	10.0	63.0	1.0	6.30	8.05		0.00	0.04
D2	11.8	72.5	2.1	6.17	7.55		0.48	0.08
D3	6.5	41.0	2.8	6.31	7.93		0.63	0.10
D4	17.6	116.0	4.6	6.60	8.03	10600	0.44	0.16
D5	6.9	46.5	5.4	6.74	8.05	12200	0.44	0.18
D6	26.8	182.0	8.3	6.79	8.03	12200	0.45	0.28
D7	25.0	169.0	10.9	6.76	8.05	9900	0.44	0.37
D8	31.0	205.0	14.2	6.61	8.06	10600	0.43	0.48
D9	21.0	142.0	16.5	6.76	8.06	12300	0.44	0.55
D10	25.0	165.0	19.1	6.60	8.06	11600	0.43	0.64
D11	27.0	180.0	21.9	6.67	8.06	12300	0.44	0.74
D12	30.0	200.0	25.1	6.67	8.06	12300	0.44	0.85
D13	25.6	167.0	27.7	6.53	7.99		0.45	0.93
D14	26.0	174.0	30.5	6.69	7.80		0.44	1.03
D15	20.0	134.0	32.6	6.70	7.93		0.43	1.10
D16	32.0	215.0	36.0	6.72	7.75	12500	0.44	1.21
D17	23.0	150.0	38.4	6.52	8.01	12800	0.43	1.29
D18	42.0	278.0	42.8	6.62	7.50	12500	0.44	1.44
D19	35.0	230.0	46.5	6.57	7.51	12400	0.44	1.56
D20	26.7	176.0	49.3	6.59	7.45	12400	0.43	1.66
D21	30.0	195.0	52.4	6.50	7.39	12500	0.44	1.76
D22	38.0	250.0	56.3	6.58	7.35	12000	0.44	1.90
D23	35.0	231.0	60.0	6.60	7.37	12000	0.43	2.02
D24	45.0	295.0	64.7	6.56	7.35	12000	0.44	2.18
D25	32.0	214.0	68.1	6.69	7.34	12000	0.44	2.29
D26	31.0	206.0	71.3	6.65	7.35	12200	0.44	2.40
D27	74.0	489.0	79.1	6.61	7.35	12000	0.45	2.66
D28	45.0	300.0	83.9	6.67	7.16	12000	0.44	2.82
D29	60.0	400.0	90.2	6.67	4.62	11000	0.44	3.03
D30	70.5	464.0	97.6	6.58	4.24	10600	0.43	3.28
D31	65.0	430.0	104.4	6.62	4.23	10000	0.43	3.51
D32	69.0	453.0	111.6	6.57	4.10	11850	0.44	3.75
D33	72.0	478.0	119.2	6.64	4.02	8400	0.44	4.01
D34	77.0	502.0	127.1	6.52	4.01	12000	0.44	4.28
D35	75.0	492.0	134.9	6.56	4.00	8400	0.43	4.54
D36	60.0	400.0	141.3	6.67	3.89		0.44	4.75
D37	45.0	296.0	146.0	6.58	3.69	12800	0.44	4.91
D38*	60.0	400.0	152.3	6.67	3.76	12500	1.90	5.76
D39	68.0	444.0	159.4	6.53	3.85	12500	1.92	6.69
D40	50.0	326.0	164.5	6.52	3.80	5000	2.12	7.38
D41	76.0	495.0	172.4	6.51	3.77	13000	2.38	8.40
D42	77.0	500.0	180.3	6.49	3.94	11400	2.60	9.41
D43	62.0	400.0	186.7	6.45	3.86	12000	2.87	10.21
D44	88.0	570.0	195.7	6.48	4.06	11000	3.07	11.34
D45	77.0	496.0	203.6	6.44	4.12	10000	3.50	12.30
D46	37.5	241.0	207.4	6.43	4.10	4600	4.01	12.75
D47	120.0	775.0	219.7	6.46	3.97	4500	6.09	14.01
D48	38.0	245.0	223.6	6.45	3.99	5200	7.78	14.36
D49	69.0	447.0	230.7	6.48	3.66	6200	10.50	14.86
D50	46.0	293.0	235.3	6.37	3.80	8400	12.00	15.13
D51	60.0	386.0	241.4	6.43	3.82	10000	14.50	15.38
D52	83.0	533.0	249.9	6.42	3.55	9500	16.50	15.60

D53	65.0	415.0	256.5	6.38	3.46	9500	18.50	15.67
D54	75.0	476.0	264.0	6.35	3.45	6800	20.00	15.67
D55	67.0	425.0	270.8	6.34	3.33	6800	20.00	15.67
D56	31.5	200.0	273.9	6.35	3.21	6800	20.00	15.67
D57	72.0	455.0	281.2	6.32	3.21	6800	20.00	15.67
D58	71.0	450.0	288.3	6.34	3.20	6800	20.00	15.67
D59	29.0	181.0	291.2	6.24	3.11	6800	20.00	15.67
D60	32.0	200.0	294.3	6.25	3.12	6800	20.00	15.67
D61**	77.0	479.0	301.9	6.22	3.10		20.00	17.35
D62	78.0	482.0	309.6	6.18	3.07		20.00	19.04
D63	61.0	376.0	315.6	6.16	3.10		20.00	20.36
D64	48.5	300.0	320.3	6.19	3.10		20.00	21.41
D65	124.0	761.0	332.4	6.14	3.31		20.00	24.08
D66	43.0	266.0	336.6	6.19	3.38		27.00	24.80
D67	69.0	427.0	343.4	6.19	3.40		29.00	25.84
D68	39.0	240.0	347.2	6.15	3.37		30.39	26.39
D69	6.2	38.0	347.8	6.13	3.39		40.18	26.44
D70**	29.0	178.0	350.6	6.14	3.31		45.83	35.89
D71	34.6	213.0	354.0	6.16	3.20		226.50	42.70
D72	36.5	225.0	357.6	6.16	3.21		280.60	48.47
D73	45.0	278.0	362.0	6.18	3.35		358.30	53.08
D74	33.0	203.0	365.2	6.15	3.13		385.30	55.80
D75	72.5	445.0	372.3	6.14	3.12		467.00	57.52
D76	51.0	310.0	377.2	6.08	3.10		499.00	57.55
D77	71.0	430.0	384.0	6.06	3.09		503.00	57.40
D78	84.0	510.0	392.1	6.07	2.94		505.00	57.10
D79	43.5	263.0	396.3	6.05	2.79		507.00	56.89
D80	84.5	510.0	404.4	6.04	2.75		506.00	56.53
DP1*	11.0	63.0	405.4	5.73	2.89		512.00	3.77
DP2	14.5	80.0	406.6	5.52	3.00		660.00	9.94
DP3	8.9	48.5	407.4	5.45	3.49		264.00	11.44
DP4	23.0	123.0	409.3	5.35	3.88		57.12	12.26
DP5	22.0	117.0	411.2	5.32	7.41		16.45	12.49
DP6	38.0	202	414.4	5.32	7.56		7.45	12.66
DP7	59.0	310	419.3	5.25	7.54		2.79	12.76
DP8	58.0	305	424.2	5.26	7.67		1.44	12.82
DP9	96.0	503	432.1	5.24	7.69		1.35	12.90
DP10	96.0	504	440.1	5.25	7.71		0.79	12.94

D38* Influent Cr(VI) 20 mg/L in 0.1 M NaCl + 12.5 ml/L HCl
D61** Influent Cr(VI) 50 mg/L in 0.1 M NaCl + 12.5 ml/L HCl
D70** Influent Cr(VI) 500 mg/L in 0.1 M NaCl + 12.5 ml/L HCl
DP1* Desorption with 0.5 M phosphate at pH = 8.0

Table 45: Soil column experiment # 8

Sample no.	time (hr)	Sample vol. (ml)	Cumu. pore (vol.)	Flow rate (ml/hr)	pH	Cr(VI) conc. (mg/L)	Cr(VI) adsorb. (mmol/kg)	C/C0
C1	30.0	28.0	1.0	0.93	8.20	0.0	3.00	0.000
C2	17.0	14.0	1.5	0.82	8.17	30.2	4.41	0.060
C3	16.9	14.0	2.0	0.83	8.04	169.2	3.99	0.338
C4	17.0	14.0	2.4	0.82	7.98	270.2	4.68	0.540
C5	30.0	29.0	3.5	0.97	8.04	351.0	5.60	0.702
C6	52.0	56.0	5.4	1.08	8.21	415.7	6.62	0.831
C7	75.0	83.0	8.3	1.11	8.28	473.0	7.10	0.946
C8	85.0	95.5	11.6	1.12	8.17	473.0	7.65	0.946
C9	54.0	57.0	13.6	1.06	8.12	473.0	7.98	0.946
C10	54.0	57.0	15.6	1.06	8.07	473.0	8.31	0.946
C11	70.0	75.0	18.2	1.07	8.06	474.0	8.72	0.948
C12	70.0	75.0	20.8	1.07	8.07	475.0	9.13	0.950
C13	63.0	67.0	23.2	1.06	8.02	474.0	9.50	0.948
C14	16.0	16.5	23.8	1.03	8.05	475.0	9.59	0.950
C15	83.0	90.0	26.9	1.08	8.05	474.0	10.09	0.948
C16	62.0	65.0	29.2	1.05	8.07	473.0	10.46	0.946
C17	71.0	73.0	31.7	1.03	8.07	474.0	10.87	0.948
C18	63.0	66.0	34.0	1.05	8.13	473.0	11.25	0.946
C19	65.0	68.5	36.4	1.05	8.13	475.0	11.62	0.950
C20	44.0	43.5	37.9	0.99	8.11	475.0	11.85	0.950
C21	26.0	23.0	38.7	0.88	8.12	480.0	11.95	0.960
C22	23.0	20.0	39.4	0.87	7.99	487.0	12.01	0.974
C23	27.0	25.0	40.3	0.93	7.95	500.0	12.01	1.000
C24	45.0	45.0	41.9	1.00	7.96	500.0	12.01	1.000
C25	63.0	65.0	44.1	1.03	7.98	500.0	12.01	1.000
C26	59.0	60.0	46.2	1.02	7.97	500.0	12.01	1.000
C27	102.0	108.0	50.0	1.06	7.96	500.0	12.01	1.000
C28*	47.0	46.0	51.6	0.98	8.01	477.0	12.23	0.954
C29	64.0	62.0	53.8	0.97	8.01	412.0	13.40	0.824
C30	102.0	87.0	56.8	0.85	7.89	412.8	15.03	0.826
C31	153.0	127.0	61.2	0.83	7.79	412.0	17.42	0.824
C32	50.0	40.0	62.6	0.80	7.75	412.0	18.17	0.824
C33	72.0	57.0	64.6	0.79	7.81	413.0	19.24	0.826
C34	100.0	68.0	67.0	0.68	7.97	411.0	20.53	0.822
C35	155.0	97.0	70.4	0.63	7.94	414.0	22.32	0.828
C36	289.0	178.0	76.6	0.62	7.91	413.0	25.64	0.826
C37	337.0	205.0	83.7	0.61	7.95	414.0	29.41	0.828
C38	234.0	138.0	88.5	0.59	7.99	413.0	31.98	0.826
C39	330.0	190.0	95.2	0.58	7.92	415.0	35.44	0.830
C40	345.0	197.0	102.0	0.57	7.85	412.0	39.15	0.824
C41	456.0	242.0	110.5	0.53	7.71	411.0	43.77	0.822
C42	446.0	213.0	117.9	0.48	7.70	411.0	47.83	0.822
C43**	67.0	31.0	119.0	0.46	7.85	411.0	2.73	0.822
C44	114.0	48.0	120.7	0.42	7.99	965.0	12.65	1.930
C45	111.0	48.0	122.3	0.43	8.02	110.0	13.78	0.220
C46	156.0	65.0	124.6	0.42	8.01	41.5	14.36	0.083
C47	109.0	45.0	126.2	0.41	8.01	20.1	14.55	0.040
C48	85.0	34.0	127.4	0.40	7.99	6.7	14.60	0.013
C49	61.0	25.0	128.2	0.41	8.02	2.1	14.61	0.004
C50	78.0	31.0	129.3	0.40	7.99	0.7	14.62	0.001
C51	62.0	24.0	130.1	0.39	8.01	0.5	14.62	0.001

C52	56.0	21.0	130.9	0.38	8.03	0.4	14.62	0.001
C53	31.0	12.0	131.3	0.39	8.00	0.3	14.62	0.001

C28* New influent 500 mg/L Cr(VI) in 0.01 M NaCl + 12.5 ml/L HC
C43** Desorption with 0.5 M phosphate solution at pH = 8

Table 46: Thermodynamic calculations of $BaCrO_4$

Well No.	pH	Ba+2 (ppb)	log(Ba+2) (mol/L)	Cr(VI) (ppb)	Cr(VI) (mol/L)	logCr(VI) (mol/L)	log(Ba+2) & logCr(VI) (mol/L)
EW-8	3.84	242.0	-5.7497	1.76E+06	3.38E-02	-1.4705	-7.2202
EW-9	5.66	60.0	-6.3553	6.44E+06	1.24E-01	-0.9071	-7.2625
EW-13	6.57	13.0	-7.0195	4.46E+05	8.58E-03	-2.0667	-9.0863
EW-16	6.12	29.0	-6.6711	3.00E+06	5.77E-02	-1.2389	-7.9100
EW-19	7.24	31.0	-6.6421	1.54E+03	2.96E-05	-4.5285	-11.1707
EW-21	6.78	18.0	-6.8782	7.18E+05	1.38E-02	-1.8599	-8.7381
EW-23	7.10	26.0	-6.7185	5.57E+04	1.07E-03	-2.9701	-9.6887
BG-2	7.45	96.0	-6.1512	2.00E+00	3.85E-08	-7.4150	-13.5662
DW-2	7.46	17.0	-6.9030	7.25E+03	1.39E-04	-3.8557	-10.7588
DW-7	7.28	24.0	-6.7533	2.00E+00	3.85E-08	-7.4150	-14.1683

Table 47: Thermodynamic calculations of $BaSO_4$

Well no.	pH	SO4-- (ppb)	SO4-- (mol/L)	log(SO4--) (mol/L)	log(Ba+2) & log(SO4--) (mol/L)
EW-8	3.84	69.2	7.2E-04	-3.14216	-8.89188
EW-9	5.66	271.0	2.8E-03	-2.54930	-8.90468
EW-13	6.57	47.2	4.9E-04	-3.30832	-10.3279
EW-16	6.12	207.0	2.2E-03	-2.66630	-9.33744
EW-19	7.24	24.5	2.6E-04	-3.59310	-10.2352
EW-21	6.78	82.4	8.6E-04	-3.06634	-9.94461
EW-23	7.10	21.1	2.2E-04	-3.65798	-10.3765
BG-2	7.45	13.8	1.4E-04	-3.84239	-9.99365
DW-2	7.46	85.9	8.9E-04	-3.04827	-9.95136
DW-7	7.28	2.2	2.3E-05	-4.63984	-11.3931

APPENDIX 3

FITEQL AND HYDRAQL Input and Output Tables

This appendix contains tables for FITEQL and HYDRAQL input and output data for chromium(VI) adsorption in NaCl electrolyte solution and competing oxyanions.

Table 48: Reaction stoichiometries considered for TLM calculations

Surface complexation reactions from Table II.2:

	FeOH	AlOH	ADS	CrO_4^{2-}	Cl^-	Na^+	H^+	$e^{-F\psi o/RT}$	$e^{(-F\psi\beta/RT}$
1.	1	0	0	0	0	0	1	1	0
2.	1	0	0	0	0	0	-1	-1	0
3.	0	1	0	0	0	0	1	1	0
4.	0	1	0	0	0	0	-1	-1	0
5.	1	0	0	0	0	1	-1	-1	1
6.	1	0	0	0	1	0	1	1	-1
7.	0	1	0	0	0	1	-1	-1	1
8.	0	1	0	0	1	0	1	1	-1
9.	1	0	1	1	0	0	1	1	-2
10.	1	0	1	1	0	0	2	1	-1
11.	0	1	1	1	0	0	1	1	-2
12.	0	1	1	1	0	0	2	1	-1
13.	1	0	1	1	0	0	1	1	-1
14.	1	0	1	1	0	0	2	1	-2

Aqueous speciation reactions from Table II.2:

15.	0	0	0	1	0	0	1	1	-1
16.	0	0	0	1	0	0	2	1	-1
17.	0	0	0	1	0	1	0	0	0
18.	0	0	0	2	0	0	2	2	-2

Table 49: TLM input data, 0.1 mM Cr(VI) adsorption for varying pH

```
         1
         1
         1
         1
         1
        30
         5          1          3          1
00001  -6.0   1.30E-4   SOH
00002  -6.0   4.40E-5   TOH
00160  -1.0   0.00E00   PSI0
00161  -1.0   0.00E00   PSIB
00162  -1.3   0.00E00   PSID
00010  0.0    0.00E00   ADS
00101  0.0    0.00E00   CrO4
00050  0.0    0.00E00   H+
00005  0.0    0.00E00   NaCl

00050  0.0     01 00 010 00 101 00 050 01 005 00 160 00 161 00
00100  -13.9   01 00 010 00 101 00 050 -1 005 00 160 00 161 00
00102  6.51    01 00 010 00 101 01 050 01 005 00 160 01 161 -1
00103  5.56    01 00 010 00 101 01 050 02 005 00 160 01 161 -1
00104  0.70    01 00 010 00 101 01 050 00 005 01 160 00 161 00
00105  14.56   01 00 010 00 101 02 050 02 005 00 160 02 161 -2
00001  0.0     01 01                                    161 00
01050  -4.3    01 01 010 00 101 00 050 01 005 00 160 01 161 00
01100  -9.8    01 01 010 00 101 00 050 -1 005 00 160 -1 161 00
01055  -9.3    01 01 010 00 101 00 050 -1 005 01 160 -1 161 01
01105  5.4     01 01 010 00 101 00 050 01 005 01 160 01 161 -1
00002  0.0     02 01                                    161 00
02050  -6.3    02 01 010 00 101 00 050 01 005 00 160 01 161 00
02100  -12.0   02 01 010 00 101 00 050 -1 005 00 160 -1 161 00
02055  -9.2    02 01 010 00 101 00 050 -1 005 01 160 -1 161 01
02105  7.9     02 01 010 00 101 00 050 01 005 01 160 01 161 -1
00401  11.0    01 01 010 01 101 01 050 01 005 00 160 01 161 -2
00402  18.0    01 01 010 01 101 01 050 02 005 00 160 01 161 -1
00801  9.4     02 01 010 01 101 01 050 01 005 00 160 01 161 -2
00802  15.9    02 01 010 01 101 01 050 02 005 00 160 01 161 -1


00004   18.0  40.0   1.25   0.2
0.01   1.0
         2          2          0
       401
       402
       001
       002
        12          1          3          0
        10
0.0000144
0.0000274
0.0000606
0.0001010
0.0001125
0.0001365
0.0001529
0.0001635
```

```
0.0001685
0.0001707
0.0001726
0.0001755
       101
-4.0059
-4.0127
-4.0347
-4.0402
-4.0439
-4.0467
-4.0485
-4.0495
-4.0532
-4.0542
-4.0551
-4.0765
         5
-2.
-2.
-2.
-2.
-2.
-2.
-2.
-2.
-2.
-2.
-2.
-2.
        50
-7.94
-7.75
-7.45
-6.99
-6.82
-6.38
-5.82
-5.00
-4.45
-4.00
-3.66
-3.45
         1          1
       010       0.02
       101       0.02
```

Table 50: TLM output data, 0.1 mM Cr(VI) for varying pH

INPUT DATA FOR VERIFICATION

CHEMICAL EQUILIBRIUM PROBLEM

ID	X	LOGX	T	GROUP	NAME
1	1.00E-06	-6.00	1.30E-04	I: T	SOH
2	1.00E-06	-6.00	4.40E-05	I: T	TOH
160	1.00E-01	-1.00	0.00E-01	I: T	PSI0
161	1.00E-01	-1.00	0.00E-01	I: T	PSIB
162	5.01E-02	-1.30	0.00E-01	I: T	PSID
10	1.00E+00	0.00	0.00E-01	II: T,X	ADS
101	1.00E+00	0.00	0.00E-01	III:X	CrO4
50	1.00E+00	0.00	0.00E-01	III:X	H+
5	1.00E+00	0.00	0.00E-01	III:X	NaCl

MATRIX A

ID	LOGK	1	2	160	161	162	10
50	0.00	0.00	0.00	0.00	0.00	0.00	0.00
100	-13.90	0.00	0.00	0.00	0.00	0.00	0.00
102	6.51	0.00	0.00	1.00	-1.00	0.00	0.00
103	5.56	0.00	0.00	1.00	-1.00	0.00	0.00
104	0.70	0.00	0.00	0.00	0.00	0.00	0.00
105	14.56	0.00	0.00	2.00	-2.00	0.00	0.00
1	0.00	1.00	0.00	0.00	0.00	0.00	0.00
1050	-4.20	1.00	0.00	1.00	0.00	0.00	0.00
1100	-10.80	1.00	0.00	-1.00	0.00	0.00	0.00
1055	-9.30	1.00	0.00	-1.00	1.00	0.00	0.00
1105	5.40	1.00	0.00	1.00	-1.00	0.00	0.00
2	0.00	0.00	1.00	0.00	0.00	0.00	0.00
2050	-6.30	0.00	1.00	1.00	0.00	0.00	0.00
2100	-12.00	0.00	1.00	-1.00	0.00	0.00	0.00

2055	-9.20	0.00	1.00	-1.00	1.00	0.00	0.00
2105	7.90	0.00	1.00	1.00	-1.00	0.00	0.00
401	11.00	1.00	0.00	1.00	-2.00	0.00	1.00
402	18.00	1.00	0.00	1.00	-1.00	0.00	1.00
801	9.40	0.00	1.00	1.00	-2.00	0.00	1.00
802	15.90	0.00	1.00	1.00	-1.00	0.00	1.00

MATRIX B

ID	LOGK	1	2	160	161	162	10
50	0.00	0.00	0.00	0.00	0.00	0.00	0.00
100	-13.90	0.00	0.00	0.00	0.00	0.00	0.00
102	6.51	0.00	0.00	1.00	-1.00	0.00	0.00
103	5.56	0.00	0.00	1.00	-1.00	0.00	0.00
104	0.70	0.00	0.00	0.00	0.00	0.00	0.00
105	14.56	0.00	0.00	2.00	-2.00	0.00	0.00
1	0.00	1.00	0.00	0.00	0.00	0.00	0.00
1050	-4.20	1.00	0.00	1.00	0.00	0.00	0.00
1100	-10.80	1.00	0.00	-1.00	0.00	0.00	0.00
1055	-9.30	1.00	0.00	-1.00	1.00	0.00	0.00
1105	5.40	1.00	0.00	1.00	-1.00	0.00	0.00
2	0.00	0.00	1.00	0.00	0.00	0.00	0.00
2050	-6.30	0.00	1.00	1.00	0.00	0.00	0.00
2100	-12.00	0.00	1.00	-1.00	0.00	0.00	0.00
2055	-9.20	0.00	1.00	-1.00	1.00	0.00	0.00
2105	7.90	0.00	1.00	1.00	-1.00	0.00	0.00
401	11.00	1.00	0.00	1.00	-2.00	0.00	1.00
402	18.00	1.00	0.00	1.00	-1.00	0.00	1.00
801	9.40	0.00	1.00	1.00	-2.00	0.00	1.00
802	15.90	0.00	1.00	1.00	-1.00	0.00	1.00

TRIPLE LAYER MODEL

S M**2/G = 18.0 A G/L = 40.000

C1 F/M**2 = 1.250 C2 F/M**2 = 0.200

ELECTROLYTE CONCENTRATION MOL/L = 0.010000 ELECTROLYTE VA
PARAMETERS FOR OPTIMIZATION:

LOG K FOR SPECIES: 401 402

T FOR COMPONENTS: 1 2
INPUT DATA FOR VERIFICATION

SERIAL DATA AND ERROR ESTIMATES

TOTAL CONCENTRATION FOR COMPONENT:

	10
1	1.440E-05
2	2.740E-05
3	6.060E-05
4	1.010E-04
5	1.125E-04
6	1.365E-04
7	1.529E-04
8	1.635E-04
9	1.685E-04
10	1.707E-04
11	1.726E-04
12	1.755E-04

LOG FREE CONCENTRATION FOR COMPONENT:

	101	5	50
1	-4.01	-2.00	-7.94
2	-4.01	-2.00	-7.75
3	-4.03	-2.00	-7.45
4	-4.04	-2.00	-6.99
5	-4.04	-2.00	-6.82
6	-4.05	-2.00	-6.38
7	-4.05	-2.00	-5.82
8	-4.05	-2.00	-5.00
9	-4.05	-2.00	-4.45
10	-4.05	-2.00	-4.00
11	-4.06	-2.00	-3.66
12	-4.08	-2.00	-3.45

STANDARD DEVIATION OF FREE CONCENTRATION:

COMPONENT 101 RELATIVE 0.0200 ABSOLUTE 0.000E-01

STANDARD DEVIATION OF TOTAL CONCENTRATION:

COMPONENT 10 RELATIVE 0.0200 ABSOLUTE 0.000E-01
VALUES OF ADJUSTABLE PARAMETERS AT EACH ITERATION: LOG K, T, L

I	V(Y): SOS/DF	401	402	1	2
0		1.100E+01	1.800E+01	1.300E-04	4.400E-05
	2.615E+02				
1		1.125E+01	1.846E+01	1.253E-04	4.820E-05
	5.555E+01				
2		1.081E+01	1.879E+01	1.275E-04	4.598E-05
	1.260E+01				
3		1.048E+01	1.891E+01	1.288E-04	4.462E-05

	5.475E+00				
4		1.039E+01	1.894E+01	1.285E-04	4.494E-05
	5.227E+00				
5		1.037E+01	1.894E+01	1.284E-04	4.508E-05
	5.224E+00				
6		1.037E+01	1.894E+01	1.283E-04	4.510E-05
	5.224E+00				
7		1.037E+01	1.894E+01	1.283E-04	4.511E-05
	5.224E+00				

**** OPTIMIZATION PROCEDURE CONVERGED

7	5.22E+00	1.037E+01	1.894E+01	1.283E-04	4.511E-05

DESCRIPTION OF CHEMICAL EQUILIBRIUM: (T,Y)

	10	10	101	101
1	1.440E-05	2.070E-07	0.000E-01	2.295E-05
2	2.740E-05	-3.079E-07	0.000E-01	3.684E-05
3	6.060E-05	-2.506E-06	0.000E-01	7.074E-05
4	1.010E-04	6.776E-06	0.000E-01	1.301E-04
5	1.125E-04	5.335E-06	0.000E-01	1.466E-04
6	1.365E-04	-6.760E-06	0.000E-01	1.892E-04
7	1.529E-04	-1.121E-05	0.000E-01	2.809E-04
8	1.635E-04	1.628E-06	0.000E-01	5.149E-04
9	1.685E-04	2.661E-06	0.000E-01	7.150E-04
10	1.707E-04	1.988E-06	0.000E-01	8.971E-04
11	1.726E-04	5.176E-07	0.000E-01	1.043E-03
12	1.755E-04	-2.255E-06	0.000E-01	1.126E-03

DESCRIPTION OF CHEMICAL EQUILIBRIUM: -LOG C

	50	100	102	103	104	105	1	1050	1100
1	7.94	5.96	5.47	14.36	5.31	9.40	3.94	16.06	6.83
2	7.75	6.15	5.31	14.01	5.31	9.08	3.99	15.93	7.06
3	7.45	6.45	5.10	13.50	5.33	8.65	4.15	15.84	7.46
4	6.99	6.91	4.75	12.69	5.34	7.96	4.67	16.03	8.31
5	6.82	7.08	4.62	12.39	5.34	7.69	4.94	16.17	8.71
6	6.38	7.52	4.26	11.59	5.35	6.98	5.69	16.57	9.81
7	5.82	8.08	3.87	10.64	5.35	6.21	6.63	17.12	11.15
8	5.00	8.90	3.47	9.42	5.35	5.40	7.85	17.96	12.74
9	4.45	9.45	3.28	8.68	5.35	5.03	8.59	18.52	13.66
10	4.00	9.90	3.16	8.11	5.35	4.79	9.16	18.98	14.35
11	3.66	10.24	3.09	7.70	5.36	4.63	9.58	19.32	14.84
12	3.45	10.45	3.05	7.45	5.38	4.56	9.83	19.51	15.14

DESCRIPTION OF CHEMICAL EQUILIBRIUM: C (MOL/L)

	50	100	102	103
1	1.148E-08	1.096E-06	3.398E-06	4.377E-15
2	1.778E-08	7.079E-07	4.882E-06	9.741E-15
3	3.548E-08	3.548E-07	8.015E-06	3.191E-14
4	1.023E-07	1.230E-07	1.773E-05	2.035E-13
5	1.514E-07	8.318E-08	2.419E-05	4.109E-13
6	4.169E-07	3.020E-08	5.479E-05	2.563E-12
7	1.514E-06	8.318E-09	1.334E-04	2.266E-11
8	1.000E-05	1.259E-09	3.374E-04	3.786E-10
9	3.548E-05	3.548E-10	5.206E-04	2.073E-09
10	1.000E-04	1.259E-10	6.872E-04	7.711E-09
11	2.188E-04	5.754E-11	8.185E-04	2.009E-08
12	3.548E-04	3.548E-11	8.929E-04	3.555E-08

DESCRIPTION OF CHEMICAL EQUILIBRIUM: C (MOL/L)

	1105	2	2050	2100
1	3.038E-09	4.459E-05	2.717E-19	3.668E-09
2	3.952E-09	4.439E-05	4.061E-19	2.432E-09
3	4.748E-09	4.390E-05	7.072E-19	1.366E-09
4	3.209E-09	4.238E-05	1.471E-18	6.122E-10
5	2.403E-09	4.133E-05	1.936E-18	4.423E-10
6	9.590E-10	3.625E-05	3.799E-18	1.734E-10
7	2.702E-10	2.308E-05	5.979E-18	4.465E-11
8	4.111E-11	4.313E-06	2.666E-18	3.497E-12
9	1.169E-11	9.361E-07	8.692E-19	5.052E-13
10	4.157E-12	2.620E-07	3.182E-19	1.082E-13
11	1.904E-12	1.017E-07	1.469E-19	3.530E-14
12	1.233E-12	5.768E-08	9.533E-20	1.749E-14

OUTPUT OF EQUILIBRIUM DATA: ELECTROSTATICS

	T0(MOL/L)	(C/M**2)	LOG X0	PSI0(V)	TB(MOL/L)
1	1.815E-05	0.0024	0.025	-0.0015	-2.087E-05
2	3.239E-05	0.0043	0.011	-0.0007	-3.568E-05
3	6.699E-05	0.0090	-0.043	0.0025	-7.069E-05
4	1.275E-04	0.0171	-0.170	0.0100	-1.304E-04
5	1.448E-04	0.0194	-0.209	0.0124	-1.473E-04
6	1.902E-04	0.0255	-0.300	0.0177	-1.923E-04
7	2.848E-04	0.0382	-0.467	0.0276	-2.872E-04
8	5.144E-04	0.0689	-0.909	0.0538	-5.155E-04
9	7.119E-04	0.0954	-1.282	0.0758	-7.123E-04
10	8.932E-04	0.1197	-1.616	0.0956	-8.933E-04
11	1.038E-03	0.1392	-1.880	0.1112	-1.038E-03
12	1.122E-03	0.1503	-2.032	0.1202	-1.122E-03

DESCRIPTION OF CHEMICAL EQUILIBRIUM: EXPERIMENTAL DATA

T, LOG X

	1	2	160	161
1	1.283E-04	4.511E-05	1.815E-05	-2.087E-05
2	1.283E-04	4.511E-05	3.239E-05	-3.568E-05
3	1.283E-04	4.511E-05	6.699E-05	-7.069E-05
4	1.283E-04	4.511E-05	1.275E-04	-1.304E-04
5	1.283E-04	4.511E-05	1.448E-04	-1.473E-04
6	1.283E-04	4.511E-05	1.902E-04	-1.923E-04
7	1.283E-04	4.511E-05	2.848E-04	-2.872E-04
8	1.283E-04	4.511E-05	5.144E-04	-5.155E-04
9	1.283E-04	4.511E-05	7.119E-04	-7.123E-04
10	1.283E-04	4.511E-05	8.932E-04	-8.933E-04
11	1.283E-04	4.511E-05	1.038E-03	-1.038E-03
12	1.283E-04	4.511E-05	1.122E-03	-1.122E-03

ESTIMATED STANDARD DEVIATION IN EXPERIMENTAL DATA

ST, SX

	1	2	160	161	1
1	0.000E-01	0.000E-01	0.000E-01	0.000E-01	0.000E-
2	0.000E-01	0.000E-01	0.000E-01	0.000E-01	0.000E-
3	0.000E-01	0.000E-01	0.000E-01	0.000E-01	0.000E-
4	0.000E-01	0.000E-01	0.000E-01	0.000E-01	0.000E-
5	0.000E-01	0.000E-01	0.000E-01	0.000E-01	0.000E-
6	0.000E-01	0.000E-01	0.000E-01	0.000E-01	0.000E-

7	0.000E-01	0.000E-01	0.000E-01	0.000E-01	0.000E-
8	0.000E-01	0.000E-01	0.000E-01	0.000E-01	0.000E-
9	0.000E-01	0.000E-01	0.000E-01	0.000E-01	0.000E-
10	0.000E-01	0.000E-01	0.000E-01	0.000E-01	0.000E-
11	0.000E-01	0.000E-01	0.000E-01	0.000E-01	0.000E-
12	0.000E-01	0.000E-01	0.000E-01	0.000E-01	0.000E-

OPTIMIZATION PROCEDURE: FINAL STEP

NORMAL MATRIX: SUM OF U*V*(DY/DU)*(DY/DV)/(SY*SY)

	401	402	1	2
401	3.394E+01	2.323E+02	3.339E+02	1.454E+00
402	2.323E+02	1.903E+03	3.352E+03	1.522E+01
1	3.339E+02	3.352E+03	1.983E+04	2.631E+03
2	1.454E+00	1.522E+01	2.631E+03	8.060E+02

RIGHT HAND SIDE OF NORMAL EQUATIONS: SUM OF U*(DY/DU)*Y/(SY*SY

401	402	1	2
-2.185E-04	-5.144E-03	6.692E-04	2.420E-03

INVERSE OF NORMAL MATRIX = COVARIANCE MATRIX: S(U,V)*S(U,V)/(U

	401	402	1	2
401	2.182E-01	-3.173E-02	2.934E-03	-9.368E-03
402	-3.173E-02	5.687E-03	-7.418E-04	2.371E-03
1	2.934E-03	-7.418E-04	2.210E-04	-7.127E-04
2	-9.368E-03	2.371E-03	-7.127E-04	3.539E-03

SOLUTION TO NORMAL EQUATIONS: DELTA K/K, DELTA T/T, DELTA X/X

401	402	1	2
9.484E-05	-1.708E-05	1.598E-06	-2.062E-06

STATISTICS:

STANDARD DEVIATION: S(LOG K), S(T), S(LOG X)

401	402	1	2
2.029E-01	3.275E-02	1.908E-06	2.683E-06

LINEAR CORRELATION COEFFICIENTS: S(U,V)*S(U,V)/(S(U,U)*S(V,V))

	401	402	1	2
401	1.000E+00	-9.007E-01	4.224E-01	-3.372E-01
402	-9.007E-01	1.000E+00	-6.617E-01	5.285E-01
1	4.224E-01	-6.617E-01	1.000E+00	-8.058E-01
2	-3.372E-01	5.285E-01	-8.058E-01	1.000E+00

Table 51: HYDRAQL input, 0.1 mM chromate adsorption in 0.01 M NaCl

```
0.0100 0 0.0000 25.00 1.000E-03 1 100 /XMU KEYMU ACTCOR TEMP EPS NCASES ITMAX
1    1     1      1      1     1      /IHYDRA IINPUT ICHARG IPDIST IPCENT IALLPC
1    2     4   0          80000         /KEY IADS MODEL IDIFOP LIMADS
1.25 0.2  0   686. 1.25 0.2 0   34.    /C11 C21 C31 AREA1 C12 C22 C32 AREA2
179 50 86130 86132 86152 86150 0 0 0 0 0 0 0 0 0 0 0 0 0 0 /
3.00  9.01  0.1                        /
179   -6.000   1.000E-4                /DATA FOR COMPONENTS  CrO4--
157   -2.000   1.000E-2                /                     Cl-
 50   -4.000   0.000E-0                /                     H+
  5   -2.000   1.000E-2                /                     Na+
184   -6.000   5.130E-6                /                     SOH
180   -1.000   0.000                   /                     PSI0
182   -1.000   0.000                   /                     PSIB
183   -1.300   0.000                   /                     PSID
194   -6.000   1.800E-6                /                     TOH
190   -1.000   0.000                   /                     PSI0
192   -1.000   0.000                   /                     PSIB
193   -1.300   0.000                   /                     PSID
  0    0.000   0.000                   /
2                                      /
86105   -9.8  184 1  50 -1  180  -1    0  0     0  0   0   0 /
86110    4.3  184 1  50  1  180   1    0  0     0  0   0   0 /
86115   -9.3  184 1  50 -1  180  -1    5  1   182  1   0   0 /
86120    5.4  184 1  50  1  180   1  157  1   182 -1   0   0 /
86130   10.4  184 1  50  1  180   1  179  1   182 -2   0   0 /
86150   18.9  184 1  50  2  180   1  179  1   182 -1   0   0 /
86107  -12.0  194 1  50 -1  190  -1    0  0     0  0   0   0 /
86112    6.3  194 1  50  1  190   1    0  0     0  0   0   0 /
86117   -9.2  194 1  50 -1  190  -1    5  1   192  1   0   0 /
86122    7.9  194 1  50  1  190   1  157  1   192 -1   0   0 /
86132    9.4  194 1  50  1  190   1  179  1   192 -2   0   0 /
86152   15.9  194 1  50  2  190   1  179  1   192 -1   0   0 /
    0    0.0    0 0   0  0    0   0    0  0     0  0   0   0 /
3                                                            /
50      4.00  0 0 0 0 0 0 0 0 0 0 0 0 0 0 0 0 0 0 0 0 0 0 0 0 0 0 0 0 0 0 0 /
0       0.00  0 0 0 0 0 0 0 0 0 0 0 0 0 0 0 0 0 0 0 0 0 0 0 0 0 0 0 0 0 0 0 /
6                                                                           /
180     0.00  0 0 0 0 0 0 0 0 0 0 0 0 0 0 0 0 0 0 0 0 0 0 0 0 0 0 0 0 0 0 0 /
182     0.00  0 0 0 0 0 0 0 0 0 0 0 0 0 0 0 0 0 0 0 0 0 0 0 0 0 0 0 0 0 0 0 /
183     0.00  0 0 0 0 0 0 0 0 0 0 0 0 0 0 0 0 0 0 0 0 0 0 0 0 0 0 0 0 0 0 0 /
190     0.00  0 0 0 0 0 0 0 0 0 0 0 0 0 0 0 0 0 0 0 0 0 0 0 0 0 0 0 0 0 0 0 /
192     0.00  0 0 0 0 0 0 0 0 0 0 0 0 0 0 0 0 0 0 0 0 0 0 0 0 0 0 0 0 0 0 0 /
193     0.00  0 0 0 0 0 0 0 0 0 0 0 0 0 0 0 0 0 0 0 0 0 0 0 0 0 0 0 0 0 0 0 /
 0 0 0 0 0 0 0 0 0 0 0 0 0 0 0 0 0 0 0 0 0 0 0 0 0 0 0 0 0 0 0 0 0 0 0 0 0 /
 0 0 0 0 0 0 0 0 0 0 0 0 0 0 0 0 0 0 0 0 0 0 0 0 0 0 0 0 0 0 0 0 0 0 0 0 0 /
```

Table 52: HYDRAQL output, 0.1 mM chromate adsorption in 0.01 M NaCl

pH	179[a]	86150[b]	86132[c]	86152[d]	86130[e]	50[f]	T-ADS[g]
3.0	7.4097	5.2899	11.0792	5.7929	10.8346	2.9553	1.685E-01
3.1	7.3098	5.2899	10.9792	5.7930	10.7346	3.0553	1.685E-01
3.2	7.2098	5.2899	10.8792	5.7930	10.6346	3.1553	1.685E-01
3.3	7.1099	5.2899	10.7793	5.7930	10.5346	3.2553	1.685E-01
3.4	7.0100	5.2899	10.6793	5.7930	10.4346	3.3553	1.685E-01
3.5	6.9101	5.2899	10.5793	5.7930	10.3346	3.4553	1.685E-01
3.6	6.8103	5.2899	10.4793	5.7931	10.2346	3.5553	1.685E-01
3.7	6.7105	5.2899	10.3793	5.7931	10.1346	3.6553	1.685E-01
3.8	6.6107	5.2899	10.2794	5.7932	10.0346	3.7553	1.685E-01
3.9	6.5110	5.2899	10.1794	5.7932	9.9347	3.8553	1.685E-01
4.0	6.4114	5.2899	10.0795	5.7933	9.8347	3.9553	1.685E-01
4.1	6.3118	5.2899	9.9795	5.7934	9.7347	4.0553	1.685E-01
4.2	6.2124	5.2899	9.8796	5.7935	9.6347	4.1553	1.685E-01
4.3	6.1132	5.2900	9.7797	5.7937	9.5347	4.2553	1.684E-01
4.4	6.0141	5.2900	9.6798	5.7939	9.4347	4.3553	1.684E-01
4.5	5.9153	5.2900	9.5800	5.7942	9.3347	4.4553	1.684E-01
4.6	5.8168	5.2900	9.4802	5.7945	9.2347	4.5553	1.684E-01
4.7	5.7187	5.2900	9.3805	5.7949	9.1348	4.6553	1.683E-01
4.8	5.6211	5.2901	9.2808	5.7954	9.0348	4.7553	1.683E-01
4.9	5.5240	5.2901	9.1813	5.7961	8.9349	4.8553	1.682E-01
5.0	5.4277	5.2901	9.0818	5.7969	8.8349	4.9553	1.681E-01
5.1	5.3322	5.2902	8.9825	5.7980	8.7350	5.0553	1.680E-01
5.2	5.2379	5.2903	8.8835	5.7993	8.6351	5.1553	1.679E-01
5.3	5.1450	5.2904	8.7846	5.8010	8.5352	5.2553	1.677E-01
5.4	5.0537	5.2905	8.6861	5.8032	8.4354	5.3553	1.675E-01
5.5	4.9645	5.2907	8.5881	5.8060	8.3355	5.4553	1.673E-01
5.6	4.8776	5.2909	8.4907	5.8095	8.2358	5.5553	1.669E-01
5.7	4.7937	5.2912	8.3941	5.8141	8.1361	5.6553	1.665E-01
5.8	4.7130	5.2916	8.2986	5.8200	8.0366	5.7553	1.659E-01
5.9	4.6363	5.2921	8.2046	5.8277	7.9371	5.8553	1.652E-01
6.0	4.5638	5.2928	8.1127	5.8377	7.8379	5.9553	1.643E-01
6.1	4.4962	5.2937	8.0236	5.8508	7.7389	6.0553	1.631E-01
6.2	4.4337	5.2950	7.9385	5.8680	7.6402	6.1553	1.615E-01
6.3	4.3767	5.2967	7.8586	5.8904	7.5420	6.2553	1.595E-01
6.4	4.3254	5.2990	7.7857	5.9197	7.4445	6.3553	1.570E-01
6.5	4.2797	5.3023	7.7220	5.9578	7.3481	6.4553	1.538E-01
6.6	4.2395	5.3070	7.6698	6.0066	7.2530	6.5553	1.498E-01
6.7	4.2045	5.3138	7.6316	6.0682	7.1601	6.6553	1.451E-01
6.8	4.1743	5.3235	7.6092	6.1443	7.0701	6.7553	1.394E-01
6.9	4.1485	5.3375	7.6041	6.2361	6.9845	6.8553	1.327E-01
7.0	4.1264	5.3576	7.6165	6.3438	6.9051	6.9553	1.248E-01
7.1	4.1077	5.3862	7.6456	6.4670	6.8343	7.0553	1.155E-01
7.2	4.0916	5.4264	7.6896	6.6042	6.7749	7.1553	1.046E-01
7.3	4.0779	5.4813	7.7462	6.7537	6.7303	7.2553	9.204E-02
7.4	4.0660	5.5540	7.8131	6.9134	6.7033	7.3553	7.820E-02
7.5	4.0559	5.6466	7.8880	7.0815	6.6960	7.4553	6.384E-02
7.6	4.0474	5.7597	7.9691	7.2564	6.7092	7.5553	5.001E-02
7.7	4.0403	5.8925	8.0550	7.4368	6.7418	7.6553	3.769E-02
7.8	4.0345	6.0425	8.1445	7.6216	6.7916	7.7553	2.749E-02
7.9	4.0300	6.2066	8.2368	7.8099	6.8555	7.8553	1.956E-02
8.0	4.0264	6.3818	8.3312	8.0009	6.9305	7.9553	1.368E-02
8.1	4.0237	6.5651	8.4271	8.1940	7.0138	8.0553	9.480E-03
8.2	4.0216	6.7544	8.5242	8.3887	7.1033	8.1553	6.549E-03
8.3	4.0199	6.9481	8.6220	8.5847	7.1973	8.2553	4.529E-03

8.4	4.0187	7.1451	8.7205	8.7816	7.2948	8.3553	3.147E-03
8.5	4.0177	7.3447	8.8194	8.9793	7.3952	8.4553	2.201E-03
8.6	4.0169	7.5465	8.9187	9.1775	7.4979	8.5553	1.551E-03
8.7	4.0164	7.7503	9.0183	9.3763	7.6030	8.6553	1.102E-03
8.8	4.0159	7.9560	9.1181	9.5754	7.7103	8.7553	7.895E-04
8.9	4.0155	8.1637	9.2182	9.7749	7.8201	8.8553	5.691E-04
9.0	4.0152	8.3737	9.3185	9.9746	7.9325	8.9553	4.124E-04

179[a] -log [CrO_4^{2-}] concentration (mol/L)
86150[b] -log [$FeOH_2^+$-$HCrO_4^-$] concentration (mol/L)
86130[c] -log [$FeOH_2^+$-CrO_4^{2-}] concentration (mol/L)
86132[d] -log [$AlOH_2^+$-$HCrO_4^-$] concentration (mol/L)
86152[e] -log [$AlOH_2^+$-CrO_4^{2-}] concentration (mol/L)
50[f] -log [H^+] concentration (mol/L)
T-ADS[g] -log [$FeOH_2^+$-$HCrO_4^-$] -log [$FeOH_2^+$-CrO_4^{2-}] -log [$AlOH_2^+$-$HCrO_4^-$] -log [$AlOH_2^+$-CrO_4^{2-}] concentration (mmol/kg)

Table 53: HYDRAQL input, 0.1 mM chromate adsorption in 0.1 M NaCl

```
0.1000 0 0.0000 25.00 1.000E-03 1 100 /XMU KEYMU ACTCOR TEMP EPS NCASES ITMAX
1    1     1      1      1     1      /IHYDRA IINPUT ICHARG IPDIST IPCENT IALLPC
1    2     4   0         80000         /KEY IADS MODEL IDIFOP LIMADS
1.25 0.2  0   686. 1.25 0.2 0   34.   /C11 C21 C31 AREA1 C12 C22 C32 AREA2
179 50 86130 86132 86152 86150 0 0 0 0 0 0 0 0 0 0 0 0 0 0 /
3.00   9.01  0.1                      /
179    -6.000    1.000E-4             /DATA FOR COMPONENTS  CrO4--
157    -2.000    1.000E-1             /                     Cl-
 50    -4.000    0.000E-0             /                     H+
  5    -2.000    1.000E-1             /                     Na+
184    -6.000    5.130E-6             /                     SOH
180    -1.000    0.000                /                     PSI0
182    -1.000    0.000                /                     PSIB
183    -1.300    0.000                /                     PSID
194    -6.000    1.800E-6             /                     TOH
190    -1.000    0.000                /                     PSI0
192    -1.000    0.000                /                     PSIB
193    -1.300    0.000                /                     PSID
  0     0.000    0.000                /
2                                     /
86105    -9.8  184 1  50 -1  180  -1    0  0     0  0    0    0 /
86110     4.3  184 1  50  1  180   1    0  0     0  0    0    0 /
86115    -9.3  184 1  50 -1  180  -1    5  1   182  1    0    0 /
86120     5.4  184 1  50  1  180   1  157  1   182 -1    0    0 /
86130    10.4  184 1  50  1  180   1  179  1   182 -2    0    0 /
86150    18.1  184 1  50  2  180   1  179  1   182 -1    0    0 /
86107   -12.0  194 1  50 -1  190  -1    0  0     0  0    0    0 /
86112     6.3  194 1  50  1  190   1    0  0     0  0    0    0 /
86117    -9.2  194 1  50 -1  190  -1    5  1   192  1    0    0 /
86122     7.9  194 1  50  1  190   1  157  1   192 -1    0    0 /
86132     9.4  194 1  50  1  190   1  179  1   192 -2    0    0 /
86152    15.9  194 1  50  2  190   1  179  1   192 -1    0    0 /
    0     0.0    0 0   0  0    0   0    0  0     0  0    0    0 /
3                                                                /
50      4.00  0 0 0 0 0 0 0 0 0 0 0 0 0 0 0 0 0 0 0 0 0 0 0 0 0 0 0 0 0 0 0 /
0       0.00  0 0 0 0 0 0 0 0 0 0 0 0 0 0 0 0 0 0 0 0 0 0 0 0 0 0 0 0 0 0 0 /
6                                                                           /
180     0.00  0 0 0 0 0 0 0 0 0 0 0 0 0 0 0 0 0 0 0 0 0 0 0 0 0 0 0 0 0 0 0 /
182     0.00  0 0 0 0 0 0 0 0 0 0 0 0 0 0 0 0 0 0 0 0 0 0 0 0 0 0 0 0 0 0 0 /
183     0.00  0 0 0 0 0 0 0 0 0 0 0 0 0 0 0 0 0 0 0 0 0 0 0 0 0 0 0 0 0 0 0 /
190     0.00  0 0 0 0 0 0 0 0 0 0 0 0 0 0 0 0 0 0 0 0 0 0 0 0 0 0 0 0 0 0 0 /
192     0.00  0 0 0 0 0 0 0 0 0 0 0 0 0 0 0 0 0 0 0 0 0 0 0 0 0 0 0 0 0 0 0 /
193     0.00  0 0 0 0 0 0 0 0 0 0 0 0 0 0 0 0 0 0 0 0 0 0 0 0 0 0 0 0 0 0 0 /
 0 0 0 0 0 0 0 0 0 0 0 0 0 0 0 0 0 0 0 0 0 0 0 0 0 0 0 0 0 0 0 0 0 0 0 0 0 /
 0 0 0 0 0 0 0 0 0 0 0 0 0 0 0 0 0 0 0 0 0 0 0 0 0 0 0 0 0 0 0 0 0 0 0 0 0 /
```

Table 54: HYDRAQL output, 0.1 mM chromate adsorption in 0.1 M NaCl

pH	179[a]	86150[b]	86132[c]	86152[d]	86130[e]	50[f]	T-ADS[g]
3.0	7.2219	5.2901	10.9259	5.9589	10.0971	2.8930	1.557E-01
3.1	7.1219	5.2901	10.8259	5.9590	9.9971	2.9930	1.557E-01
3.2	7.0220	5.2901	10.7260	5.9590	9.8971	3.0930	1.557E-01
3.3	6.9222	5.2901	10.6260	5.9591	9.7971	3.1930	1.557E-01
3.4	6.8223	5.2901	10.5261	5.9591	9.6971	3.2930	1.557E-01
3.5	6.7225	5.2901	10.4262	5.9592	9.5971	3.3930	1.557E-01
3.6	6.6228	5.2901	10.3263	5.9593	9.4971	3.4930	1.557E-01
3.7	6.5231	5.2901	10.2264	5.9595	9.3971	3.5930	1.556E-01
3.8	6.4236	5.2901	10.1266	5.9597	9.2971	3.6930	1.556E-01
3.9	6.3241	5.2902	10.0268	5.9599	9.1971	3.7930	1.556E-01
4.0	6.2247	5.2902	9.9271	5.9602	9.0972	3.8930	1.556E-01
4.1	6.1256	5.2902	9.8274	5.9606	8.9972	3.9930	1.556E-01
4.2	6.0266	5.2902	9.7279	5.9610	8.8972	4.0930	1.555E-01
4.3	5.9279	5.2903	9.6284	5.9616	8.7973	4.1930	1.555E-01
4.4	5.8296	5.2903	9.5291	5.9624	8.6973	4.2930	1.554E-01
4.5	5.7317	5.2904	9.4299	5.9633	8.5974	4.3930	1.554E-01
4.6	5.6343	5.2905	9.3310	5.9645	8.4975	4.4930	1.553E-01
4.7	5.5375	5.2906	9.2324	5.9660	8.3976	4.5930	1.552E-01
4.8	5.4415	5.2907	9.1341	5.9678	8.2978	4.6930	1.551E-01
4.9	5.3466	5.2909	9.0362	5.9701	8.1980	4.7930	1.549E-01
5.0	5.2529	5.2911	8.9389	5.9731	8.0982	4.8930	1.547E-01
5.1	5.1606	5.2914	8.8423	5.9767	7.9986	4.9930	1.545E-01
5.2	5.0702	5.2918	8.7466	5.9813	7.8990	5.0930	1.541E-01
5.3	4.9820	5.2923	8.6519	5.9871	7.7995	5.1930	1.537E-01
5.4	4.8963	5.2929	8.5586	5.9943	7.7002	5.2930	1.533E-01
5.5	4.8138	5.2937	8.4670	6.0032	7.6010	5.3930	1.527E-01
5.6	4.7348	5.2947	8.3774	6.0144	7.5021	5.4930	1.519E-01
5.7	4.6599	5.2960	8.2904	6.0282	7.4035	5.5930	1.510E-01
5.8	4.5896	5.2977	8.2066	6.0453	7.3054	5.6930	1.499E-01
5.9	4.5243	5.3000	8.1266	6.0663	7.2079	5.7930	1.485E-01
6.0	4.4643	5.3031	8.0513	6.0921	7.1112	5.8930	1.468E-01
6.1	4.4099	5.3072	7.9815	6.1234	7.0156	5.9930	1.447E-01
6.2	4.3613	5.3128	7.9183	6.1612	6.9216	6.0930	1.422E-01
6.3	4.3182	5.3206	7.8626	6.2064	6.8298	6.1930	1.391E-01
6.4	4.2805	5.3313	7.8156	6.2600	6.7410	6.2930	1.352E-01
6.5	4.2479	5.3461	7.7782	6.3227	6.6564	6.3930	1.305E-01
6.6	4.2198	5.3668	7.7511	6.3952	6.5777	6.4930	1.246E-01
6.7	4.1958	5.3953	7.7349	6.4780	6.5070	6.5930	1.172E-01
6.8	4.1753	5.4343	7.7298	6.5714	6.4467	6.6930	1.081E-01
6.9	4.1577	5.4867	7.7358	6.6752	6.3997	6.7930	9.722E-02
7.0	4.1427	5.5552	7.7527	6.7892	6.3687	6.8930	8.482E-02
7.1	4.1299	5.6421	7.7800	6.9132	6.3557	6.9930	7.148E-02
7.2	4.1190	5.7481	7.8171	7.0466	6.3618	7.0930	5.815E-02
7.3	4.1100	5.8731	7.8633	7.1890	6.3864	7.1930	4.571E-02
7.4	4.1025	6.0151	7.9178	7.3397	6.4279	7.2930	3.492E-02
7.5	4.0966	6.1716	7.9798	7.4979	6.4837	7.3930	2.610E-02
7.6	4.0918	6.3399	8.0483	7.6629	6.5515	7.4930	1.922E-02
7.7	4.0881	6.5172	8.1225	7.8338	6.6281	7.5930	1.404E-02
7.8	4.0851	6.7011	8.2014	8.0098	6.7116	7.6930	1.023E-02
7.9	4.0828	6.8901	8.2844	8.1902	6.8001	7.7930	7.472E-03
8.0	4.0810	7.0827	8.3707	8.3743	6.8925	7.8930	5.481E-03
8.1	4.0796	7.2780	8.4599	8.5615	6.9877	7.9930	4.045E-03
8.2	4.0785	7.4755	8.5514	8.7514	7.0852	8.0930	3.006E-03
8.3	4.0777	7.6748	8.6448	8.9434	7.1846	8.1930	2.248E-03
8.4	4.0770	7.8756	8.7399	9.1374	7.2857	8.2930	1.692E-03

8.5	4.0765	8.0780	8.8364	9.3330	7.3884	8.3930	1.279E-03
8.6	4.0761	8.2818	8.9341	9.5299	7.4928	8.4930	9.709E-04
8.7	4.0757	8.4872	9.0330	9.7282	7.5990	8.5930	7.387E-04
8.8	4.0755	8.6944	9.1330	9.9276	7.7071	8.6930	5.626E-04
8.9	4.0753	8.9037	9.2340	10.1282	7.8176	8.7930	4.281E-04
9.0	4.0751	9.1153	9.3362	10.3299	7.9306	8.8930	3.252E-04

179* -log [CrO_4^{2-}] concentration (mol/L)
86150* -log [$FeOH_2^+$-$HCrO_4^-$] concentration (mol/L)
86130* -log [$FeOH_2^+$-CrO_4^{2-}] concentration (mol/L)
86132* -log [$AlOH_2^+$-$HCrO_4^-$] concentration (mol/L)
86152* -log [$AlOH_2^+$-CrO_4^{2-}] concentration (mol/L)
50* -log [H^+] concentration (mol/L)
T-ADS* -log [$FeOH_2^+$-$HCrO_4^-$] -log [$FeOH_2^+$-CrO_4^{2-}] -log [$AlOH_2^+$-$HCrO_4^-$] -log [$AlOH_2^+$-CrO_4^{2-}] concentration (mmol/kg)

Table 55: HYDRAQL input , 0.1 mM chromate adsorption in 0.5 M NaCl

```
0.1000 0 0.0000 25.00 1.000E-03 1 100 /XMU KEYMU ACTCOR TEMP EPS NCASES ITMAX
1    1     1      1      1     1      /IHYDRA IINPUT ICHARG IPDIST IPCENT IALLPC
1    2     4   0          80000        /KEY IADS MODEL IDIFOP LIMADS
1.25 0.2  0   686. 1.25 0.2 0   34.   /C11 C21 C31 AREA1 C12 C22 C32 AREA2
179 50 86130 86132 86152 86150 0 0 0 0 0 0 0 0 0 0 0 0 0 0 /
3.00  9.01  0.1                       /
179   -6.000   1.000E-4               /DATA FOR COMPONENTS  CrO4--
157   -2.000   5.000E-1               /                     Cl-
 50   -4.000   0.000E-0               /                     H+
  5   -2.000   5.000E-1               /                     Na+
184   -6.000   5.130E-6               /                     SOH
180   -1.000   0.000                  /                     PSIO
182   -1.000   0.000                  /                     PSIB
183   -1.300   0.000                  /                     PSID
194   -6.000   1.800E-6               /                     TOH
190   -1.000   0.000                  /                     PSIO
192   -1.000   0.000                  /                     PSIB
193   -1.300   0.000                  /                     PSID
  0    0.000   0.000                  /
2                                     /
86105   -9.8  184 1  50 -1  180  -1    0  0     0  0   0   0 /
86110    4.3  184 1  50  1  180   1    0  0     0  0   0   0 /
86115   -9.3  184 1  50 -1  180  -1    5  1   182  1   0   0 /
86120    5.4  184 1  50  1  180   1  157  1   182 -1   0   0 /
86130   10.4  184 1  50  1  180   1  179  1   182 -2   0   0 /
86150   18.1  184 1  50  2  180   1  179  1   182 -1   0   0 /
86107  -12.0  194 1  50 -1  190  -1    0  0     0  0   0   0 /
86112    6.3  194 1  50  1  190   1    0  0     0  0   0   0 /
86117   -9.2  194 1  50 -1  190  -1    5  1   192  1   0   0 /
86122    7.9  194 1  50  1  190   1  157  1   192 -1   0   0 /
86132    9.4  194 1  50  1  190   1  179  1   192 -2   0   0 /
86152   17.3  194 1  50  2  190   1  179  1   192 -1   0   0 /
    0    0.0    0 0   0  0    0   0    0  0     0  0   0   0 /
3                                                             /
50      4.00  0 0 0 0 0 0 0 0 0 0 0 0 0 0 0 0 0 0 0 0 0 0 0 0 0 0 0 0 0 0 0 /
0       0.00  0 0 0 0 0 0 0 0 0 0 0 0 0 0 0 0 0 0 0 0 0 0 0 0 0 0 0 0 0 0 0 /
6                                                                           /
180     0.00  0 0 0 0 0 0 0 0 0 0 0 0 0 0 0 0 0 0 0 0 0 0 0 0 0 0 0 0 0 0 0 /
182     0.00  0 0 0 0 0 0 0 0 0 0 0 0 0 0 0 0 0 0 0 0 0 0 0 0 0 0 0 0 0 0 0 /
183     0.00  0 0 0 0 0 0 0 0 0 0 0 0 0 0 0 0 0 0 0 0 0 0 0 0 0 0 0 0 0 0 0 /
190     0.00  0 0 0 0 0 0 0 0 0 0 0 0 0 0 0 0 0 0 0 0 0 0 0 0 0 0 0 0 0 0 0 /
192     0.00  0 0 0 0 0 0 0 0 0 0 0 0 0 0 0 0 0 0 0 0 0 0 0 0 0 0 0 0 0 0 0 /
193     0.00  0 0 0 0 0 0 0 0 0 0 0 0 0 0 0 0 0 0 0 0 0 0 0 0 0 0 0 0 0 0 0 /
 0 0 0 0 0 0 0 0 0 0 0 0 0 0 0 0 0 0 0 0 0 0 0 0 0 0 0 0 0 0 0 0 0 0 0 0 0 /
 0 0 0 0 0 0 0 0 0 0 0 0 0 0 0 0 0 0 0 0 0 0 0 0 0 0 0 0 0 0 0 0 0 0 0 0 0 /
```

Table 56: HYDRAQL output, 0.1 mM chromate adsorption in 0.5 M NaCl

pH	179*	86150*	86132*	86152*	86130*	50*	T-ADS*
3.0	7.1325	5.2912	11.4504	6.5599	9.9912	3.0000	1.348E-01
3.1	7.0327	5.2912	11.3506	6.5601	9.8911	3.1000	1.347E-01
3.2	6.9331	5.2912	11.2508	6.5604	9.7911	3.2000	1.347E-01
3.3	6.8335	5.2912	11.1512	6.5607	9.6912	3.3000	1.347E-01
3.4	6.7340	5.2912	11.0516	6.5612	9.5912	3.4000	1.347E-01
3.5	6.6346	5.2912	10.9522	6.5617	9.4912	3.5000	1.347E-01
3.6	6.5354	5.2912	10.8528	6.5624	9.3912	3.6000	1.347E-01
3.7	6.4364	5.2912	10.7537	6.5633	9.2912	3.7000	1.347E-01
3.8	6.3377	5.2912	10.6548	6.5643	9.1912	3.8000	1.347E-01
3.9	6.2393	5.2913	10.5562	6.5657	9.0913	3.9000	1.346E-01
4.0	6.1413	5.2913	10.4579	6.5674	8.9913	4.0000	1.346E-01
4.1	6.0438	5.2913	10.3600	6.5696	8.8913	4.1000	1.346E-01
4.2	5.9469	5.2914	10.2627	6.5722	8.7914	4.2000	1.345E-01
4.3	5.8508	5.2915	10.1660	6.5756	8.6915	4.3000	1.345E-01
4.4	5.7557	5.2916	10.0702	6.5798	8.5916	4.4000	1.344E-01
4.5	5.6618	5.2917	9.9754	6.5850	8.4917	4.5000	1.343E-01
4.6	5.5693	5.2918	9.8819	6.5915	8.3918	4.6000	1.342E-01
4.7	5.4786	5.2920	9.7899	6.5995	8.2920	4.7000	1.340E-01
4.8	5.3900	5.2922	9.6998	6.6095	8.1923	4.8000	1.339E-01
4.9	5.3040	5.2925	9.6120	6.6216	8.0926	4.9000	1.337E-01
5.0	5.2209	5.2929	9.5268	6.6365	7.9930	5.0000	1.334E-01
5.1	5.1414	5.2934	9.4448	6.6546	7.8935	5.1000	1.331E-01
5.2	5.0659	5.2940	9.3665	6.6763	7.7942	5.2000	1.327E-01
5.3	4.9949	5.2948	9.2924	6.7023	7.6951	5.3000	1.323E-01
5.4	4.9289	5.2959	9.2230	6.7329	7.5962	5.4000	1.318E-01
5.5	4.8682	5.2973	9.1588	6.7688	7.4977	5.5000	1.311E-01
5.6	4.8131	5.2993	9.1001	6.8101	7.3998	5.6000	1.304E-01
5.7	4.7638	5.3019	9.0472	6.8573	7.3025	5.7000	1.295E-01
5.8	4.7201	5.3055	9.0002	6.9103	7.2063	5.8000	1.284E-01
5.9	4.6820	5.3105	8.9590	6.9692	7.1115	5.9000	1.269E-01
6.0	4.6491	5.3175	8.9236	7.0337	7.0187	6.0000	1.251E-01
6.1	4.6209	5.3274	8.8935	7.1037	6.9288	6.1000	1.226E-01
6.2	4.5969	5.3413	8.8684	7.1786	6.8431	6.2000	1.192E-01
6.3	4.5766	5.3609	8.8478	7.2580	6.7631	6.3000	1.146E-01
6.4	4.5594	5.3885	8.8313	7.3415	6.6911	6.4000	1.085E-01
6.5	4.5447	5.4268	8.8185	7.4287	6.6297	6.5000	1.004E-01
6.6	4.5321	5.4787	8.8091	7.5192	6.5821	6.6000	9.037E-02
6.7	4.5212	5.5474	8.8029	7.6128	6.5509	6.7000	7.856E-02
6.8	4.5118	5.6349	8.7999	7.7096	6.5386	6.8000	6.571E-02
6.9	4.5038	5.7423	8.8002	7.8098	6.5460	6.9000	5.279E-02
7.0	4.4971	5.8692	8.8041	7.9134	6.5726	7.0000	4.082E-02
7.1	4.4916	6.0134	8.8115	8.0206	6.6165	7.1000	3.056E-02
7.2	4.4872	6.1725	8.8234	8.1321	6.6753	7.2000	2.231E-02
7.3	4.4837	6.3434	8.8397	8.2481	6.7459	7.3000	1.600E-02
7.4	4.4810	6.5232	8.8607	8.3687	6.8253	7.4000	1.137E-02
7.5	4.4789	6.7097	8.8868	8.4943	6.9115	7.5000	8.056E-03
7.6	4.4773	6.9011	8.9183	8.6252	7.0027	7.6000	5.713E-03
7.7	4.4761	7.0962	8.9555	8.7618	7.0977	7.7000	4.071E-03
7.8	4.4751	7.2942	8.9986	8.9044	7.1956	7.8000	2.920E-03
7.9	4.4744	7.4946	9.0480	9.0532	7.2960	7.9000	2.110E-03
8.0	4.4738	7.6972	9.1038	9.2083	7.3986	8.0000	1.536E-03
8.1	4.4734	7.9018	9.1662	9.3701	7.5034	8.1000	1.126E-03
8.2	4.4730	8.1085	9.2351	9.5384	7.6103	8.2000	8.298E-04
8.3	4.4727	8.3176	9.3106	9.7134	7.7197	8.3000	6.141E-04
8.4	4.4725	8.5293	9.3928	9.8950	7.8317	8.4000	4.555E-04

8.5	4.4724	8.7439	9.4814	10.0832	7.9468	8.5000	3.380E-04
8.6	4.4722	8.9618	9.5766	10.2780	8.0652	8.6000	2.504E-04
8.7	4.4721	9.1836	9.6783	10.4794	8.1876	8.7000	1.848E-04
8.8	4.4720	9.4096	9.7865	10.6872	8.3143	8.8000	1.356E-04
8.9	4.4720	9.6403	9.9012	10.9017	8.4458	8.9000	9.874E-05
9.0	4.4719	9.8762	10.0224	11.1227	8.5824	9.0000	7.128E-05

179* -log [CrO_4^{2-}] concentration (mol/L)
86150* -log [$FeOH_2^+$-$HCrO_4^-$] concentration (mol/L)
86130* -log [$FeOH_2^+$-CrO_4^{2-}] concentration (mol/L)
86132* -log [$AlOH_2^+$-$HCrO_4^-$] concentration (mol/L)
86152* -log [$AlOH_2^+$-CrO_4^{2-}] concentration (mol/L)
50* -log [H^+] concentration (mol/L)
T-ADS* -log [$FeOH_2^+$-$HCrO_4^-$] -log [$FeOH_2^+$-CrO_4^{2-}] -log [$AlOH_2^+$-$HCrO_4^-$] -log [$AlOH_2^+$-CrO_4^{2-}] concentration (mmol/kg)

Table 57: HYDRAQL input, 0.1 mM chromate adsorption in 0.01 M sulfate

```
0.0100 0 0.0000 25.00 1.000E-03 1 100 /XMU KEYMU ACTCOR TEMP EPS NCASES ITMAX
0    0     0      1      0     0      /IHYDRA IINPUT ICHARG IPDIST IPCENT IALLPC
1    2     4   0         80000         /KEY IADS MODEL IDIFOP LIMADS
1.25 0.2  0   686. 1.25 0.2 0   34.    /C11 C21 C31 AREA1 C12 C22 C32 AREA2
179 50 86130 86132 86152 86150 0 0 0 0 0 0 0 0 0 0 0 0 0 0 /
3.00  9.01  0.1                        /
179   -6.000   1.000E-4                /DATA FOR COMPONENTS  CrO4--
102   -6.000   1.000E-2                /                     SO4--
157   -2.000   1.000E-2                /                     Cl-
 50   -4.000   0.000E-0                /                     H+
  5   -2.000   1.000E-2                /                     Na+
184   -6.000   5.130E-6                /                     SOH
180   -1.000   0.000                   /                     PSI0
182   -1.000   0.000                   /                     PSIB
183   -1.300   0.000                   /                     PSID
194   -6.000   1.800E-6                /                     TOH
190   -1.000   0.000                   /                     PSI0
192   -1.000   0.000                   /                     PSIB
193   -1.300   0.000                   /                     PSID
  0    0.000   0.000                   /
2                                      /
86105   -9.8  184 1  50 -1  180  -1    0  0     0  0   0   0 /
86110    4.3  184 1  50  1  180   1    0  0     0  0   0   0 /
86115   -9.3  184 1  50 -1  180  -1    5  1   182  1   0   0 /
86120    5.4  184 1  50  1  180   1  157  1   182 -1   0   0 /
86130   10.4  184 1  50  1  180   1  179  1   182 -2   0   0 /
86150   18.9  184 1  50  2  180   1  179  1   182 -1   0   0 /
86107  -12.0  194 1  50 -1  190  -1    0  0     0  0   0   0 /
86112    6.3  194 1  50  1  190   1    0  0     0  0   0   0 /
86117   -9.2  194 1  50 -1  190  -1    5  1   192  1   0   0 /
86122    7.9  194 1  50  1  190   1  157  1   192 -1   0   0 /
86132    9.4  194 1  50  1  190   1  179  1   192 -2   0   0 /
86152   17.7  194 1  50  2  190   1  179  1   192 -1   0   0 /
86160   11.6  184 1  50  1  180   1  102  1   182 -2   0   0 /
86170   17.3  184 1  50  2  180   1  102  1   182 -1   0   0 /
    0    0.0    0 0   0  0    0   0    0  0     0  0   0   0 /
3                                                            /
50      4.00  0 0 0 0 0 0 0 0 0 0 0 0 0 0 0 0 0 0 0 0 0 0 0 0 0 0 0 0 0 0 0 /
0       0.00  0 0 0 0 0 0 0 0 0 0 0 0 0 0 0 0 0 0 0 0 0 0 0 0 0 0 0 0 0 0 0 /
6                                                                           /
180     0.00  0 0 0 0 0 0 0 0 0 0 0 0 0 0 0 0 0 0 0 0 0 0 0 0 0 0 0 0 0 0 0 /
182     0.00  0 0 0 0 0 0 0 0 0 0 0 0 0 0 0 0 0 0 0 0 0 0 0 0 0 0 0 0 0 0 0 /
183     0.00  0 0 0 0 0 0 0 0 0 0 0 0 0 0 0 0 0 0 0 0 0 0 0 0 0 0 0 0 0 0 0 /
190     0.00  0 0 0 0 0 0 0 0 0 0 0 0 0 0 0 0 0 0 0 0 0 0 0 0 0 0 0 0 0 0 0 /
192     0.00  0 0 0 0 0 0 0 0 0 0 0 0 0 0 0 0 0 0 0 0 0 0 0 0 0 0 0 0 0 0 0 /
193     0.00  0 0 0 0 0 0 0 0 0 0 0 0 0 0 0 0 0 0 0 0 0 0 0 0 0 0 0 0 0 0 0 /
 0 0 0 0 0 0 0 0 0 0 0 0 0 0 0 0 0 0 0 0 0 0 0 0 0 0 0 0 0 0 0 0 0 0 0 0 0 /
 0 0 0 0 0 0 0 0 0 0 0 0 0 0 0 0 0 0 0 0 0 0 0 0 0 0 0 0 0 0 0 0 0 0 0 0 0 /
```

Table 58: HYDRAQL output, 0.1 mM chromate adsorption in 0.01 M sulfate

pH	179[a]	86150[b]	86132[c]	86152[d]	86130[e]	50[f]	T-ADS[g]
3.0	7.3871	11.0795	5.7908	12.5651	7.0202	2.9553	4.286E-02
3.1	7.2873	10.9795	5.7908	12.3734	6.9284	3.0553	4.342E-02
3.2	7.1874	10.8795	5.7908	12.1811	6.8361	3.1553	4.412E-02
3.3	7.0877	10.7795	5.7909	11.9887	6.7436	3.2553	4.497E-02
3.4	6.9879	10.6795	5.7909	11.7965	6.6512	3.3553	4.604E-02
3.5	6.8883	10.5795	5.7909	11.6048	6.5594	3.4553	4.736E-02
3.6	6.7887	10.4795	5.7910	11.4140	6.4685	3.5553	4.895E-02
3.7	6.6893	10.3795	5.7911	11.2245	6.3788	3.6553	5.089E-02
3.8	6.5899	10.2796	5.7912	11.0368	6.2909	3.7553	5.323E-02
3.9	6.4907	10.1796	5.7913	10.8512	6.2050	3.8553	5.602E-02
4.0	6.3917	10.0796	5.7914	10.6683	6.1218	3.9553	5.930E-02
4.1	6.2928	9.9797	5.7916	10.4885	6.0417	4.0553	6.311E-02
4.2	6.1942	9.8798	5.7917	10.3125	5.9652	4.1553	6.748E-02
4.3	6.0958	9.7799	5.7920	10.1405	5.8928	4.2553	7.236E-02
4.4	5.9977	9.6800	5.7923	9.9732	5.8250	4.3553	7.774E-02
4.5	5.8999	9.5801	5.7926	9.8109	5.7621	4.4553	8.355E-02
4.6	5.8025	9.4803	5.7931	9.6539	5.7045	4.5553	8.964E-02
4.7	5.7055	9.3806	5.7936	9.5023	5.6523	4.6553	9.590E-02
4.8	5.6090	9.2809	5.7942	9.3563	5.6056	4.7553	1.022E-01
4.9	5.5130	9.1813	5.7949	9.2158	5.5645	4.8553	1.083E-01
5.0	5.4178	9.0819	5.7959	9.0806	5.5286	4.9553	1.141E-01
5.1	5.3233	8.9826	5.7970	8.9504	5.4978	5.0553	1.194E-01
5.2	5.2299	8.8835	5.7984	8.8250	5.4717	5.1553	1.242E-01
5.3	5.1378	8.7846	5.8002	8.7037	5.4498	5.2553	1.284E-01
5.4	5.0472	8.6861	5.8024	8.5864	5.4319	5.3553	1.320E-01
5.5	4.9585	8.5881	5.8052	8.4725	5.4174	5.4553	1.349E-01
5.6	4.8722	8.4906	5.8088	8.3617	5.4059	5.5553	1.372E-01
5.7	4.7886	8.3940	5.8134	8.2537	5.3973	5.6553	1.388E-01
5.8	4.7082	8.2984	5.8193	8.1483	5.3911	5.7553	1.398E-01
5.9	4.6316	8.2044	5.8270	8.0452	5.3872	5.8553	1.401E-01
6.0	4.5593	8.1124	5.8369	7.9443	5.3854	5.9553	1.398E-01
6.1	4.4917	8.0233	5.8499	7.8457	5.3857	6.0553	1.388E-01
6.2	4.4292	7.9380	5.8669	7.7494	5.3881	6.1553	1.370E-01
6.3	4.3721	7.8579	5.8892	7.6556	5.3928	6.2553	1.344E-01
6.4	4.3206	7.7848	5.9183	7.5646	5.4000	6.3553	1.308E-01
6.5	4.2746	7.7207	5.9560	7.4767	5.4100	6.4553	1.262E-01
6.6	4.2341	7.6681	6.0043	7.3924	5.4233	6.5553	1.206E-01
6.7	4.1988	7.6293	6.0654	7.3123	5.4405	6.6553	1.140E-01
6.8	4.1683	7.6063	6.1409	7.2373	5.4625	6.7553	1.063E-01
6.9	4.1421	7.6005	6.2320	7.1681	5.4902	6.8553	9.784E-02
7.0	4.1199	7.6122	6.3391	7.1060	5.5248	6.9553	8.869E-02
7.1	4.1011	7.6407	6.4619	7.0521	5.5678	7.0553	7.905E-02
7.2	4.0853	7.6845	6.5989	7.0077	5.6207	7.1553	6.914E-02
7.3	4.0720	7.7412	6.7485	6.9742	5.6850	7.2553	5.920E-02
7.4	4.0609	7.8085	6.9087	6.9526	5.7623	7.3553	4.948E-02
7.5	4.0517	7.8841	7.0776	6.9439	5.8536	7.4553	4.028E-02
7.6	4.0442	7.9661	7.2533	6.9484	5.9592	7.5553	3.194E-02
7.7	4.0380	8.0528	7.4346	6.9660	6.0788	7.6553	2.470E-02
7.8	4.0330	8.1430	7.6201	6.9958	6.2117	7.7553	1.866E-02
7.9	4.0290	8.2358	7.8089	7.0369	6.3564	7.8553	1.383E-02
8.0	4.0258	8.3306	8.0003	7.0882	6.5114	7.9553	1.011E-02
8.1	4.0233	8.4267	8.1936	7.1483	6.6753	8.0553	7.311E-03
8.2	4.0213	8.5239	8.3885	7.2162	6.8466	8.1553	5.256E-03

8.3	4.0198	8.6219	8.5845	7.2908	7.0243	8.2553	3.769E-03
8.4	4.0186	8.7204	8.7815	7.3713	7.2073	8.3553	2.703E-03
8.5	4.0177	8.8194	8.9792	7.4571	7.3950	8.4553	1.944E-03
8.6	4.0169	8.9187	9.1775	7.5476	7.5868	8.5553	1.403E-03
8.7	4.0163	9.0183	9.3763	7.6424	7.7823	8.6553	1.017E-03
8.8	4.0159	9.1181	9.5754	7.7413	7.9812	8.7553	7.403E-04
8.9	4.0155	9.2182	9.7748	7.8443	8.1835	8.8553	5.410E-04
9.0	4.0152	9.3185	9.9746	7.9512	8.3890	8.9553	3.965E-04

179[a] -log [CrO_4^{2-}] concentration (mol/L)
86150[b] -log [$FeOH_2^+$-$HCrO_4^-$] concentration (mol/L)
86130[c] -log [$FeOH_2^+$-CrO_4^{2-}] concentration (mol/L)
86132[d] -log [$AlOH_2^+$-$HCrO_4^-$] concentration (mol/L)
86152[e] -log [$AlOH_2^+$-CrO_4^{2-}] concentration (mol/L)
50[f] -log [H^+] concentration (mol/L)
T-ADS[g] -log [$FeOH_2^+$-$HCrO_4^-$] -log [$FeOH_2^+$-CrO_4^{2-}] -log [$AlOH_2^+$-$HCrO_4^-$]
-log [$AlOH_2^+$-CrO_4^{2-}] concentration (mmol/kg)